Jurassic and Cretaceous strata of the Lamu Embayment, Kenya.

Their petrography, stratigraphy, depositional environments and diagenesis, with particular emphasis on the Kambe Formation.

by

Peter K. Thuo

A thesis presented for the degree of Master of Science in the Faculty of Science at the University of St. Andrews, 1992.

Declaration

a). I *Peter K. Thuo* hereby certify that this thesis has been written by me, that it is a record of my own work and that it has not been submitted in any previous application for a higher degree.

Signature of candidate_____ Date 23.12.92

b). I hereby certify that the candidate has fulfilled the conditions of the Resolutions and Regulations appropriate to the degree of Master of Science and that he is qualified to submit this thesis in application for that degree.

Signature of supervisor_____ Date 5.1.93

Copyright Declaration

UNRESTRICTED

In submitting this thesis to the University of St. Andrews I understand that I am giving permission for it to be made available for use in accordance with the regulations of the University Library for the time being in force, subject to any copyright vested in the work not being affected thereby. I also understand that the title and abstract will be published and that a copy of the work may be made and supplied to any bona fide library or research worker.

Abstract

The development of the Lamu Embayment began with the deposition of Karroo sediments during the rift phase of the passive margin evolution. The top of the Karroo sequence is marked by the Mazeras sandstones.

The Jurassic Kambe limestones of the Lamu Embayment were deposited in shallow water environments within the epicontinental sea which developed during the separation of Madagascar from Africa. The limestones overlie the mainly continental clastic sediments of the Karroo. The Cretaceous Freretown limestones are separated from the Kambe limestones by a thick sequence of Upper Jurassic shales.

The depositional model proposed for the Kambe limestones invokes the presence of a wide epeiric shelf within which grainstone shoals and patch reefs were developed while oolite grainstone complexes formed at the shelf margin. The composition of the limestones has enabled their subdivision into 6 petrofacies, each of which formed in a particular subenvironment within the carbonate platform. The diagenetic sequence for the Kambe limestones is interpreted as having proceeded from the seafloor and shallow submarine environment into the deep burial environment. There is no evidence for subearial exposure or meteoric diagenesis. The trace element composition of the limestones indicates a high-Mg precursor sediment with no evidence of aragonitic material in the cements. Dolomitization is only locally important as a late

diagenetic process.

Based on thin section evaluation, the reservoir potential of the Mazeras sandstones and the Kambe limestones is poor due to extensive cementation. The Freretown limestones have good interparticle and intraparticle porosity and are possible good reservoir targets.

Acknowledgment

This project was carried out under the supervision of Dr R. Duck and Professor E. K. Walton. I wish to thank them most sincerely for their stimulating supervision and encouragement during the course of the project and for their very constructive criticism of the draft chapters of the thesis. Helpful contributions were made by Dr R. MacGregor (petrography) and Dr A. J. Weir (stratigraphy) for which I owe them both much gratitude. I would also like to thank Dr J. Kinnaird of the University College, Cork for her assistance with fluid inclusion work. I am also very grateful for the help I received from the staff of the SURRC, particularly Dr A. Fallick, in isotope analysis.

Technical staff were helpful and co-operative all the way. I would particularly like to express my appreciation for the help received from Andy Mackie (thin section and miscellaneous problems), Jim Allan (photography), Donald Herd (microprobe) and Irvine Davidson (SEM).

I am greatly indebted to the National Oil Corporation of Kenya (NOCK) for generously providing funds without which this project would never have been carried out. To NOCK management and staff, I say thank you very much indeed.

Not forgotten are my wife, Wambui and daughter, Ciru who bravely bore the burden of loneliness during the long year that I was away from home. I thank them both for their understanding and unfailing support.

Contents

List of Figures

List of Tables

List of Plates

1.0 INTRODUCTION

1.1 OBJECTIVES

The objectives of this study are as outlined below :

1 to review the stratigraphy of the Lamu Embayment from published data with particular emphasis on the Jurassic and Cretaceous strata

2 to identify the different facies of the Jurassic Kambe limestones based on their petrographic characteristics such as the lithological composition and textural features

3 to propose a depositional and diagenetic model for the Jurassic and Cretaceous strata

4 to determine the hydrocarbon reservoir potential of the Mazeras sandstones, Kambe limestones and the Freretown limestones.

1.2 LOCATION, GEOLOGICAL SETTING AND BASIN EVOLUTION

The Lamu Embayment extends from the Oddo Alimo region in Somalia, south through Kenya to the Tanzanian border and inland from the Kenya coast to the Precambrian basement

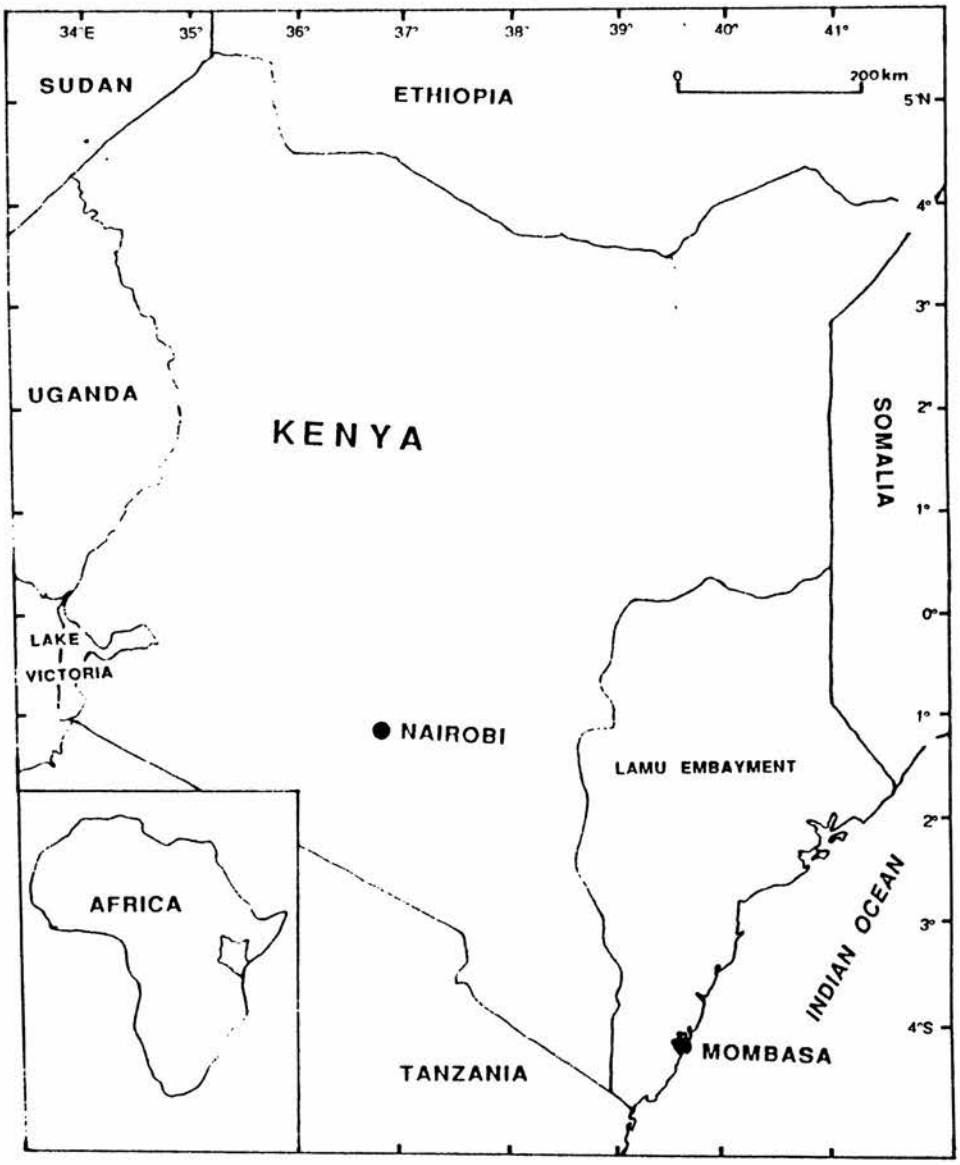

Figure 1-1

Location of the Lamu Embayment

outcrops (Figure 1-1). Thus the basin extends inland westwards to c.38°30'E. The Kenyan portion of the Embayment includes the present day Tana valley and north to the middle reaches of the intermittent Uaso Nyiro river (Walters & Linton,1973; Coffin & Rabinowitz,1988).

The Lamu Embayment of coastal Kenya contains up to 10,000m of sediments ranging in age from Carboniferous-Permian (Karroo) to Quaternary (Walters & Linton,1973). The Lamu Embayment is Kenya's largest basinal area encompassing 132,770 km^2. Successively older beds become exposed as one passes inland as the sediments of the basins of East Africa prograde oceanwards (McKinnon-Wood,1938; Coffin & Rabinowitz,1988).

The Lamu Embayment is a typical passive margin whose development started with continental rifting, followed by continental spreading, juvenile oceanic spreading, and finally formation of the mature basin. Three stages are recognized in the development of the basin. These stages are referred to as the pre-rift, the syn-rift and the post-rift stages with respect to the continental rifting associated with the break-up of Gondwanaland. The pre-rift phase corresponds to Precambrian to Carboniferous prior to the break-up of Gondwanaland. The Basement System rocks in this period consist of gneisses and schists (metamorphics formed from the sediments of the Mozambique Orogenic Belt). Rifting during the Permian marked the initial tensional breakdown of the

continental margin (Kent,1972).

The continental margin bordering Tanzania and most of Kenya is a manifestation of the transform motion between Madagascar and Africa while the margin of Northeast Kenya was formed by the rifting and the drifting between Madagascar and Africa. The motion of Madagascar is, in this case, assumed to have been from the north, as shown by marine magnetic measurements (Rabinowitz,1983). The trajectory of Madagascar was in two phases according to Reeves *et al* (1986). The first was a relatively small, east-west separation with rifting parallel to the existing coastline during Karroo times. The main translational movement of Madagascar began after the domal uplift below the mid-Jurassic triple junction. This motion was in a southerly direction with respect to Africa at the rate of 1.8cm/year.

Deposition of continental clastic material dominated the rifting phase with only minor marine incursions. Evaporites typify the closed lake basins of the rift stage and the first marine incursion during the incipient ocean (Allen and Allen,1990). These evaporites become mobile when buried under the overburden of the passive margin sediments and the resulting salt diapirism frequently followed pre-existing faults. In the East African margin, evaporites have been reported from Tanzania, Somalia and off-shore Kenya. Significant thicknesses of early Jurassic evaporites are reported to have been deposited during the rift and early

drift phases of the separation of Madagascar from Africa. The salt diapirs occur only on the portions of continental margin formed by the rifting and not on the transform margin (Kent and Perry,1973; Kamen-Kaye and Barnes,1973; Rabinowitz *et al* ,1982).

During the Jurassic, marine waters flooded across lowlands and invaded the Karroo evaporite troughs, transgressing across the major fault margins. Extensional faulting died out in the post-rift phase with only minor reactivation of older normal faults. Growth faults are common in areas of high sedimentation. In East Africa, the phase of vertical movements associated with subsidence ended in the middle Jurassic, by which time shallow water limestones had been widely deposited along the line of the present coast. The post-rift phase in the Lamu Embayment encompasses the time from middle Jurassic to Recent (Kent and Perry,1973; Kent,1982; Allen and Allen,1990).

The early, sediment-starved phase of passive margin development is generally followed by an increase in continental- derived clastic sediments forming thick seaward -prograding wedges (Allen and Allen,1990). In the Lamu Embayment, shale deposition was dominant in the Upper Jurassic and early Tertiary, largely in progradational series (Kent,1982). Sedimentation was controlled by intermittent tectonic activity and eustatic sea- level changes. A general regression occurred as a result of uplift at the end of the

Jurassic with the formation of horst structures resulting in regional unconformities at the Jurassic-Cretaceous boundary. From Cretaceous through Eocene time, basement uplift caused wide scale erosion in many western areas of the Lamu Embayment. During this period, continental clastic sediments advanced from the north-west with continued subsidence offshore. Eocene through Recent sedimentation is characterized by overall regressive sequences of continental, deltaic and marine facies (Western Atlas International, Inc.1990).

1.3 PREVIOUS WORK

Among the earliest geological reports of the Kenya coast region were those of Gregory (1921), Parsons (1928) and McKinnon-Wood (1930; 1938). The first two were geological reports of the regional stratigraphy of the coastal districts and formation names. The reports by McKinnon-Wood provided the first comprehensive palaeontological dating of the sedimentary rocks of the Kenya coast. These reports form the basic stratigraphic model on which subsequent work was based. The Geological Survey of Kenya carried out more detailed work on the coastal geology and produced reports in the 1950s and 1960s. These include reports by Dodson (1966), Sanders (1959), Miller (1952), Thompson (1956) and Caswell (1953; 1956).

Several oil companies have carried out geological surveys covering the Lamu Embayment but most of the reports are unpublished. Oil exploration in the Lamu Embayment began in

the early 1950s resulting in the drilling of several wildcat wells by BP-Shell. From the mid-1970s to the mid-1980s, field geological surveys and core-drilling were carried out by Chevron and UNOCAL, among others. During this period, 9 oil companies were active in the exploration of the off-shore Lamu Embayment. The exploration resulted in the drilling of 3 off-shore wells which tested Cretaceous carbonates and sandstones associated with salt-related anticlines and horst-blocks. All the wells were abandoned as dry holes with non-economic gas shows. A total of 15,977 line-km of seismic data have been recorded onshore in the Lamu Embayment with another 11,671 line-km off-shore (Nyagah,1992).

1.4 METHODS

Standard thin sections were used for petrography. All carbonate thin sections were stained on one half using a solution of Potassium Ferricyanide and Alizarin Red-S following the procedure outlined by Dickson (1966) to enable the identification of carbonate minerals. Friable sandstone samples and any others with apparent porosity were impregnated with blue-dyed epoxy resin to facilitate thin section preparation and to aid in identification and quantification of porosity.

For SEM petrography, selected specimens were sampled by breaking off a cube of rock of about 1 cm dimensions and mounting this on an aluminium or steel stub. Six samples were

mounted on each stub and were then sputter-coated with gold to provide a conductive surface. The equipment used was a JEOL JSM-35CF scanning microscope with an energy-dispersive X-ray analyzer.

Polished thin sections were used for electron microprobe analysis and cathodoluminescence (CL) petrography. The CL machine used was a Technosyn 2001 operating at 250mA gun current and 15kV accelerating voltage. CL photographs were taken at various exposure times starting at 5 seconds and progressively doubling this up to 320 seconds. The optimum exposure time was found to be around 20 seconds. Microprobe analysis was carried out on a JEOL superprobe JCXA-733 machine with a backscattered electron detector. The polished sections were carbon-coated before being analyzed.

Stable isotope analysis was carried out on coarse vein cements and whole rock samples. A surgical scalpel was used to scratch out small quantities of material from a sample viewed under a binocular microscope. The sampled material was weighed (a minimum of 1mg was required) and digested in 100% phosphoric acid. The sample and acid were mixed under vacuum and the temperature was maintained at a constant 25°C . The reaction was allowed to proceed overnight for calcite and 3 days for dolomites. After removal of volatiles and water vapour, the carbon dioxide gas produced by the reaction was fed into a mass spectrometer to obtain its carbon and oxygen isotopic composition. The isotope analyses were performed at

the Scottish Universities Reactor and Research Center (SURRC) in East Kilbride, Glasgow.

2.0 STRATIGRAPHY

2.1 KARROO SEDIMENTS

The Karroo is the oldest non-metamorphic sedimentary succession in the Lamu Embayment and is locally known as the Duruma Sandstone Group. It is divided into four main formations with coarser beds at the top and bottom, separated by a relatively finer grained formation. The Karroo is assumed to persist beneath the Lamu Embayment in a northerly direction, being represented north of Wajir in north-eastern Kenya by the Mansa Guda Formation (Walters & Linton,1973). Figure 2-1 shows the general stratigraphy of the Lamu Embayment.

2.1.1 Taru Formation

The Taru Formation which forms the base of the Karroo Supergroup, is shown by the presence of the freshwater bivalve *Palaeonodonta fisheri* to be Upper Permian in age (McKinnon-Wood,1938). It is of fluviatile origin with possible marine horizons, with fresh feldspathic grits (coarse-grained sandstones) and sandstones derived from the basement to the west. Deposition of the Karroo Supergroup was initiated by major faulting in late Carboniferous or early Permian time (Coffin & Rabinowitz, 1988). The Taru Formation appear to be c.2700m thick west of Mombasa (maximum thickness) while further north, only half of this thickness is known (Walters & Linton,1973). At the base of the Taru Grits are tilloids

Age	Thickness	Lithology	Formation	Description
Pleistocene	100 m		Reef Complex	Coral Reef Lagoonal Dune Beach Sands
Pliocene	100 m		Magarini Formation	Uniform Sands and Sandstones Basal Conglomerate
Miocene	600 m		Marafa Fm. Baratumu Fm.	Shale,sandstones,Sands and Limestones
Creataceous	1790 m		Upper Mtomkuu	Dark Grey Shale with Sandstone and Limestone Bands
Upper Jurassic			Middle Mtomkuu	Dark Grey or Brown Shales, Silty and Sandy
	180 m		Lower Mtomkuu	Grey Brown Sandy Micaceous Shale,with Sandstone and Limestone
Middle Jurassic	150 m		Kambe Formation	Dark Grey Oolitic Limestones and Shale,Basal Conglomerate
Lower Jurassic	1000 m		Upper Mazeras	Coarse Pebbly Sandstone
			Middle Mazeras	Cross-bedded Coarse Arkosic Sandstone
				Shale/Siltstone , Silicified wood
Triassic	2000 m		Lower Mazeras	Banded coarse to Medium Grained Sandstones with Shale
			Upper Mariakani	Medium-Fine grained Sandstone with Basal shale/siltstone horizon
			Middle Mariakani	Flaggy Sandstones with Shale / Siltstone Intercalations
			Lower Mariakani	Mottled Sandstones with Basal Shale/ Siltstone Horizon
Permian	4500 m		Upper Maji-ya-Chumvi	Flaggy Sandstones
			Middle Maji-ya-Chumvi	Grey-green Shales with *Estheria*
			Fish Bed Lower Maji-ya-Chumvi	Blue Micaceous Shale with Fish Remains Carbonaceous Shaly Siltstones Sandstones with Fish Remains
			Upper Taru	Arkoses,Shales and Sandstones
Carboniferous			Middle Taru	Coarse Sanstones,Arkoses Shales and Minor Limestones and Conglomerates
			Lower Taru	Tillites
Precambrian			Basement System	Gneisses and Schists

Figure 2-1
A generalized stratigraphy of the Lamu Embayment (after Karanja,1984).

comparable in age to the tillites found in the Morondava Basin of Madagascar (Coffin & Rabinowitz,1988).

Miller (1952) subdivided the Taru Formation into two while Sanders (1959) and Karanja (1980) proposed a three-fold subdivision of the Taru Formation into the Lower, Middle and Upper Members. According to Sanders (1959) the Basal Taru consists of tillites and arkoses/conglomerates, the former being poorly stratified, pale yellow-grey, indurated rocks resting unconformably on basement rocks. Karanja (1980) noted that, though the Lower Taru sediments are limited in extent in Kenya, their similarities to the glacial deposits of the Dwyka Tillites of the South African Karroo would possibly confirm the extension of the Upper Carboniferous glaciation to East Africa.

The Middle member of the Taru Formation comprises well -defined units of coarse-grained arkosic and pebbly sandstones with well-developed shale/siltstone horizons towards the base (Karanja,1980).

The Upper Member of the Taru Formation comprises mainly arkosic sandstones associated with polymict conglomerate lenticles. Subordinate shale/siltstone horizons are abundant towards the top and thin coaly partings and coaly beds occur associated with the grits of the Upper Taru (Karanja,1980).

2.1.2 Maji-ya-Chumvi Formation

Overlying the Taru Formation are the Maji-ya-Chumvi Beds

which represent a change from fluviatile to lacustrine conditions (Coffin & Rabinowitz,1988). These consist of shales and sandstones containing Triassic plant remains and the lower Triassic *Estheria greyi* (McKinnon-Wood,1938). The Maji-ya-Chumvi Formation can be subdivided into the Lower, Middle and Upper members as suggested by Karanja (1980). The Lower Member comprises sandstones, shales, siltstones and subordinate limestones. The Middle Member has dominant shales with fish remains while the Upper Member is dominated by a sandstone/shale /siltstone lithology. A recently discovered fossil has been identified as *Australosomus* of early Triassic age (Cannon *et al*,1981).

The Maji-ya-Chumvi Formation reaches a maximum thickness of 1200m and the beds frequently exhibit ripple marks, cross-bedding, sun cracks and rain pits. The lower half of the beds (550m) is continental, containing plant fragments and is overlain by a thin layer of Lower Triassic marine shale containing fish fossils while the Upper part of the unit (650m) indicates by the presence of a fresh water brachiopod, a fresh or possibly brackish lacustrine environment. The plant remains in the lower part of the unit include *Voltzia* and *Ulmania*, while above it, an incursion of the sea dated as early Triassic, resulted in the formation of a thin shale sequence (The Triassic Fish Bed) which contains scales similar to those of the fish *Boreosumus gillioti* (Walters & Linton,1973).

2.1.3 Mariakani Formation

This includes sediments of both arenaceous and argillaceous grade (Thompson,1956). The Majority of the sandstones are cemented by calcareous matter. Walters and Linton (1973) consider the Mariakani Formation to represent a fresh cycle of coarser deposition, following the quieter Maji-ya-Chumvi deposition. Coffin and Rabinowitz (1988) put the total thickness of the Mariakani Formation at between 2900m and 3400m.

The older sediments are essentially sandstones while the upper and younger horizons are mainly siltstones shales and mudstones with sandstone intercalations. Essentially the Mariakani Formation comprises thin bedded, fine grained, flaggy sandstones. Cross-bedding is common, more so in the finer sandstones and siltstones. In addition to calcite, other cementing materials include chlorite, iron ores (usually limonite) and in some cases, clay minerals (Thompson,1956). Only unidentifiable, poorly preserved plant remains have been found in the Mariakani Formation and these are believed to be Triassic in age (Walters & Linton,1973).

Karanja (1980) distinguishes three members of the Formation, all characterized coarsening-upward cycles.

2.1.4 Mazeras Formation

The Mazeras Formation which tops the Karroo sequence consists of massive, coarse, cross-bedded sandstones with

interbedded siltstones. Silicified wood fragments are common in the Mazeras Formation (Coffin & Rabinowitz,1988; Walters & Linton,1973). The unit ranges in age from Triassic through early Jurassic, and consists of 450m of sediment. The sandstones are flaggy and cross-bedded at the base, with more massive beds at higher horizons, which are also commonly cross-bedded (Thompson,1956). Intercalated argillaceous beds are not common in the Mazeras Formation. The sandstones have suffered faulting resulting in the formation of fault breccias which have undergone initial silicification followed by later partial ferruginisation (Thompson,1956). The lower sandstones were probably deposited in extensive deltas as the lakes gradually sanded up, but the upper beds are aeolian sandstones and probably represent coastal dunes formed during more arid conditions prevailing towards the end of the erosional cycle (Walters & Linton,1973). The basal contact with the underlying Mariakani Formation is considered an unconformity by Caswell (1956) and Thompson (1956).

2.2 POST-KARROO SEDIMENTS

At the end of early Jurassic, a major episode of faulting brought about the end of the predominantly continental Karroo deposition (Coffin & Rabinowitz,1988). Marine conditions became established in the Lamu Embayment during middle Jurassic times.

2.2.1 Kambe Formation

The Kambe Formation consists of dark grey, dense, oolitic and coralliferous limestones with interbedded shales. Three facies of limestones have been identified, including the dark, compact facies, the light grey coral limestone and an oolitic or pisolitic limestone found interstratified with the other two varieties (McKinnon-Wood,1930). Evidence for their Bajocian age rested on some ammonites collected by McKinnon-Wood (1930). The limestones generally occur in faulted contact with the underlying Karroo and this results in varying thicknesses reported, ranging from 150m to 600m (Walters & Linton,1973).

In the Mwachi River section the Kambe Formation is seen to rest, with a slight unconformity, directly on the Mazeras Formation of the Karroo sequence. Here, a basal conglomerate of some 12 to 15m thickness is exposed, consisting of boulders of Mazeras sandstones. A pisolitic and coral limestone interbedded with thinly laminated shale is also exposed (Walters & Linton,1973).

In the Rare valley section, the lowermost part of the Kambe Formation exposed is represented by a drab coloured, coarsely crystalline, dolomitic limestone, unfossiliferous and containing a black mineral, probably an iron ore (Thompson,1956). Higher up in the series is a yellowish, arenaceous limestone containing feldspar and quartz grains.

The Kambe Formation has been interpreted as forming in

varying shallow water environments, with a deeper water facies in the south and a shallower water environment indicated towards the north (Walters & Linton,1973; Coffin & Rabinowitz,1988).

2.2.2 Mtomkuu Formation

Karanja (1984) suggested the name Mtomkuu Formation to encompass the Upper Jurassic to Cretaceous strata of the Lamu Embayment. The Mtomkuu Formation comprises mainly shales with subordinate sandstones, limestones, marls and siltstones. The Formation is conveniently subdivided into three members .

The Lower Member consists of brown sandy micaceous shales, unfossiliferous silty sandstones and limestone bands. This member appears to rest conformably on the underlying Kambe Formation although in the Mazeras area, the Lower Mtomkuu is faulted against the Mazeras sandstones. The Lower Mtomkuu is what the earlier geologists referred to as the Kibiongoni Beds (Gregory,1921; McKinnon-Wood,1930; Caswell,1953; Caswell,1956). The base of the lower Mtomkuu is marked by a conglomerate, roughly 30cm thick, composed of subangular pebbles of limestone and quartz set in a limonitic matrix. This is overlain by a series of thin, sandy shales with interbedded micaceous and ferruginous sandstones (Caswell,1953). Near the top is a fairly massive 2.4m band of ochreous sandstone.

Many of the beds are ripple-marked and rain-pitted

(Caswell, 1953) suggesting a coastal environment of deposition, possibly estuarine. Karanja (1984) noted the presence of slumping and discordant bedding features which were interpreted as suggesting a depositional wedge prograding towards a deep sea along a steep slope.

The Lower Mtomkuu sequences are Callovian in age (Walters & Linton,1973). Caswell (1953) has postulated that the Lower Mtomkuu (or Kibiongoni Beds as he refers to them) are a lateral facies equivalent of the Kambe limestones formed in the estuaries of rivers that were discharging sand into the middle Jurassic sea.

The Middle Mtomkuu comprises grey gritty shales and clays with very rare local limestone and sandstone interbeds (Karanja,1984). The Middle Mtomkuu is apparently what Caswell (1953; 1956) and other writers refer to as the Upper Jurassic Shales and Limestones. They have been subdivided into Miritini Shales, Rabai Shales, Changamwe Shales and Coroa Mombasa Limestones. This nomenclature is rather confusing as the beds were given locality names which resulted in the same formation having several different names at different localities. It is therefore more convenient to follow the Karanja (1984) nomenclature of Middle Mtomkuu to encompass the Upper Jurassic shales and limestones.

The lower beds of the member consist mainly of dark grey, well laminated calcareous siltstones which on weathering become a yellowish drab colour (Thompson,1956). The lower

Mtomkuu normally passes into the middle member without any obvious stratigraphic break (Karanja,1984) and Caswell (1956) observed that the main difference between the two members is an upward gradation with a reduction in sand content. White sandy, ferruginous and sometimes micaceous bands are known, the majority of the shales are calcareous and in some places, the content of calcareous material is sufficiently high to form argillaceous limestones. These are of lenticular development and are rarely more than 33m thick. Septarian nodules occur throughout the succession, especially in the higher horizons, where they often contain included ammonites (Caswell,1956).

The Upper Mtomkuu is distinguished from the Middle Mtomkuu by the development of abundant limestone and sandstone horizons and marks the entrance into the Cretaceous age (Karanja,1984). At the Freretown area, near Mombasa, the topmost 30m of continuous shales that have hitherto been regarded as Upper Jurassic have been proved to be Lower Cretaceous in age (Walters & Linton,1973). This has been established by means of megafossils, including ammonites.

The overlying Freretown Limestone sequence which forms part of the limestone units of the Upper Mtomkuu (Karanja,1984) indicates deposition in a shallow water shelf environment. It has been assumed that the change in sedimentary conditions between this and the underlying shales reflected a distinction between the Jurassic and Cretaceous

environments (Walters & Linton,1973). It has now been established that this lithological change took place entirely within the Neocomian and that the Jurassic/ Cretaceous boundary lies within the shale sequence. A possibly significant facies difference between the Neocomian and the underlying Jurassic shales (i.e. between the Middle and Upper Mtomkuu) is the apparent lack of concretions in the former. Thin sections of the Freretown Limestone contain *Orbitolina bulgarica janenschi* and *O. kurdica* which, being Barremian-Aptian, agrees with the megafossil dating and the Freretown Limestone is regarded as probably late Neocomian/early Aptian in age (Walters & Linton,1973). In the Freretown area c.20m of bluish grey mudstones of Aptian age overlie the Freretown Limestone. These mudstones contain *Planomalina (Globigerinelloides) algeriana.*

Borehole data have shown that at least 1500m of Neocomian beds followed by 250m of Aptian are present in the Lamu Embayment (Walters & Linton,1973), the lithology being a monotonous sequence of repeated sandstones, siltstones and dark grey shales throughout the Neocomian while the Aptian is mostly of sandstones and siltstones. These clastics represent the erosion products of the early phase of the end-Cretaceous erosional surface cycle. The presence of pure orthoquartzites in the sandstones may indicate that further west the arenaceous sediments of the Karroo were being actively eroded.

In the Freretown area, above the sandstone band which is taken as the top of the Aptian, there is a marked lithological change to about 30m of massive, blocky, bluish-grey to brownish grey shales with abundant microfauna of Albian to Cenomanian age. The fauna recovered from these shales includes *Hedbergella paradubia*, *H. trocoidea*, *Ticinella roberti* and *Planomalina buxforti* (Walters & Linton,1973; Coffin & Rabinowitz,1988). Thicknesses exceeding 1000m are known for the Albian sediments at depth. These are calcareous dark grey shales containing a planktonic foraminiferal assemblage and ammonite fragments, including the Lower Albian *Tetrahoplitoides* sp. These were probably deposited in comparatively deep undisturbed water in the center of the Lamu Embayment while in the shallower more marginal areas they grade into argillaceous limestones containing only a sparse benthonic assemblage together with *Hedbergella washitensis*. The undisturbed, relatively deep marine environment of deposition persisted over the central part of the Lamu Embayment throughout most of late Cretaceous, resulting in a thick shale sequence in which all the stages (except Coniacian) from Cenomanian to Campanian are represented (Walters & Linton,1973). The total thickness of deep water marine sediments deposited from early Cretaceous to the beginning of Cenozoic time is approximately 1200m of grey to grey-green calcareous mudstone with thin bands of argillaceous sandstone and micritic limestone (Coffin & Rabinowitz,1988).

2.2.3 Cenozoic Rocks

These are largely confined to the coastal plain and comprise representatives of the Miocene, Pleistocene and Recent sediments (Thompson,1956).

2.2.3.1 *Baratumu Formation*

This generally comprises light coloured sediments composed of yellow, sandy marls, marly limestones and sands with occasional light grey or dirty white sandy marls. Calcareous sandstones are present but not common. The sediments are lenticular in nature and are not of great lateral extent. The lenticles of yellow sands are often highly fossiliferous (foraminiferal). The presence of the *Miogypsina* sp. horizon indicates the Miocene age of the formation (Thompson,1956; Karanja,1984).

Towards the top of the Miocene beds, lenticular bands of marly fossiliferous limestone are found. From regional dip calculations, Thompson (1956) suggested that the total thickness of the Baratumu Formation does not exceed 488m. The environment of deposition was mainly shallow marine, inner shelf with, on the landward side, fluviatile influences (Karanja,1984).

2.2.3.2 *Marafa Formation*

The Marafa beds are subaqueous deposits of probably late Pliocene to early Pleistocene (previously allocated to the

Miocene:Karanja,1984) age. These are essentially light coloured, white to creamy white sands with occasional lenticular bands of red and purple sands and clays (Thompson,1956). These sands, clays and pebble beds are cross-bedded and are essentially noncalcareous, with locally accumulated fossiliferous horizons of limited extent. The fossils identified from these horizons include large and small foraminifera, bryozoa, ostracoda, cirripedia and anthozoa.

The beds are, on the whole, unconsolidated and easily eroded. In places, they show a peculiar mode of erosion where pits are formed with earth pillars, sometimes up to 33m tall, with protective caps formed of a ferricrete band more than 3m thick. In the Malindi area, the Marafa Formation probably does not exceed 107m in thickness (Thompson,1956).

2.2.3.3 *Magarini Formation*

This consists of unfossiliferous, unconsolidated poorly sorted to well sorted quartz sands which accumulated as coastal dunes. The sands show all degrees of coarseness and are often clay-bound or are grading into sandy clays. Their colour varies from dark-red to greenish-yellow (Caswell,1953; Thompson,1956; Walters & Linton,1973). The age of the formation is late Pliocene.

2.2.3.4 *Pleistocene Deposits*

The Pleistocene deposits of the Lamu Embayment comprise

the Reef Complex and the associated dune, beach and lagoonal sediments (Karanja,1984). The Reef Complex is an extremely variable complex of lithological types. The Reef itself is primarily a detrital, sandy algal limestone with scattered coral heads and may posses an open porous texture or may be hard and dense, with internal recrystallization (Walters & Linton,1973). The Reef Complex and the Kilindini Sands are lateral equivalents, evidenced by the interbedding of reef material with current-bedded sands and also lateral changes from sandy algal limestone to gravelly calcareous sands and back again which occur over very short distances. Other lithologies represented include loose, detrital, calcareous sands; coarse calcareous grits with red garnet grains; sandy shelly limestones (coquinoid with large *Ostrea*, *Pecten* and *Balanus*) and greenish-white unconsolidated quartz sands containing pebbles of fossil wood, ultimately of Karroo origin (Walters & Linton,1973).

2.3 FIELD OBSERVATIONS AND SAMPLING

The coastal belt in Kenya is characterized by poor outcrop exposure due to the generally low topographic relief and extensive soil and vegetation cover. The belt has been subdivided into four physiographic units which coincide with different sedimentary deposits (Gregory,1921; Caswell,1953). These units are the coastal plain, the foot plateau, the coastal range and the Nyika. The coastal plain comprises the

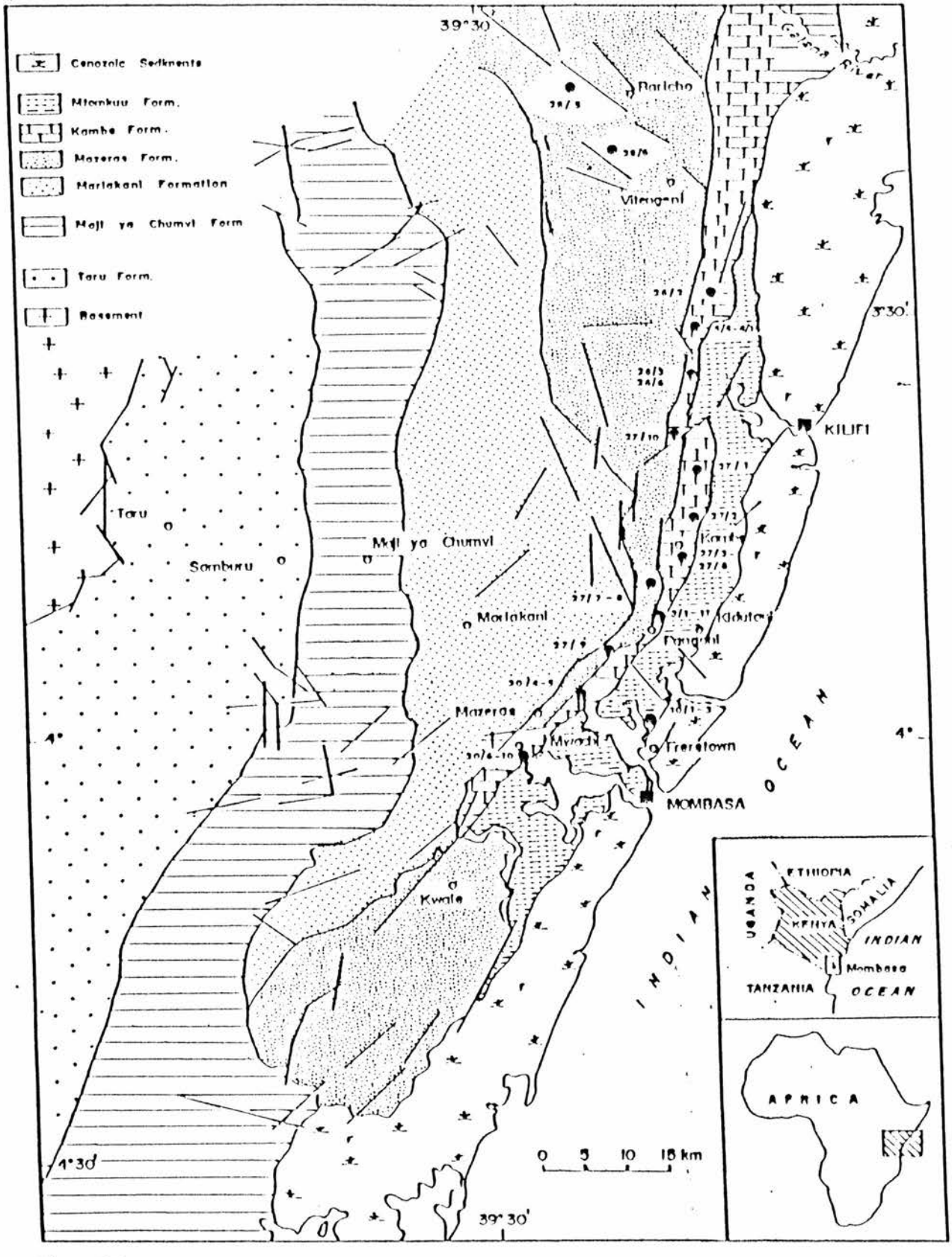

Figure 2-2
Geological and sample location map (geology modified from Rais-Assa,1988).

Cenozoic formations and generally lies below the 30m contour. The foot plateau coincides with the Jurassic deposits and the Nyika is underlain by the Karroo sandstones. The foot plateau rises to about 150m while the coastal range is 518m at its highest. The coastal range is composed of rocks of the Mazeras Formation while the Nyika is considered as the remnant of a peneplained surface of mid-Pliocene age west of the contact between the Jurassic and Triassic rocks (Caswell,1953; Thompson, 1956).

2.3.1 Mazeras sandstones

Outcrops of the Mazeras sandstones were found in the Kambe-Mikomani area where they occur as fine-grained friable, micaceous sandstones with very thin horizons of dark-grey shale. Similar varieties of the grey fine-grained sandstones were observed at an outcrop in the Makobeni-Mbungoni and Merikani area (sample 28/6). In the area around Baricho, (see figure 2-2 for locations) outcrops of the Mazeras sandstones occur as highly weathered conglomeratic sandstone (sample 28/5).

In the Miritini area along the Mombasa-Nairobi Highway, the Mazeras sandstones outcrop in the road-cut section with an apparent fault contact with shale. The beds on the upthrown side (towards the west) dip 10° towards the southwest. The sandstone unit in the upper part of the exposed section (sample 30/5) is lighter-coloured and finer-grained than the

underlying unit (sample 30/4).

2.3.2 Kambe limestones

An outcrop of Kambe biomicrites and biosparites was sampled in the Matano-Manne area (sample 26/2). The outcrop is composed of grey-coloured bioclastic limestones containing abundant corals.

In the Kachororoni area near the Rare River, medium-grey limestone with 1.2-2cm thick calcite veins filled with crystalline cement is exposed at a roadside quarry. This is composed of a massive variety of the Kambe limestones with dissolution vugs that are partially filled with crystalline cement. Sparry and micritic bioclastic limestones containing shell fragments were sampled (samples 26/3, 26/4, 26/5 and 26/6). Medium to dark-grey oolitic limestone with calcite veins outcrops in the Kidutani area. Weathering in this region produces distinctive karst topography.

Three distinct facies of the Kambe limestones were found at an outcrop in the Luandani River valley. These include a micritic variety with a coralline unit and an oolitic horizon. The three units are separated by thin whitish shale interbeds (samples 27/4, 27/5 and 27/6). In the same area, the coralline variety was sampled (sample 3/10) in the vicinity of an inferred fault-contact between the Kambe Formation and the underlying Mazeras Formation. Both formations are exposed on one side of the river but the Mazeras Formation disappears

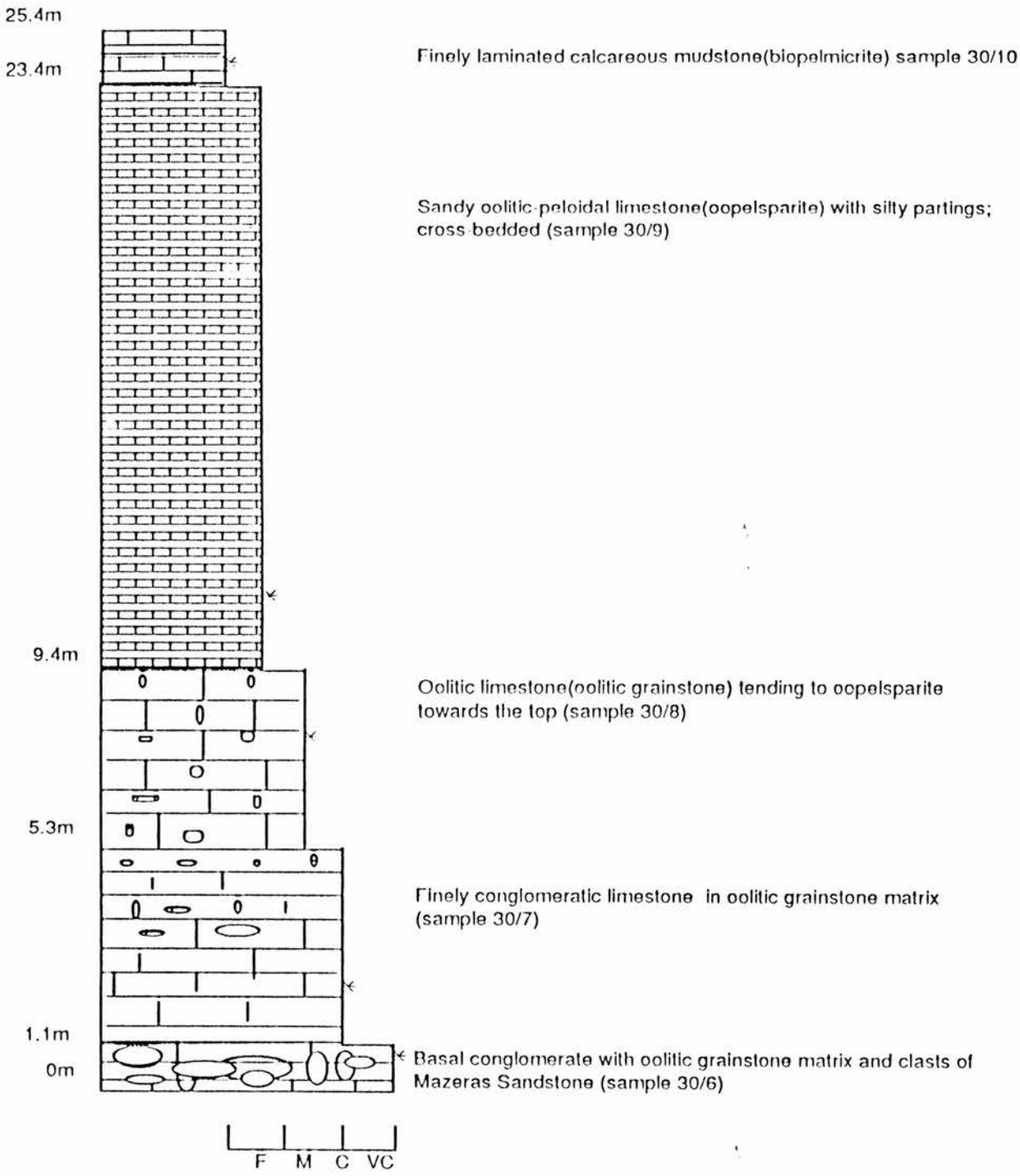

Figure 2-3
Vertical section at the Kambe Limestone Quarry. Grain size scale: F = fine, M = medium, C = coarse and VC = very coarse grained. * indicates sampling positions.

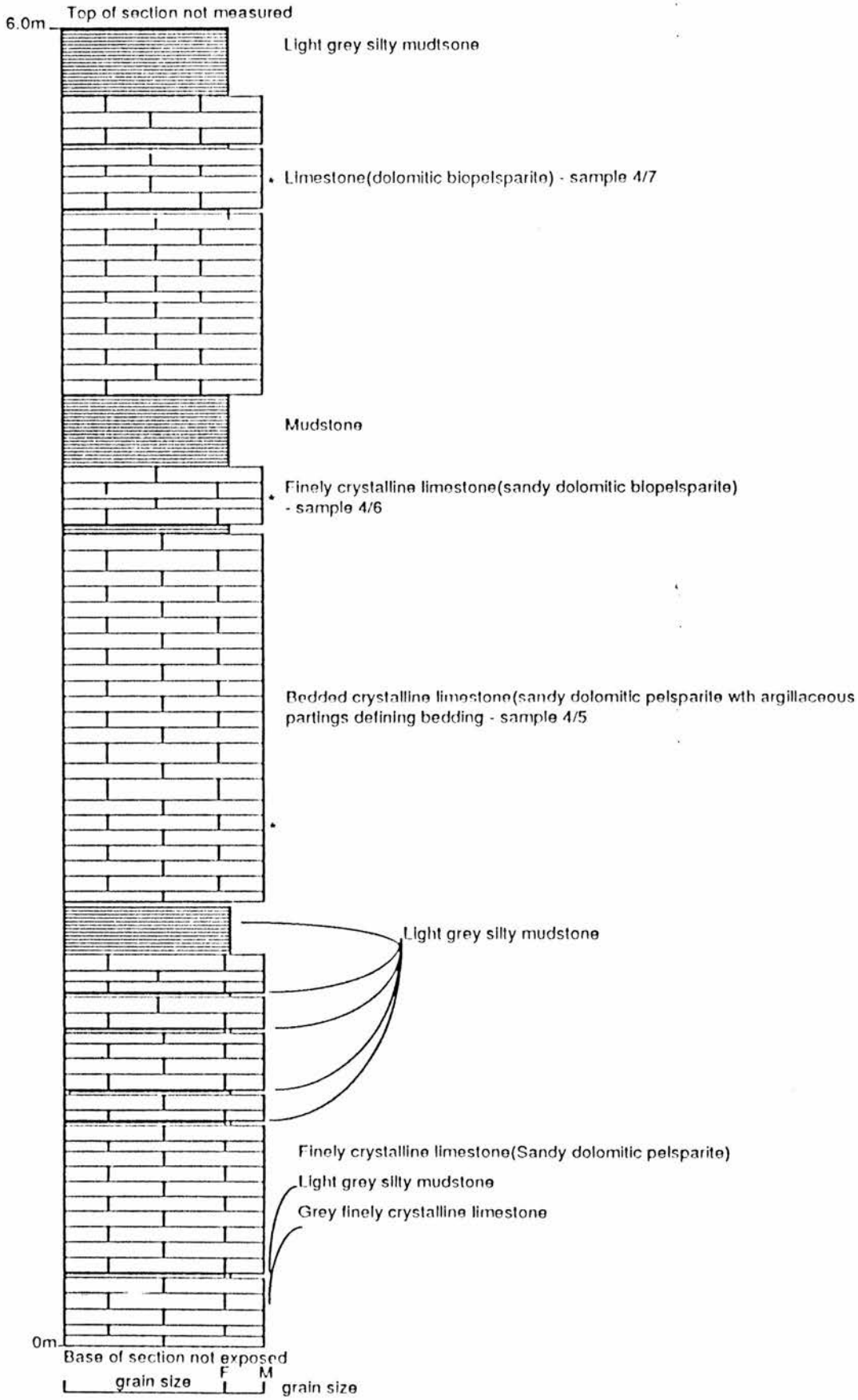

Figure 2-4
Measured section of the Kambe Formation at the Rare River cliffs, the lower units. Grain size scale: F = fine and M = medium.

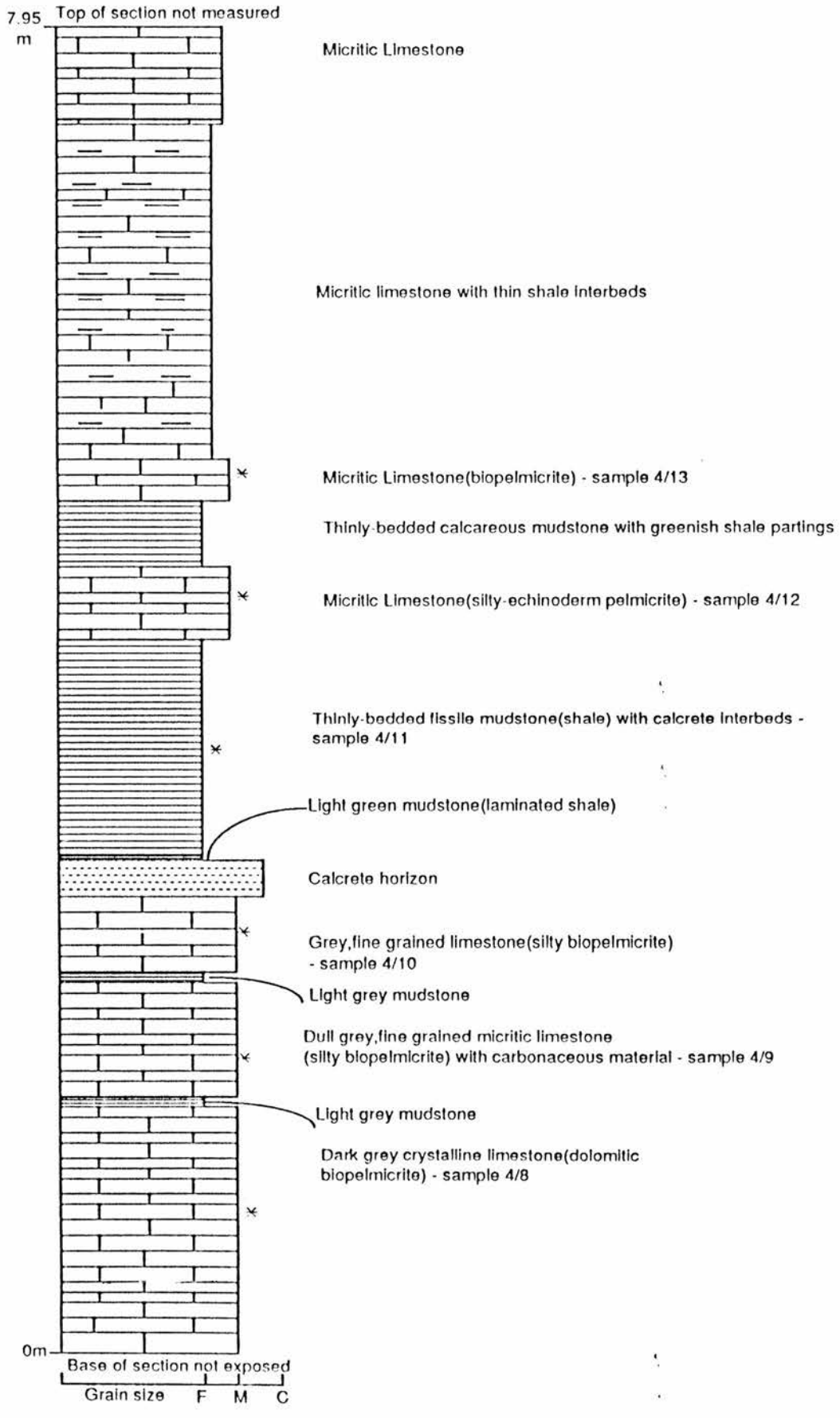

Figure 2-5
Measured section of the Kambe Formation at the Rare River cliffs, the upper units. Grain size scale: F = fine, M = medium and C = coarse grained. * indicates sample point.

across the river.

In the Jaribuni area, a highly altered sample (27/10) was collected from an outcrop with extensive black iron mineralization. This variety of limestone is locally mined as iron ore.

Different facies of the Kambe limestones were sampled in the Jongani River-Pangani area. These include bioclastic facies, micritic facies, conglomeratic limestone and the coarsely crystalline sparite facies (samples 3/1 to 3/7). Samples 3/8 and 3/9 were collected near the Pangani Primary School from an outcrop comprising the crystalline and the micritic varieties.

A typical section of the oolitic facies of the Kambe Formation is exposed in the outcrop at the Kambe Limestone quarry. In this section, the bioclastic varieties are not represented. The vertical section can be subdivided into at least four units (Figure 2-3). The lower-most unit is a basal conglomerate composed of sandstone and siltstone clasts which are up to 60cm in diameter and were probably derived from the underlying Mazeras sandstones (not exposed here). The clasts are held in a matrix made of dark-grey, massive, oolitic limestone (sample 30/6). The overlying unit is a finer-grained conglomerate relative to the lower unit. It is probably just part of the lower unit showing an upward size-grading. The unit is oolitic (sample 30/7) and shows large-scale cross-bedding. Sample 30/8 was taken from the

overlying coarsely crystalline and pebbly oolitic limestone which is in turn overlain by a crystalline unit with silty partings and abundant quartz sand grains (sample 30/9). The topmost unit is composed of a finely-laminated calcareous mudstone (sample 30/10) with up to 10cm-thick shale partings.

At the Rare River Cliffs, an estimated 60m of the fine grained variety of the Kambe limestones is exposed. Part of this outcrop was measured and sampled (Figures 2-4 and 2-5). The base of the section is not exposed while the top was inaccessible. The section is composed mainly of repetitive units of dark-grey, fine grained limestones, well-bedded calcareous mudstones and thinly-laminated light green shales (samples 4/3 to 4/13).

2.3.3 Freretown limestones

These were sampled at only one outcrop exposed in a disused quarry in the Freretown area near Mombasa. The outcrop is highly weathered and vegetation and soil cover limit the exposure of the outcrop. Three samples (30/1, 30/2 and 30/3) were collected.

3.0 PETROGRAPHY

3.1 MAZERAS SANDSTONES

The composition and classification of the Jurassic Mazeras sandstones is based on the analysis of 8 thin sections and one SEM sample. Three thin sections were point-counted (Table 3-1B). In determining the compositional percentages, a total of 1000 points were counted for every thin section.

3.1.1 Framework grains

Monocrystalline quartz is the dominant framework grain, with mean grain sizes ranging from 0.2mm (fine sand) to 0.7mm (coarse sand). The maximum grain sizes are in the range 0.3mm (medium sand) to 1.2mm (very coarse sand). Sorting ranges from poor to moderate and the grains are angular to subrounded. Most quartz grains have non-undulose extinction. Grain contacts range from straight to slightly sutured, indicating some degree of compactional deformation.

Polycrystalline quartz grains make up between 8.2 and 20.3% in the samples point-counted (table 3-1B) and are very coarse, up to 1.8mm in diameter, inclusion-rich with the inclusions displaying a preferred linear pattern. The intersubcrystal boundaries show sutured contacts.

Feldspars are abundant in some samples while others have only trace amounts indicating different levels of mineralogical maturity. Where present, potassium feldspars tend to dominate over plagioclase feldspars and show varying

degrees of alteration from fresh-looking unaltered to almost completely altered feldspar with highly birefringent alteration products. Some feldspar grains have been dissolved out leaving only traces of the original grain. Most of the feldspars are twinned (Carlsbad, albite and cross-hatched).

Micas: muscovite is present as colourless elongate flakes, sometimes squeezed between quartz and other detrital grains indicating compaction. Occasional brown to pale yellowish-green pleochroic flakes (biotite) are present.

Detrital clay clasts are rarely present squeezed between other framework grains. Most of the clay occurs as authigenic pore-lining and pore-filling kaolinite probably resulting from the alteration of feldspars since it also occurs as a replacement product of feldspar grains.

Chert occurs as fine-grained cloudy masses, abundant in some samples and absent in others.

3.1.2 Cements

Silica is the most common cement. It occurs as authigenic overgrowths precipitated onto detrital quartz grains. In some cases the overgrowths are marked by dust rims of inclusions. Calcite cement (non-ferroan) is present in some samples, clearly visible in the ones stained for carbonate identification.

Clay cement is quite common as pore-filling and pore-lining kaolinite, sometimes forming euhedral "kaolinite

booklets" as observed under the SEM.

3.1.3 Accessory minerals

Dark brown to black opaque (probably ferrous) mineralization is present especially in association with cherty material and altered feldspars.

3.1.4 Porosity

The porosity is generally poor. Most of the primary intergranular porosity has been obliterated by cementation by silica and clay minerals. Where primary intergranular porosity still exists, it is poorly interconnected. Porosity quantification by point-counting of three thin sections resulted in values of 3.1%, 5.6% and 7.8% (Table 3-1B). Secondary porosity resulting from dissolution of feldspars is abundant in some samples with fair interconnectedness which may result in some permeability. Fracture porosity is present in one sample which has a 0.07mm open fracture (this could be an induced fracture formed during thin section preparation).

3.1.5 Classification

Based on the Folk (1974) classification of sandstones, of the eight samples examined, two were classified as quartzwackes (sample numbers 27/7 and 27/8), one subarkose (27/9), one quartzarenite (3/11), one lithic arkose (30/4), two sublitharenites (28/5 and 28/6) and one a feldspathic

litharenite.

3.2 KAMBE LIMESTONES

On the basis of the analysis of 36 thin sections and 15 SEM samples, 6 different petrofacies have been recognized in the Jurassic Kambe Formation. Twenty of the thirty-six thin sections were point-counted (at 1000 points per thin section). The facies have been classified according to the Folk (1962) classification of limestones. The facies have been categorized according to the relative abundance of allochemical constituents (peloids, ooids, bioclasts and intraclasts), micrite matrix and sparry cement. The 6 facies identified are:

3.2.1 Biomicrite Facies

Most of the biomicrites of the Kambe Formation are fossiliferous wackestones and packstones on the Dunham (1962) classification (Table 3-1A). They range from mud-supported to grain-supported carbonates with bioclastic grains set in a micritic carbonate matrix. Sparry calcite cements are in most cases, significantly less than 50% and in some cases absent.

3.2.1.1 *Allochemical components*

Corals are the most abundant bioclastic constituents of the biomicrites. The samples examined contain between 7.3 and 55% coral (Table 3-1A). Their structure is preserved by faint micrite rims and are associated with encrusting algae. Most

of the original structure has been lost through neomorphism and in most cases identification is only based on the general morphology and shapes compared with published data (Adams, *et al.*, 1984; Scholle, 1978; Majewske, 1969; Bathurst, 1971). The internal structure is filled with non-ferroan calcite. The calcite is judged to be neomorphic in origin because of the abundance of non-planar crystal boundaries, patches of remnant micrite and an irregular distribution of grain sizes. The individual coral polyp outlines are generally spheroidal to ovoid in shape and appear to be unbroken. They were probably aragonitic originally and have since been recrystallized (neomorphosed) into low magnesium calcite. Coral polyp sizes range from 2mm to 6mm in diameter while the infilling neomorphic spar has crystal sizes ranging from micron-sized (microspar) to about 1mm and sometimes displays a drusy fabric in which the micron-sized crystals occur at the margins while the coarser ones are towards the center.

Echinoderm plates and spines are present in most of the samples examined, their abundance varying from 0.1 to 3% (Table 3-1A). Most of the transverse sections of the echinoderm spines are preserved whole while the plates and longitudinal sections of spines occur as fragments up to 6mm in length. Occasionally the spines occur within intraclasts. The echinoderm fragments show characteristic dusty appearance and single-crystal extinction in most cases, with syntaxial

Samples	26/2	26/4	26/6	27/4	27/6	3/1	3/6	3/7	3/10
coral	13.4	55.0	25.9	34.8	31.0	7.3	0.0	0.0	26.5
echinoderm	2.9	0.0	0.1	0.1	0.2	2.5	3.0	0.6	0.8
brachiopod	0.6	0.0	0.5	0.5	0.0	3.5	2.4	0.4	0.0
gastropod/ bivalve	3.2	0.1	2.2	0.6	2.0	6.7	19.8	0.4	3.0
calcareous sponge	0.9	0.0	0.0	0.0	0.2	2.1	5.5	0.0	0.2
algae	2.6	7.6	2.3	9.9	7.0	2.7	2.3	3.5	16.0
foraminifera	0.3	0.0	0.0	0.1	1.4	0.3	1.0	1.6	0.9
ooids/peloids/ intraclasts	5.3	2.2	11.5	4.7	4.3	13.4	7.6	1.5	2.6
micritic matrix	52.3	26.6	31.7	36.0	42.3	47.2	45.3	77.1	39.0
cement	14.1	6.9	24.2	13.1	11.3	13.6	13.0	14.8	8.0
detrital quartz	4.4	1.6	1.6	0.2	0.3	0.7	0.1	0.1	3.0
porosity	1.5	0.0	2.7	0.0	4.6	0.3	1.9	4.7	4.0
Total percentage	100.0	100.0	100.0	100.0	100.0	100.0	100.0	100.0	100.0

(A)

Samples	30/4	27/9	3/11
Monocrystalline Quartz	32.8	48.6	52.4
Polycrystalline Quartz	20.3	8.2	10.2
Feldspar	14.3	19.1	6.4
Mica	1.8	5.6	2.6
Clay	15.3	8.8	12.2
Chert	8.7	3.1	12.2
Cement (excluding silica overgroths)	6.5	5.6	3.4
Accessory minerals	0.3	1.0	0.6
Porosity	5.6	3.1	7.8
Total percentage	100.0	100.0	100.0

(B)

Table 3-1
Composition of the Kambe biomicrite facies (A) and the Mazeras sandstones (B). The numbers indicate percentages of the various components. The total percentages do not include porosity (the porosity channel was isolated during point-counting). The total number of points counted for each sample was 1000. In (A), samples 26/2, 26/4, 26/6, 27/4, 27/6, 3/1, 3/6 and 3/10 are packstones while 3/7 is a wackestone on the Dunham (1962) scheme. In (B), sample 27/9 is a subarkose, 30/4 is a lithic arkose and 3/10 a qurtzarenite on the Folk (1974) scheme.

calcite cement overgrowths around them in optical continuity. The echinoderm grains have undergone micritization around their edges. Evidence of boring is better preserved in the longitudinal sections of spines.

Brachiopod shells occur as whole shells, broken shell fragments and occasionally spines. Some of the fragments measure up to 8mm in length and show characteristic foliated wall structure and, in some, a two-walled structure where the calcitic part is preserved intact while the other (probably aragonitic originally) has been recrystallized. Both articulate and inarticulate brachiopods are present and the shell walls show endopunctate, pseudopunctate and impunctate structure. The brachiopod spines, which are rarely present, show a hollow structure with concentric calcitic fibres. The shells are occasionally coated on the outside, leaving them with a thin micrite envelope. Some of the brachiopod shells are broken and cut by later-stage fractures filled by calcite spar cement. Bivalves, where present, are recognized only by their general shape as they were originally aragonitic and have since recrystallized into calcite. There is good preservation of the structure by thin micrite envelopes that surround the entire grain. Some of the bivalve casts are up to 5mm in length, are broken and transected by later fracture-filling cement. This helps to differentiate between grains of bioclastic origin from sparry calcite resulting from aggrading neomorphism. Enclosed in the micrite envelopes is

a coarsely crystalline (4 mm plus), mainly equant spar.

Gastropods were formerly aragonitics and appear as well preserved transverse sections encased in thin micrite walls. Their inner chambers are filled with sparry calcite which may be primary cement precipitated in dissolution voids created by leaching of unstable aragonite or may be neomorphic produced by the inversion of aragonite to calcite. The transverse sections are about 1mm in diameter.

Calcareous sponges are common and show a distinctive meandering canal structure with well-preserved wavy, thin calcite crystals with indistinct crystal boundaries. The sponges are up to 4mm and their internal structure is filled partly by micrite and neomorphic spar with micrite patches. The micritic material is probably internal (geopetal) sediment or vadose silt deposited in primary voids within the calcareous sponge structure.

Ostracodes are rare occurring as whole shells and fragments. The shells are very thin and, where complete, show characteristic shell-overlap structure.

Algae: encrusting algae occur associated with the corals. These are probably coralline algae which encrust onto the coral forming laminated micritic crusts around them.

Foraminifera are rare, and are mostly *miliolids* with well preserved micritic wall structures and spar-filled chambers. Local *peneloplids* are also present.

Ooids are a rare occurrence in the biomicrites. They are up to 0.5mm in diameter, with quartz nuclei and, occasionally with micritic nuclei. The internal structure is a poorly preserved concentric lamination which has almost been completely obliterated by intense ooid micritization.

Peloids commonly occur as regular spheroids to ovoid shapes composed of well-rounded micritic masses with no distinguishable internal structure. They are up to 3mm in diameter and in some cases they occur within the micritic matrix of intraclasts.

Intraclasts are rare and occur as aggregate structures composed of peloidal micrite masses in a micritic matrix of evidently redeposited grains. They occasionally consist of angular to subangular broken bioclasts and authigenic quartz grains in micrite matrix.

3.2.1.2 *Terrigenous components*

Monocrystalline quartz, with a range in grain size from 0.15mm (fine sand) to a maximum of 1.5mm (very coarse sand) constitutes the major terrigenous component of the biomicrites. Some quartz occurs as free grains while some forms the nuclei of ooids. The grains are euhedral with straight edges, a narrow dust rim and authigenic overgrowths. The dust rims probably contain remnants of micritic carbonate material.

Matrix is microcrystalline carbonate material (micrite).

The samples analysed by point-counting between 26.6% and 77.1% matrix.

3.2.1.3 *Orthochemical components*

Neomorphic spar (pseudospar) occurs mainly within the internal structure of corals as non-ferroan calcite. Crystals range in size from micron (microspar) to 1.5mm and are patchily distributed relics of micrite and bioclastic debris.

Authigenic quartz occurs mainly as overgrowths on detrital quartz grains both within ooids (as nuclei) and in the micritic matrix. Abundance of detrital quartz ranges from 0.1% to 4.4% in the point-counted samples.

Dolomite is rare, and was seen only in one sample where it occurs as interlocked rhombohedra with indistinct zoning. The dolomite crystals are randomly distributed, measure up to 0.2mm and are most likely replacive in origin (after calcite).

3.2.1.4 *Cements*

The percentage of cement material ranges from 6.9% to 24.2% in the biomicrites examined (Table 3-1A).

Syntaxial rim cements of calcite have grown in optical continuity with echinoderm fragments.

Equant spar: non-ferroan calcite spar occurs in drusy

mosaics in which the crystal sizes increase away from substrate i.e. towards center of pores.

Isopachous rim cements: non-ferroan fine spar cements have formed around the edges of grains which are followed by a coarser, later-generation void filling spar.

Late-stage ferroan calcite cement forms as a fracture-filling cement that cuts across earlier cements and bioclastic grains and is thus interpreted as a late-stage precipitation.

Bladed crust cement is rare, but was observed to be precipitated on the surface of a bioclast and growing perpendicular to it.

3.2.1.5 *Porosity*

In almost all the biomicrites, porosity is either completely obliterated by cementation or where present, it is only in trace amounts of intraparticle and intercrystalline porosity ranging from zero to a maximum of 4.7% (Table 3-1A). Examination of the samples under the SEM shows the presence of microporosity in the micritic matrix. This, however, is unlikely to contribute to the overall rock permeability as the pore spaces are extremely small in size.

3.2.2 Biopelmicrite Facies

These are composed mainly of peloids and bioclastic grains in a micrite matrix, with relatively minor amounts of sparry calcite cement. Peloids constitute between 19.8 and

33.3%, cement 17.4 to 18.4% bioclasts 14.4 to 14.8% and micrite 14.4 to 14.8% of the samples examined (Table 3-2A).

3.2.2.1 *Allochemical components*

Foraminifera are very abundant and include both the thick calcite-walled and the micrite-walled *miliolids* with internal chambers filled with calcite spar. The *miliolids* occur in a wide variety of shapes dependent on the thin section cutting position. Occasional uniserial foraminifera are also present.

Brachiopods are not very abundant and both articulate and inarticulate varieties are present. They occur as single fragments in a sample and in most cases they are partially micritized.

Calcareous Sponges are present as traces of fragments which occur as coated bioclastic grains in peloids.

Ostracode valves are very rare and occur as thin curved shells.

Gastropod casts of transverse sections occur only as a minor component, with their structure outlined by thin micrite envelopes enclosing coarse calcite spar.

Echinoderms: mainly transverse and longitudinal sections of spines are present in most biopelmicrite samples. Most of them show a certain degree of micritization ranging from almost non-micritized to almost completely micritized grains. The almost completely micritized ones have a thick coat of

micrite surrounding the whole grain.

Bivalves are in the biopelmicrites and occur as micrite envelopes, mostly thin-walled with interiors filled with calcite spar.

Peloids are a major constituent grain of the biopelmicrites. They comprise 19.8 and 33.3% in the samples point-counted. These are generally made up of small micritic grains and may or may not be pelletal in origin. They are mostly circular to ovoid in shape, well-rounded and well-sorted, the smallest ones are 0.05mm in diameter with occasional large ones up to 1.2mm in diameter. The larger ones often contain bioclastic and occasionally terrigenous debris. They are totally lacking in internal structure and occur as darker coloured micritic masses within lighter micrite matrix. The peloids could be of various origins such as micritization of skeletal and oolitic grains, biological (including faecal), aggregation of lime mud and mechanical erosion of carbonate mud or lithified mudstone (Enos,1983). In areas of slow deposition it is difficult to determine the origin of peloids due to the rounding effects of grain micritization and hardening resulting from intraparticle cementation.

Ooids are rare and where present, they are completely micritized resulting in total destruction of internal structure. These are identified as ooids by their almost perfect spheroidal shape and presence of quartz grains as nuclei.

Matrix: the biopelmicrites are matrix-supported in microcrystalline carbonate mud, micrite.

3.2.2.2 *Terrigenous grains*

Quartz is the only detrital component. Most grains range in size from 0.03-0.1mm (medium silt to very fine sand) and show a bimodal size distribution. The coarser grains are subrounded while the finer ones are subangular. Most grains show straight to slightly undulose extinction and are inclusion-rich in the outer edges marking authigenic overgrowths which give the crystals overall euhedral shapes. The inclusions are probably remnants of micritic material through which the overgrowths have grown.

3.2.2.3 *Cements*

Isopachous rim cements of non-ferroan calcite occur as interparticle cements on grain margins. The inner interparticle pore spaces are filled with coarser ferroan and non-ferroan calcite spar in drusy mosaics.

Dolomite is present as euhedral, probably replacive, rhombohedral crystals, irregularly distributed in patches in most of the thin sections. Neomorphic spar with floating peloidal grains occurs within the micrite matrix. Syntaxial cements are common, around echinoderm fragments. Veins which cut across grains and early cement are filled with a later-generation ferroan calcite cement. Yellowish-brown clay

material is present in minor quantities especially in association with the terrigenous quartz grains.

3.2.3 Biosparite Facies

These have bioclastic grains and sparry calcite cement as the major rock constituents, with up to 35.5% fine grained matrix. They are mainly packstones and grainstones depending on the amount of carbonate matrix present; both types are grain-supported but while the packstones contain a certain amount of carbonate mud matrix, the grainstones are composed entirely of bioclastic grains in sparry calcite cement. Bioclastic grains constitute between 7.5 and 13.4% while cement abundance is in the range of 43.5 to 62.4% in the measured samples (Table 3-2A).

3.2.3.1 *Allochemical components*

The common allochemical constituents are brachiopods, echinoderms, foraminifera, corals and bivalves; while the less common ones include calcispheres, ooids, peloids, gastropods, calcareous sponges and ostracodes. Brachiopod shells are abundant as whole and broken fragments up to 3mm long. Echinoderm fragments are very common in longitudinal section. Most grains have undergone extensive micritization resulting in thick micrite walls and some peloidal grains may have been produced in this way i.e. by complete micritization of bioclastic grains. There are some perfectly shaped transverse

sections of gastropods showing structure preserved in micrite envelopes. Different sections of bivalves preserved in micrite envelopes are common, with internal structure now filled up with calcite spar and micritic material. Peloids occur mainly as small spheroidal grains with more concentrated dark coloured muddy material in a lighter coloured microcrystalline carbonate. *Miliolid* and *peneloplid* foraminifera are present. Where corals are present they have been recrystallized into neomorphic spar and they occur in association with encrusting algae. Ooids are only rarely present, as almost completely micritized grains with little internal structure preserved. Calcareous sponges are occasionally present, displaying a characteristic meandering canal structure.

3.2.3.2 *Orthochemical components*

Radioaxial fibrous calcite cement is common in the biosparites. The crystals occur as a non-ferroan calcite with undulose extinction and elongate crystal shape, extending into an extremely coarsely crystalline ferroan calcite with equant crystals. The radiaxial fibrous calcite crystals have curved twin lamellae which continue across crystal boundaries into adjacent crystals. The concave surfaces of the curved twin-lamellae face away from the substrate on which the crystals were precipitated. The crystals are made up of divergent subcrystals each of which has a slightly different extinction position giving the crystals undulose extinction. The extinction shadow swings

towards the direction of rotation of the microscope stage under crossed polars.

Neomorphic spar is frequently associated with recrystallized grains, especially corals and bivalves. Syntaxial cements are common around echinoderm fragments. Isopachous rim cements precipitated around the grain margins are commonly followed by a later generation of poikilotopic cement that completely fills up the intergranular pore space. Fractures are commonly filled with coarse non-ferroan spar. Brown-black staining (probably organic matter) is common especially along fractures and cement-substrate boundaries. Dolomite occurs as small rhombic crystals in association with the ferroan calcite cement.

3.2.4 Biopelsparite Facies

This facies is dominated by peloids and a variety of bioclasts cemented together by sparry calcite and minor amounts of microcrystalline carbonate matrix. They are classified as packstones (Dunham, 1962) and are grain-supported but contain some micritic material. The amount of cement in the samples varies between 24.2 and 44.7% (Table 3-2A).

3.2.4.1 *Allochemical components*

Peloids are the major allochemical constituent (11.7 to 41.4% abundance (Table 3-2A) and have size ranges from 0.1mm

	Biopelsparites			Oosparites			Biopelmicrites		Biosparites		
Samples	26/5	3/8	3/9	27/2	30/8	30/7	30/10	4/13	27/5	3/2	3/5
Gastropod/ bivalves	1.2	6.1	1.2	0.4	2.0	0.9	0.3	4.8	2.0	2.8	3.0
echinoderm	3.8	6.7	0.5	0.5	0.0	0.8	0.0	1.4	1.4	1.2	3.0
foraminifera	0.4	0.0	1.5	0.9	0.0	0.0	12.2	7.4	0.6	0.1	3.4
brachiopod	1.0	4.5	0.5	0.4	0.1	1.7	0.6	1.1	2.4	4.5	4.0
coral	9.0	0.4	1.2	0.0	0.0	0.0	0.0	0.0	0.0	0.0	0.0
calcareous sponge	6.0	0.0	0.0	0.0	0.0	0.0	0.0	0.0	0.1	0.0	0.0
ostracode	0.0	0.0	0.0	0.0	0.0	0.0	1.3	0.1	0.0	0.0	0.0
calcispheres	0.0	0.0	0.0	0.0	0.0	0.0	0.0	0.0	1.0	0.0	0.0
ooids	0.0	0.0	0.0	46.6	23.8	30.2	0.2	0.0	3.5	6.5	5.0
peloids	33.0	34.4	41.4	6.5	19.0	12.4	19.8	33.3	10.0	4.0	5.6
intraclasts	0.0	0.0	0.0	2.6	4.5	1.1	0.0	0.0	0.0	0.0	0.0
quartz	2.8	0.0	3.9	9.2	16.3	18.6	4.9	7.7	0.0	0.0	0.0
feldspar	0.0	0.0	0.2	0.7	2.9	2.3	0.0	0.0	0.0	0.0	0.0
cement	27.0	33.8	24.2	28.6	29.9	29.1	18.4	17.4	43.5	62.4	53.3
micrite	15.8	14.1	25.4	3.6	1.5	2.1	42.3	26.8	35.5	18.5	21.7
porosity	0.4	0.4	0.7	0.5	0.0	0.8	0.4	0.6	1.3	2.1	4.7
Total percentage	100.0	100.0	100.0	100.0	100.0	100.0	100.0	100.0	100.0	100.0	100.0

(A)

Samples	30/1	30/2	30/3
Algae	31.4	30.4	44.2
Foraminifera	17.5	30.0	12.6
Calcite cement	27.2	23.0	22.4
Micrite	16.4	13.6	10.4
Detrital quartz	7.5	3.0	10.4
Porosity	16.4	24.2	15.7
Total percentage	100.0	100.0	100.0

(B)

Table 3-2
Composition percentages for the various components for (A) some of the facies of the Kambe Formation and (B) the Freretown limestones. The figures are based on 1000 point counts for each thin section. The total percentages do not include porosity (the porosity channel was isolated during point-counting). Samples 26/5, 3/9, 27/2, 30/8, 30/7, 3/5, 30/1, 30/2 and 30/3 are grainstones; 3/8, 30/10, 4/13, 27/5 and 3/2 are packstones on the Dunham (1962) classification.

to 2.5mm, and rarely up to 6mm. The larger peloids are probably micritized bioclastic grains while the smaller ones are most likely to be pelletal. In some samples there is a distinct bimodal size distribution with smaller (pelletal) peloids being 0.15mm and larger ones 2.5mm in diameter. Most peloids are well-rounded spheroidal grains with no internal structure and commonly contain crystals of euhedral authigenic quartz. Some peloids show straight to sutured grain contacts indicating some degree of compaction and pressure-solution. Some peloidal grains may be the product of ooid micritization.

Bioclasts include bivalves in micrite envelopes enclosing neomorphic spar, echinoderm fragments at various degrees of micritization, foraminifera with well-preserved calcitic walls and micrite infilling internal structure, brachiopod shell fragments and occasional corals preserved as neomorphic spar.

3.2.4.2 *Detrital Components*

Quartz grains average 0.1mm (very fine sand) with inclusion-rich edges marking authigenic overgrowths. Coarser grains of mono- and poly-crystalline quartz are present in some samples. Some of these show undulose extinction and dust rims that mark overgrowths on detrital quartz nuclei. Some of the authigenic overgrowths transect older cement and allochemical grains (peloids and bioclasts) indicating late diagenetic precipitation of silica around detrital quartz.

Feldspar is present in trace amounts, with albite

twinning (plagioclase feldspar).

3.2.4.3 *Cements*

Finely crystalline equant ferroan and non-ferroan calcite spar cement around margins of grains with a more coarsely crystalline void-filling cement which becomes more ferroan towards the center of the pores is the common cement type. Syntaxial cements are present around echinoderm fragments. Cement also occurs as bladed, inclusion-rich calcite spar precipitated on bioclastic and micritic substrate.

Dolomite occurs as randomly distributed euhedral rhombs, 0.05-0.15mm in size, inclusion-rich with cloudy appearance and associated with dark brown to black, probably ferrous, mineralization. Saddle dolomite occurs in one sample (26/3) as very coarsely crystalline cement with curved crystal faces and sweeping extinction under cross-polarized light. It contains abundant inclusions which give it a cloudy appearance.

3.2.5 Oosparite Facies

All the oosparites of the Kambe Formation are, with the exception of one sample, grainstones composed of allochemical grains (mainly ooids and bioclasts) and orthochemical sparry calcite cement. Point-counting data from three samples shows compositions of 23.8 to 46.6% ooids, 6.5 to 19% peloids, 28.6 to 29.9% cement and only 1.5 to 3.6% micrite (Table 3-2A).

3.2.5.1 *Allochemical components*

Ooids, which are the major component of the oosparites, show both radial and concentric structure at varying degrees of preservation ranging from well-preserved to almost completely micritized. They range in size from 0.4mm to 2mm with an average diameter of 0.6mm. They are generally well-sorted. The ooids have both quartz and micrite as the common nuclei particles with occasional echinoderm and feldspar grains as nuclei. The quartz nuclei commonly have authigenic overgrowths around detrital grains. This indicates replacement of the micritic material of the ooids by silica precipitation around detrital quartz and in some ooids the replacement is almost total, leaving an ooid- shaped monocrystalline quartz grain with a single layer of oolitic coating. These could on the other hand be superficial oolites which have a characteristic large nucleus and a thin oolitic coating. The shapes of the ooids are mostly spheroidal, occasionally ovoid. A few spalled laminations are present in most of the slides which are indicative of cementation after slight compaction which resulted in the concentric oolitic laminations being sheared from the nucleus. Most ooids are not affected by the compaction. Compaction has resulted in straight grain-to-grain contacts, occasionally tending towards sutured contacts (indicating a very slight amount of pressure-solution along compactional grain contacts).

Peloids are generally large, up to 5mm in diameter, ellipsoidal micrite masses, very well-rounded with smooth even edges and no recognizable internal structure. Some are probably micritized ooids, bioclasts and aggregate grains. Some peloids contain nuclei of echinoderm fragments and are probably products of micritization of the bioclasts i.e. they are coated bioclasts. Many peloids contain small crystals of authigenic quartz and patches of finely crystalline calcite spar of possible neomorphic origin (produced by aggrading neomorphism where micrite recrystallizes into coarser crystals of calcite).

Intraclasts are large grains up to 7mm in diameter and are composed of ooids and peloids in a micritic matrix. These are reworked grains as evidenced by their well-rounded texture and their truncation of cements and other older grains. The ooids in the intraclasts show poor structural preservation and are almost completely micritized.

Other components are bioclastic grains and rare chert and quartz grains.

3.2.5.2 *Authigenic components*

Quartz is very abundant comprising between 9.2 and 18.6% in the samples point-counted. It occurs mainly as subhedral crystals of monocrystalline quartz, very coarse grained (up to 1.8mm) with abundant inclusions and probably growing around detrital grains. Most of the grains show slightly undulose

extinction. There are minor amounts of polycrystalline quartz.

Feldspar grains are rare but both potassium and plagioclase feldspars are present. They are the same size as the quartz grains and are often corroded.

3.2.5.3 *Cements*

The most common type of cement is an isopachous rim around the ooids. The crystals sometimes form compromise boundaries and are usually overlain by a coarser equant void-filling spar. Most cement is of non-ferroan calcite with occasional ferroan calcite especially at the center of pores.

Syntaxial cement is common in association with echinoderm fragments. Poikilotopic non-ferroan calcite cements are occasionally present in which a single calcite crystal cements together two or more oolitic or other grains. Ferroan calcite is also present as fracture-filling cement as a finely crystalline spar. Table 3-3 shows a petrographic summary for the various facies of the Kambe limestones.

3.2.6 Dolostone Facies

This facies is represented by one single sample (27/10) which is a totally crystalline dolomite rock with no micritic matrix and no bioclastic grains. The dolomite occurs as interlocking crystals with a maximum size of 0.66mm. The crystals are inclusion-rich giving them a cloudy appearance. The rock also shows extensive dark brown, probably iron,

	Biomicrites	Biopelmicrites	Biosparites	Biopelsparites	Oosparites
Samples	26/2,26/4, 26/6,27/4, 27/6,3/1, 3/6,3/7, 3/10.	30/10,4/3,4/4, 4/9,4/10,4/12, 4/13,4/14, 26/3	27/5,3/2, 3/3,3/4, 3/5	26/5,30/9, 3/8,4/5,4/6, 4/7,4/8	27/2,30/6,30/7 30/8,3/9
Allochemical components	**Coral, brachiopod, bivalve, calcareous sponge, algae,** echinoderm, gastropod, ostracod, foraminifera, ooids,peloids, intraclasts	**Foraminifera, brachiopod, echinoderm, peloids** calcareous sponge ostracode, gastropod, bivalve ooids	**Brachiopod, echinoderm, foraminifera coral, bivalve,** calcispheres ooids peloids gastropod calcareous sponge ostracode	**Peloids,** bivalve, echinoderm, foraminifera, brachiopod, coral	**ooids**,peloids, intraclasts, echinoderm, brachiopod, bivalve, foraminifera, coral
Detrital components	Quartz	Quartz	None	Quartz, feldspar	Quartz feldspar
Matrix	Micrite	Micrite	Micrite	Micrite	None
Orthochemical components	Neomorphic spar, authigenic quartz, dolomite, syntaxial, equant, isopachous, bladed, ferroan calcite cements	Neomorphic spar, isopachous rim cements, late-stage ferroan calcite, saddle dolomite traces of clay	Neomorphic spar, radiaxial fibrous calcite, syntaxial rim cement, isopachous cements, dolomite, Fe-calcite	Neomorphic spar, syntaxial rim cements, bladed spar, fine equant spar, dolomite rhombs, Fe-calcite	Isopachous rim cement, late pore filling Fe-calcite, syntaxial and poikilotopic cement
Porosity	Trace interparticle intercrystalline, microporosity in the micrite	trace	trace intercrystalline	trace	trace interparticle, intercrystalline
Depositional environments	Low energy shallow marine	Shallow open shelf Lagoon	High energy Winnowed platform edge	Tidal flat/ restricted shelf lagoon	High energy marine waters on tidal bars or oolite shoals

Table 3-3
Petrographic summary for the various facies of the Kambe Formation. The major components are shown in bold.

Samples	Allochemical constituents	Terrigenous constituents	Matrix	Cement	Porosity
30/1 30/2 30/3	Algae, Foraminifera, brachiopod, echinoderm, ostracode.	Quartz	Micrite	Isopachous rim cements, non-ferroan calcite in intraparticle pore-space	15.7 to 24.2% intrapartical and interpartical porosity
Depositional environment: tidal bars/channels of lagoons (restricted marine environment)					

Table 3-4
Petrographic summary for the Freretown limestones.

mineralization. In some patches, the rock has crystals of non-ferroan calcite, possibly resulting from dedolomitization. No original structures were observed; dolomitization was a complete pervasive replacement of original carbonate rock resulting in total loss of structure. The resulting texture of the dolostone is a xenotopic mosaic of non-planar, closely packed anhedral crystals with irregular intercrystalline boundaries.

While the non-ferroan calcite may be due to dedolomitization, it may also represent calcite in the original carbonate that resisted replacement into dolomite.

Fairly good intercrystalline porosity occurs especially associated with the patches containing the non-ferroan calcite. The pores are up to 1mm in diameter and suggest

solution- enlargement. The porosity may be as a result of intercrystalline pore space created during dolomitization or, more likely, solution pore space resulting from later dissolution of unreplaced calcite to produce large pores.

3.3 FRERETOWN LIMESTONES

Three hand specimens were available from which three thin sections were made and analyzed. Two SEM samples were also analyzed. On the basis of these analyses, a single facies was recognized within the Freretown limestones. They have been classified as biosparites composed mainly of algae and foraminifera (i.e. they are algal-foraminiferal grainstones) in sparry calcite cement. The major allochemical constituents are various types of algae and foraminifera with minor amounts of broken brachiopod shells, echinoderm fragments and rare ostracode valves. Algae and foraminifera constitute between 48.9 and 60.4% of the samples while the bulk of the remainder is taken up by cement (22.4 to 27.2%). Table 3-2B shows composition of the different samples while a petrographic summary for the Freretown limestones is presented in table 3-4.

3.3.1 Allochemical Components

Algae are by far the most abundant and include red algae (probably *Lithophyllum* and *Goniolithon*) with well-preserved characteristic fine cellular structure. A variety

of encrusting algae with regular structure may have contributed in binding the rock together during deposition and the rock could thus be classified as a boundstone on the Dunham (1962) scheme. Phylloid algae and vegetative green algae (*charophytes*) are also present.

Foraminifera are second in abundance after algae and include varieties of *miliolids* with micrite walls and spar-filled pores, calcite-walled foraminifera, biserial and uniserial foraminifera. Most of the foraminiferal grains occur whole and, occasionally, cementation is not complete within the internal chambers of the foraminifera preserving intraparticle porosity.

3.3.2 Terrigenous Components

Quartz occurs as monocrystalline, subrounded grains up to 1.3mm in diameter (very coarse sand) with straight to slightly undulose extinction and is inclusion-rich. The inclusions appear to be micritic material associated with authigenic replacement of carbonate mud by silica which is precipitated onto detrital quartz grains.

3.3.3 Cements

Equant non-ferroan calcite spar precipitated within the intraparticle pores of algae and foraminifera is the most common cement. Intraparticle cement occurs as isopachous rims of crystals growing around the grain margins forming

compromise boundaries with other growths from adjacent grains or bioclastic cavities.

3.3.4 Porosity

There is abundant interparticle and intraparticle porosity especially associated with algal grains. Some of the elongate pores are up to 5mm in long diameter. In some foraminiferal grains, internal cementation is incomplete, leaving a fair amount of intraparticle porosity. The three samples examined have porosities of 15.7, 16.4 and 24.2% (good to very good).

Plate 3-1

Mazeras sandstone (sample 27/11) with fracture porosity in blue and interstitial detrital clay. Micas (muscovite) are abundant and the cement is calcareous in part producing the pink stain of non-ferroan calcite. X100 PPL (plane-polarized light).

Plate 3-2

A Mazeras sandstone quartzarenite showing secondary porosity resulting from feldspar dissolution. Silica cementation is marked by dust faint rims (arrows). Alteration of feldspars has produced pore-lining and pore-bridging clays. X 50PPL

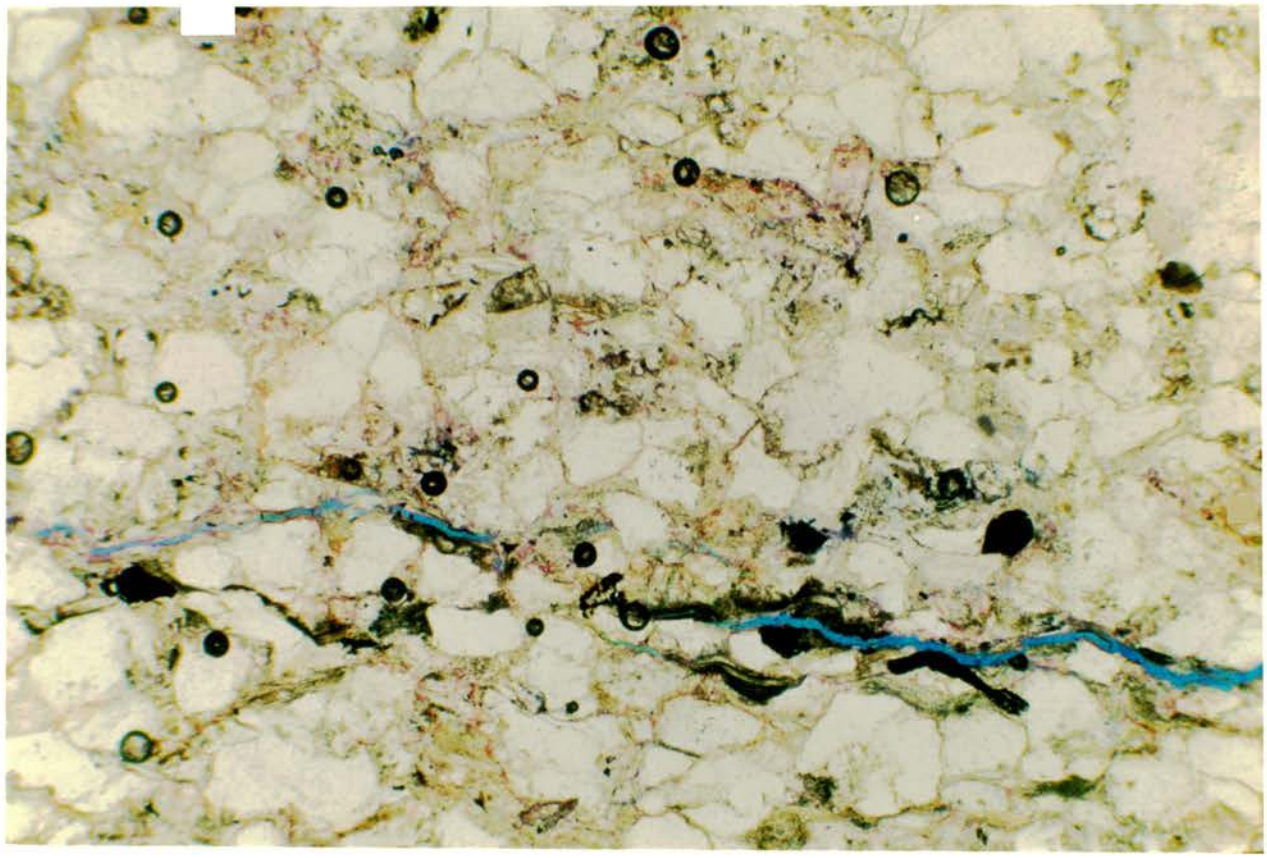

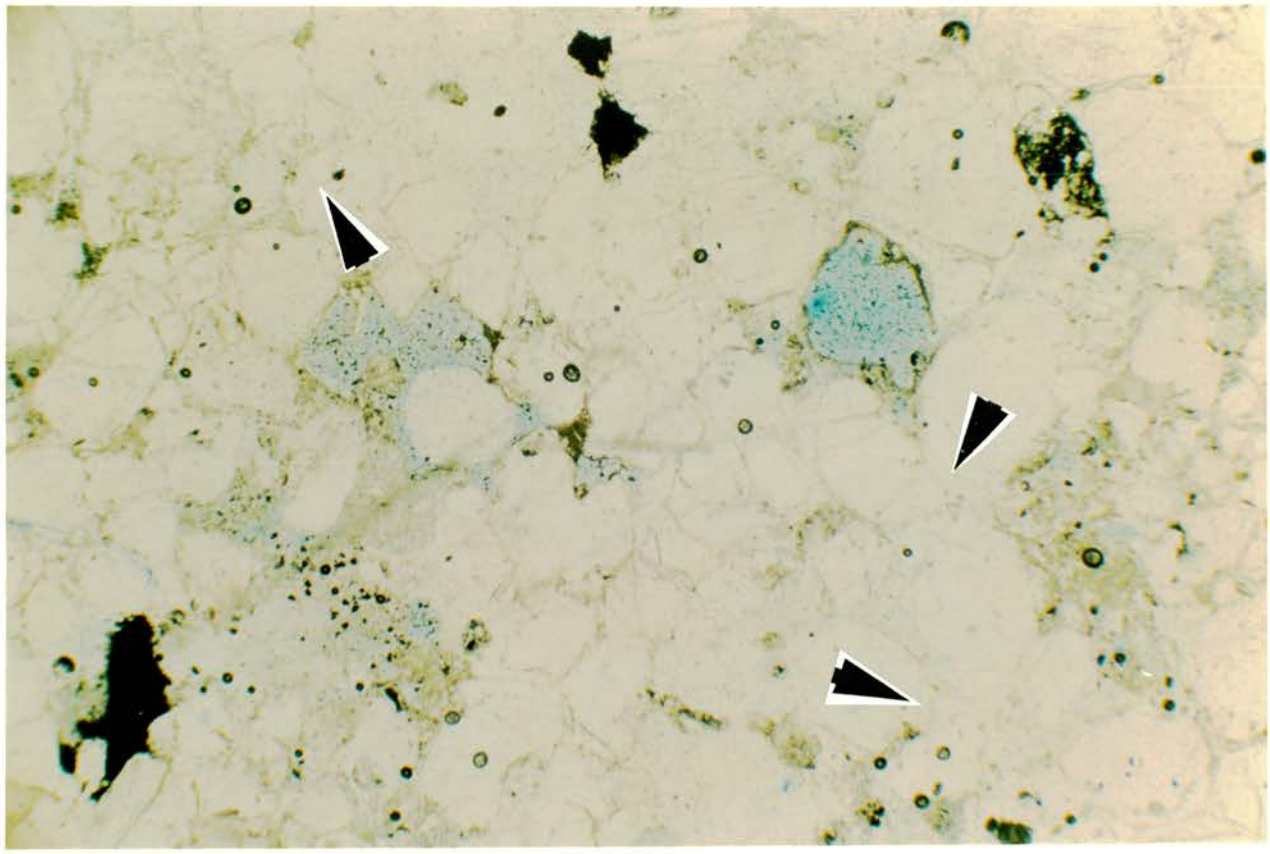

Plate 3-3

Extensive feldspar alteration (e.g. at arrows) in a lithic arkose (sample 30/4) from the Mazeras Formation. Some of the alteration products are micas (probably sericite) producing strong birefringence colours. X 50 X-P (crossed-polars).

Plate 3-4

Same as above under PPL.

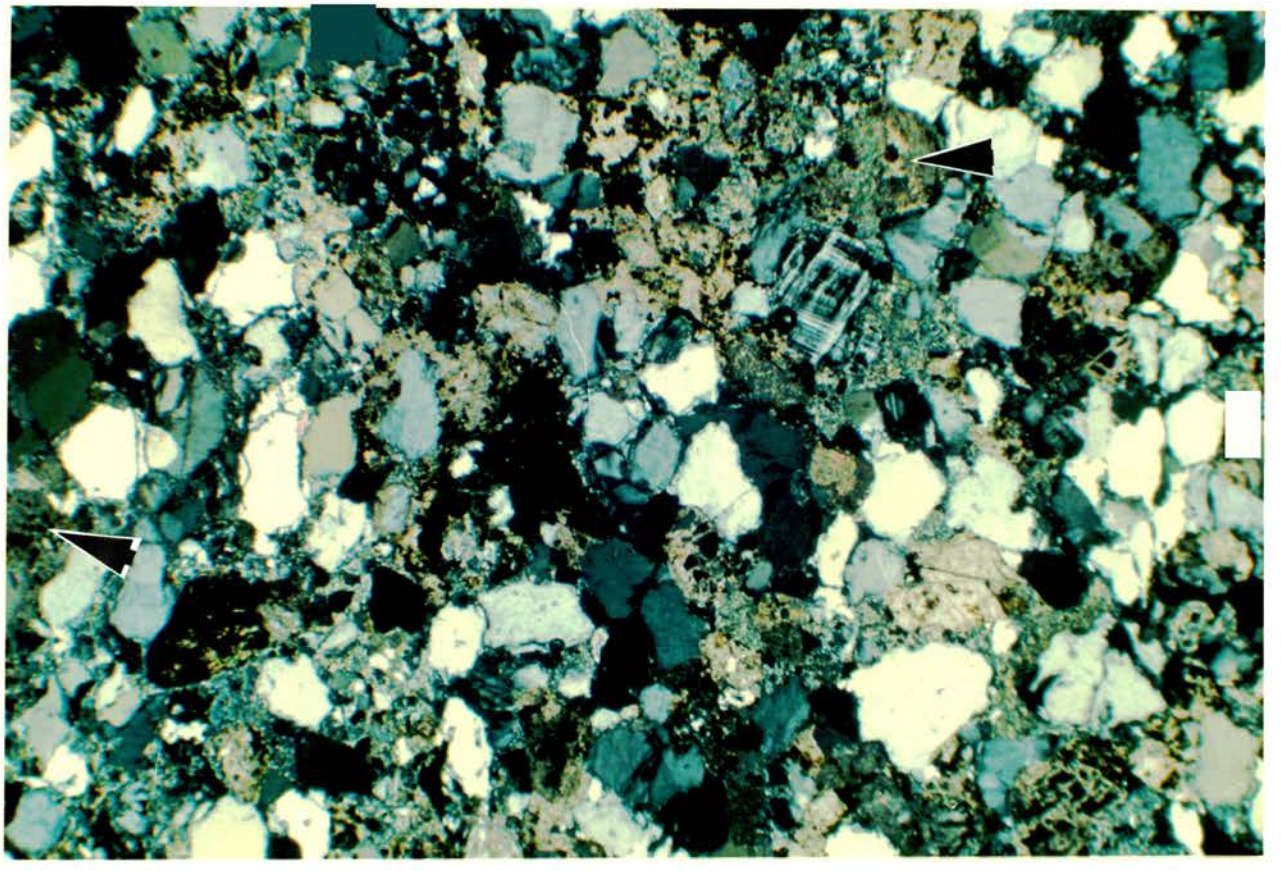

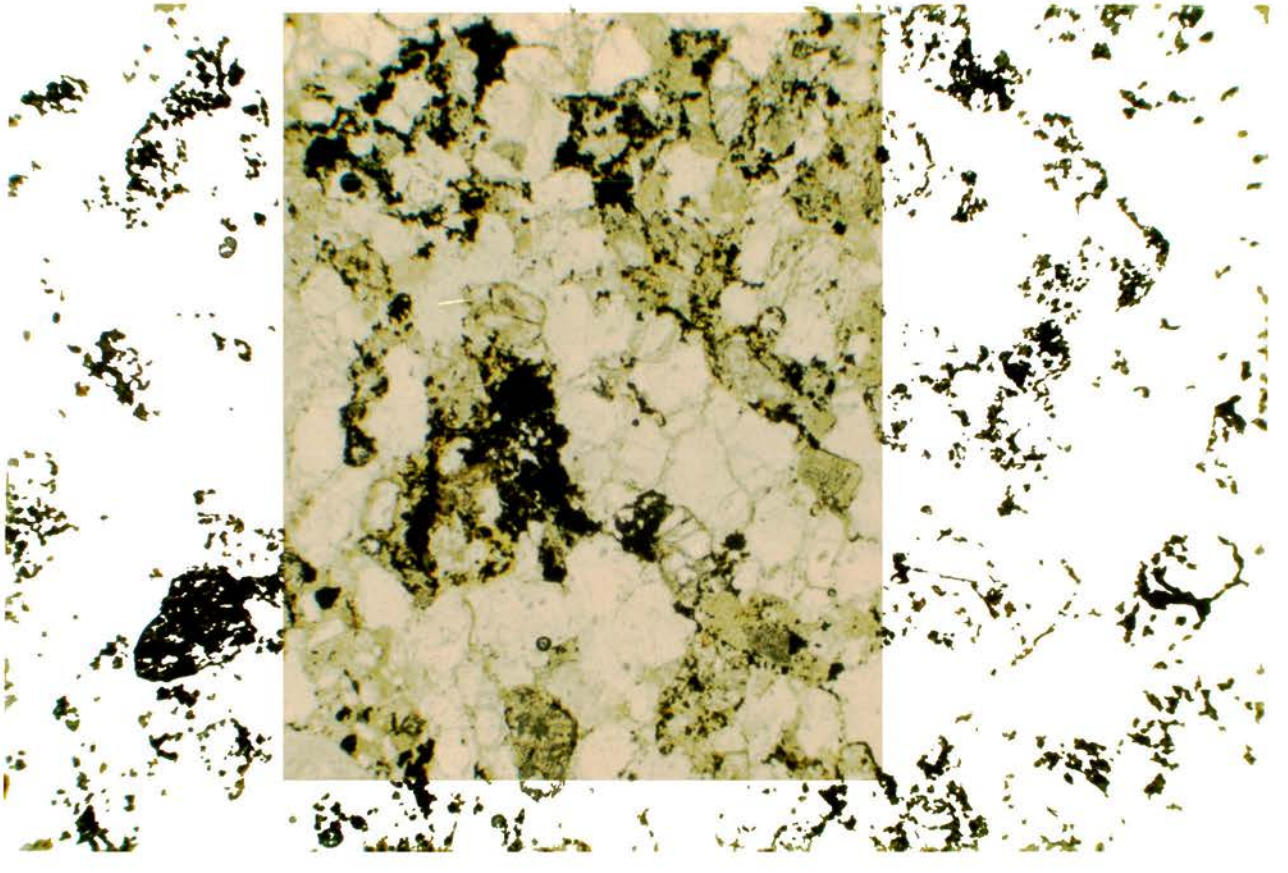

Plate 3-5

A biopelsparite from the Kambe Formation showing a calcareous sponge (arrow) with a well-preserved wall structure (sample 26/5). The hollow space is filled by equant spar, micrite and dark grey peloids. X 50PPL

Plate 3-6

A biomicrite (sample 26/6) containing coral which has undergone neomorphism and stands out against the micritic background. The remnant micritic patches form the identifying coral outline. Note the bivalve with micritized shell and sparry infilling (arrow). Stained section. X 50PPL

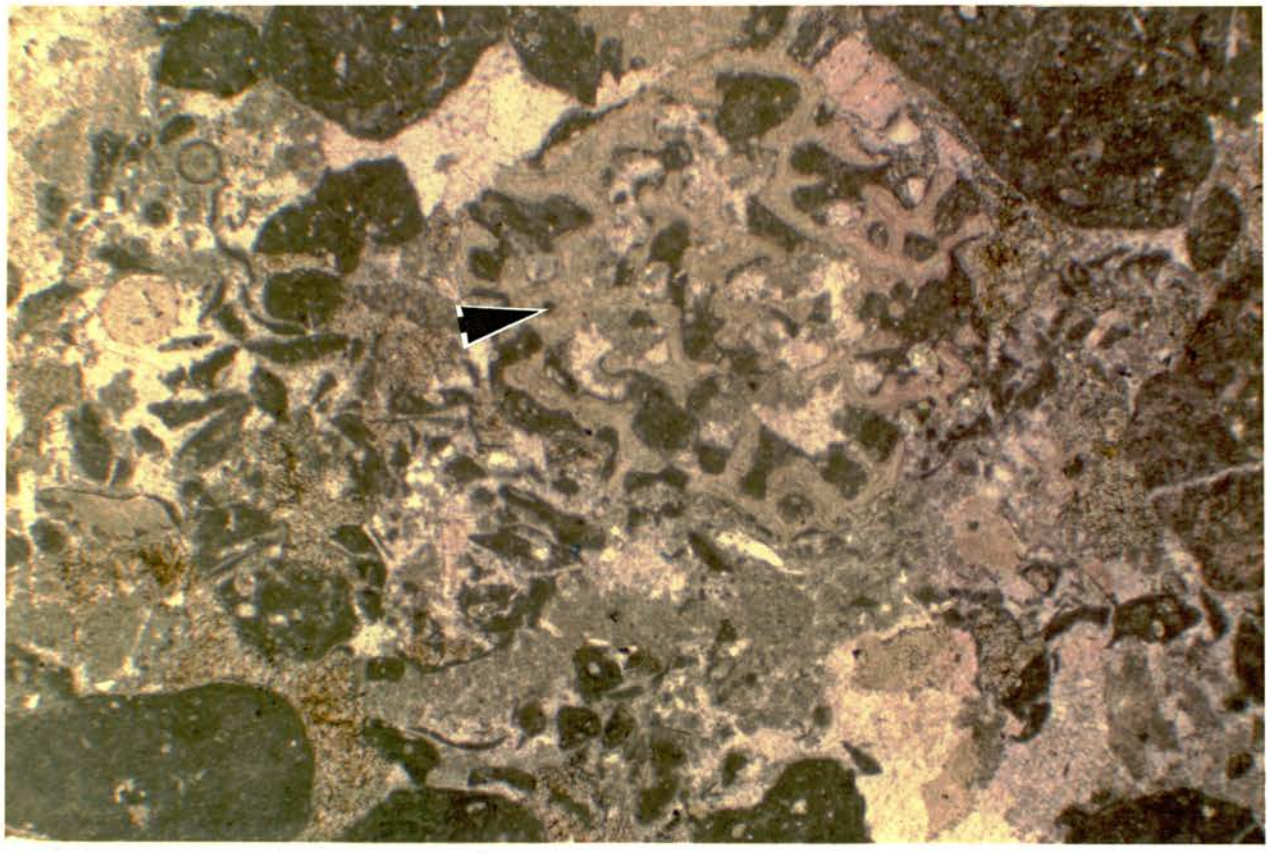

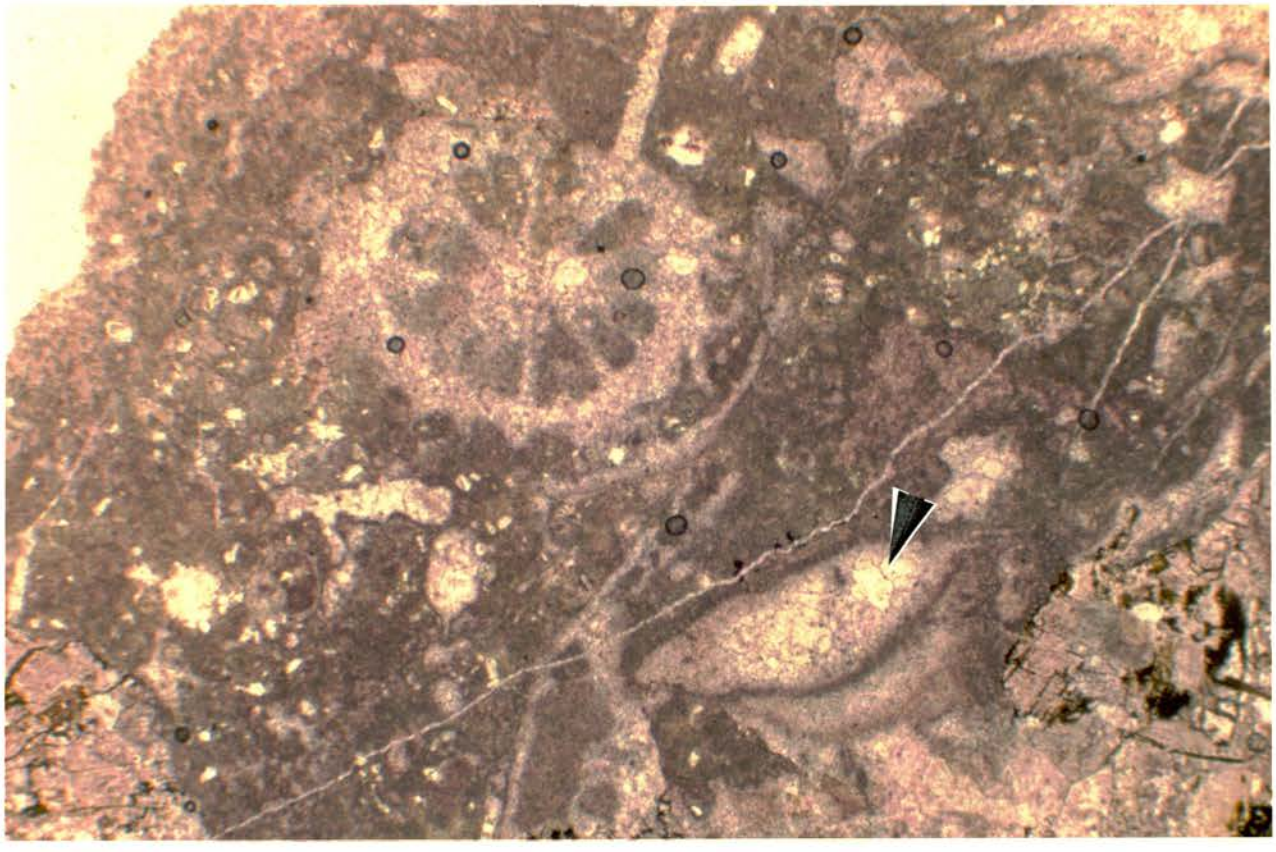

Plate 3-7

Oolitic grainstone (oosparite) showing some degree of compaction such as straight to slightly sutured grain contacts and splayed ooid cortices. The ooids have both detrital quartz and micrite nuclei. Some of the cement is poikilotopic (arrow). X50 X-P

Plate 3-8

Same as above under PPL. Most of the cement is the pink-stained non-ferroan calcite with rare bluish-stained ferroan calcite. Quartz frequently has overgrowths producing euhedral outlines. Stained section. X 50 PPL

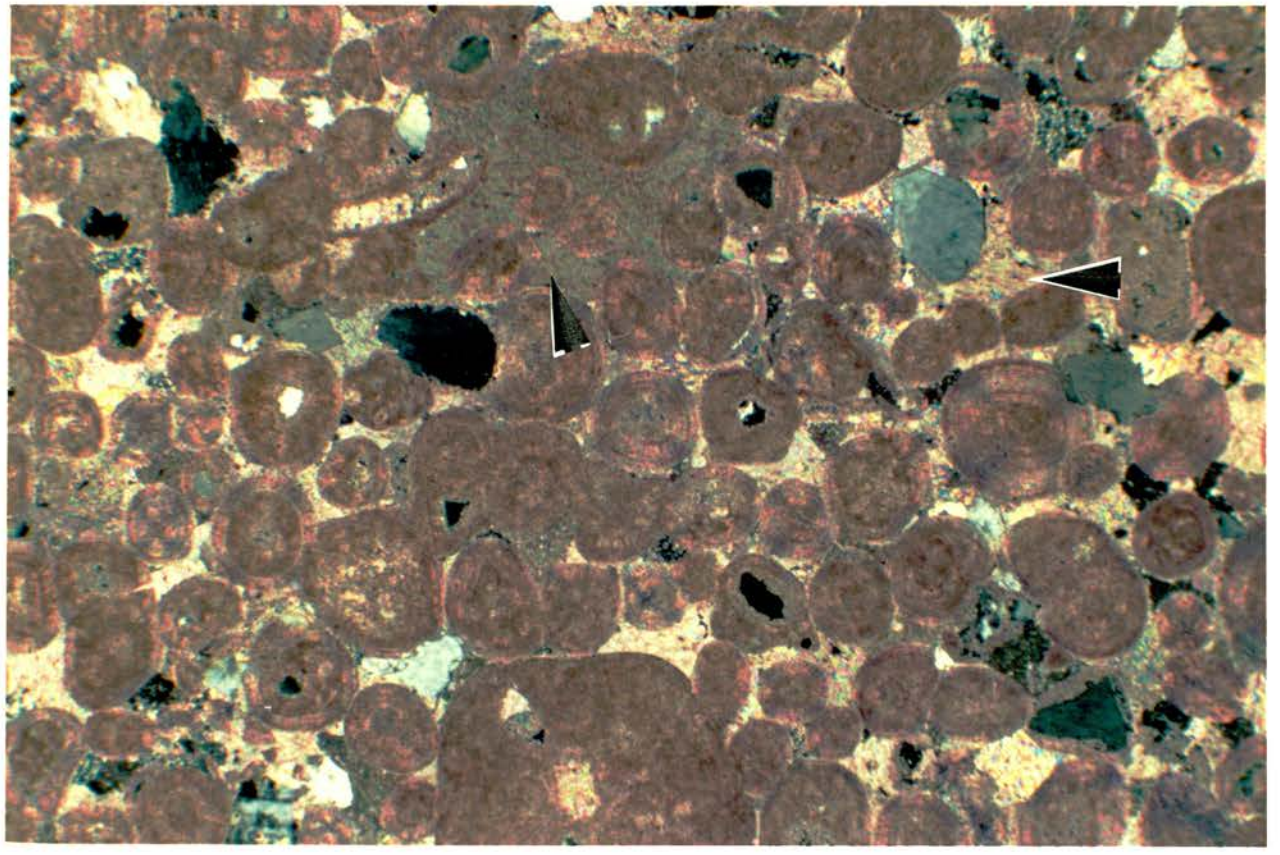

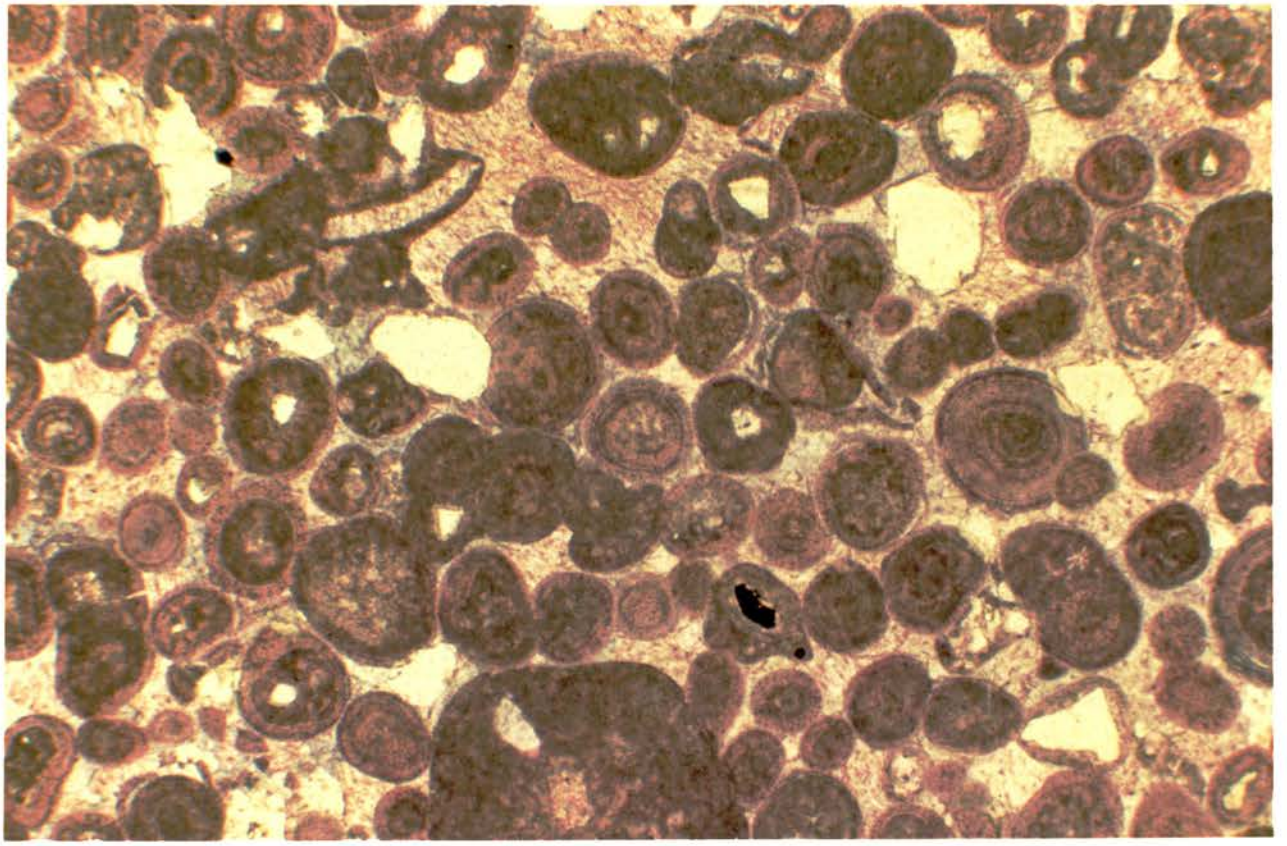

Plate 3-9

A coarsely-crystalline dolosparite. The rock was originally a limestone which has now been almost completely replaced by dolomite producing a xenotopic mosaic of anhedral crystals. This is a stained section and the absence of stain indicates the completeness of replacement. The brown mineral is probably limonite resulting from oxidation of iron. X100 PPL

Plate 3-10

The Freretown Limestone (sample 30/1) showing enlarged dissolution pores in an algal-foraminiferal biosparite (grainstone). X 50 PPL

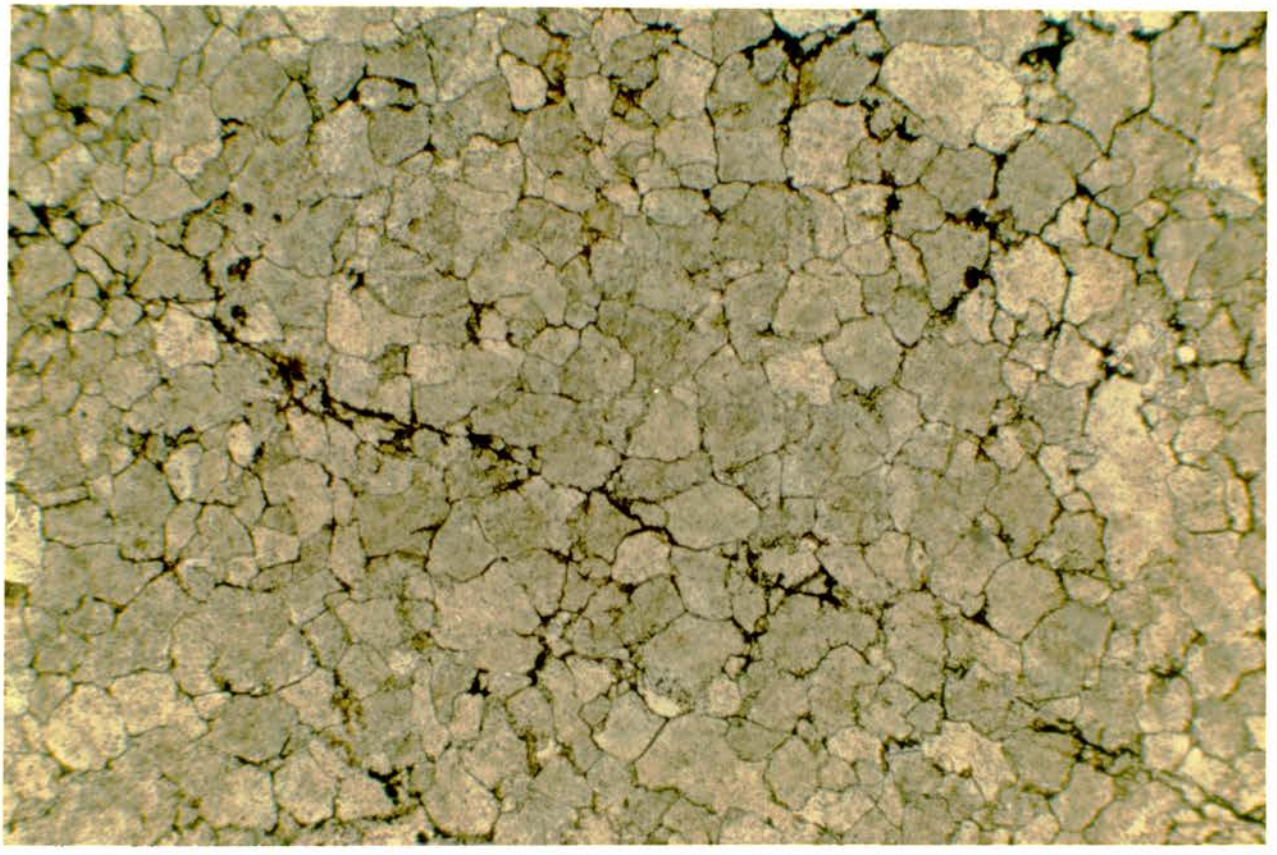

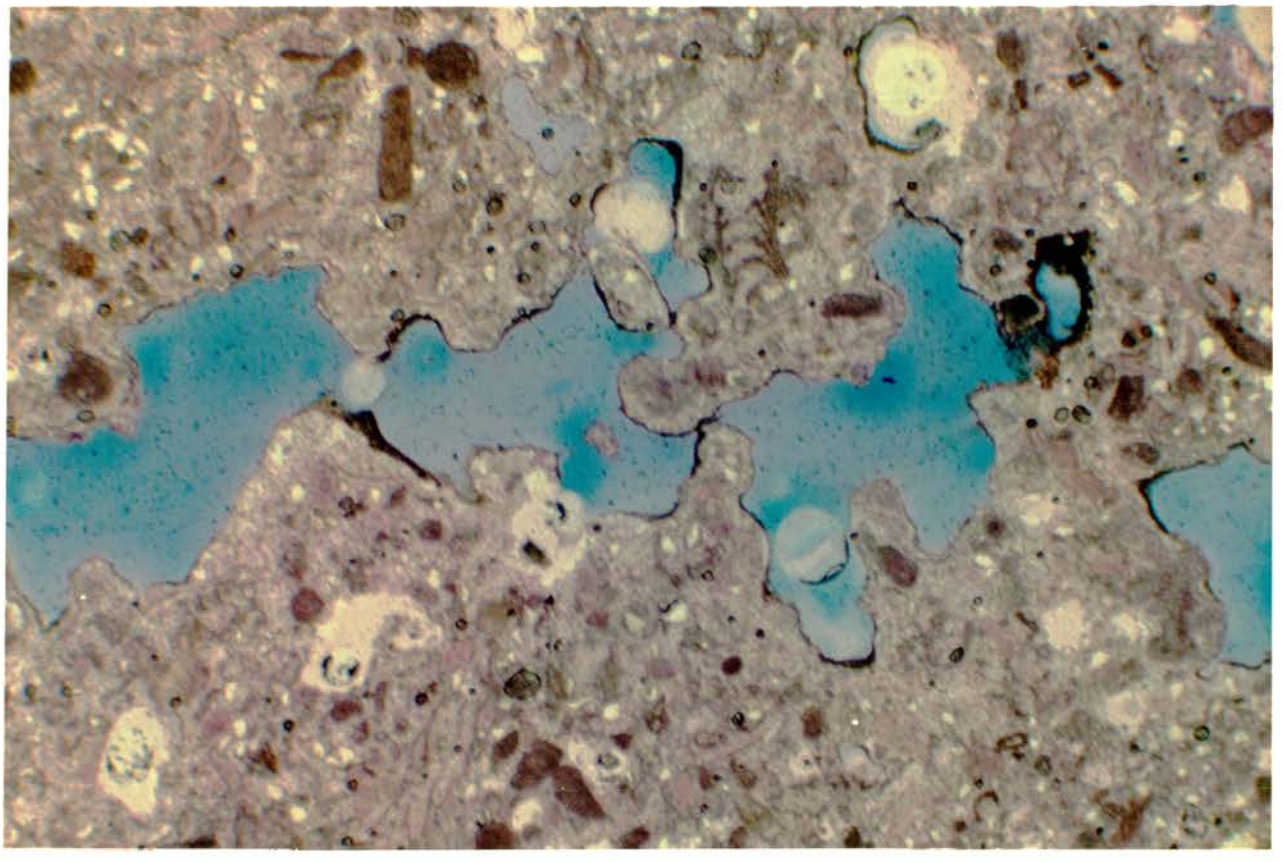

Plate 3-11

A large encrusting alga in an algal-foraminiferal grainstone (sample 30/3) from the Freretown limestones. Note the large, intraparticle, partially-cemented pores within the algal framework. X 30 PPL

Plate 3-12

A biomicrite from the Kambe Formation showing an echinoderm fragment set in a micritic matrix (sample 26/2). Stained section. X50 PPL.

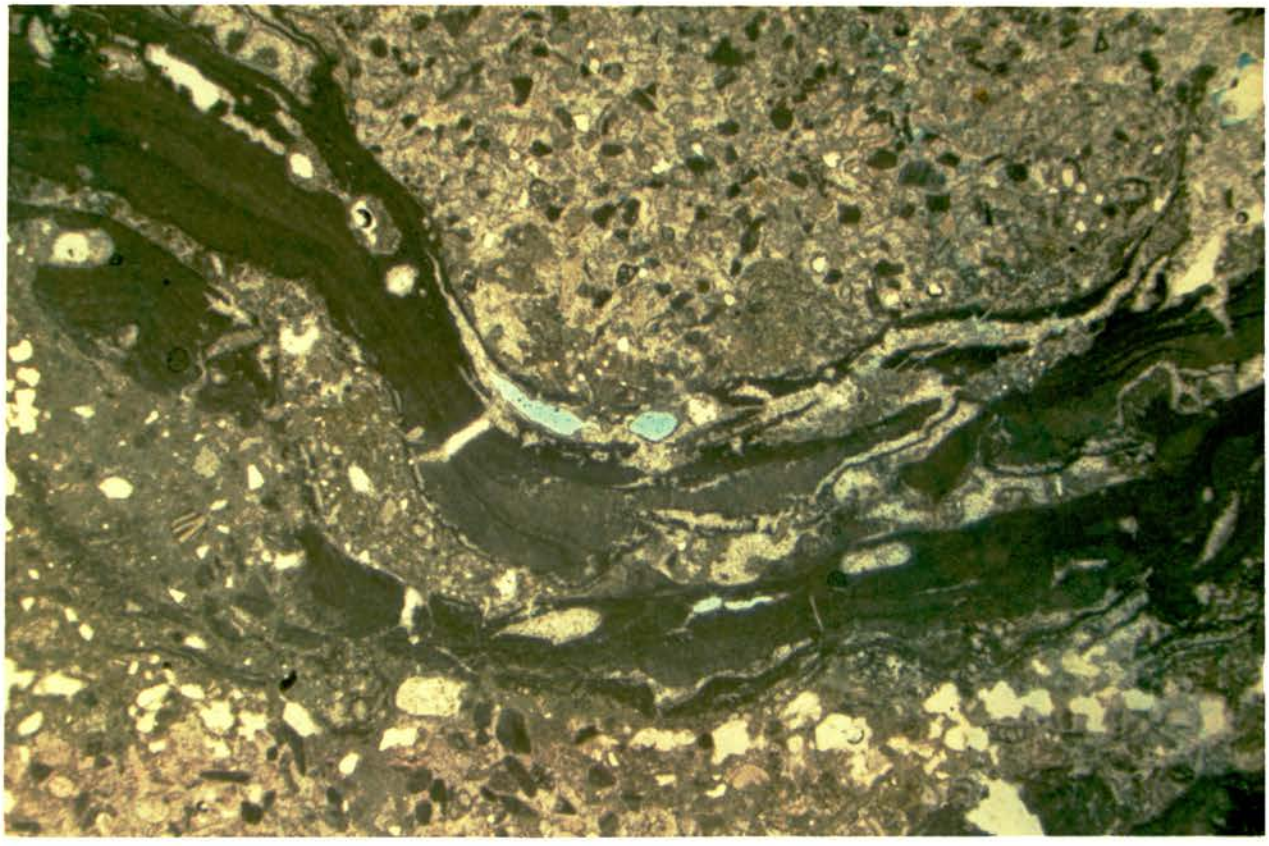

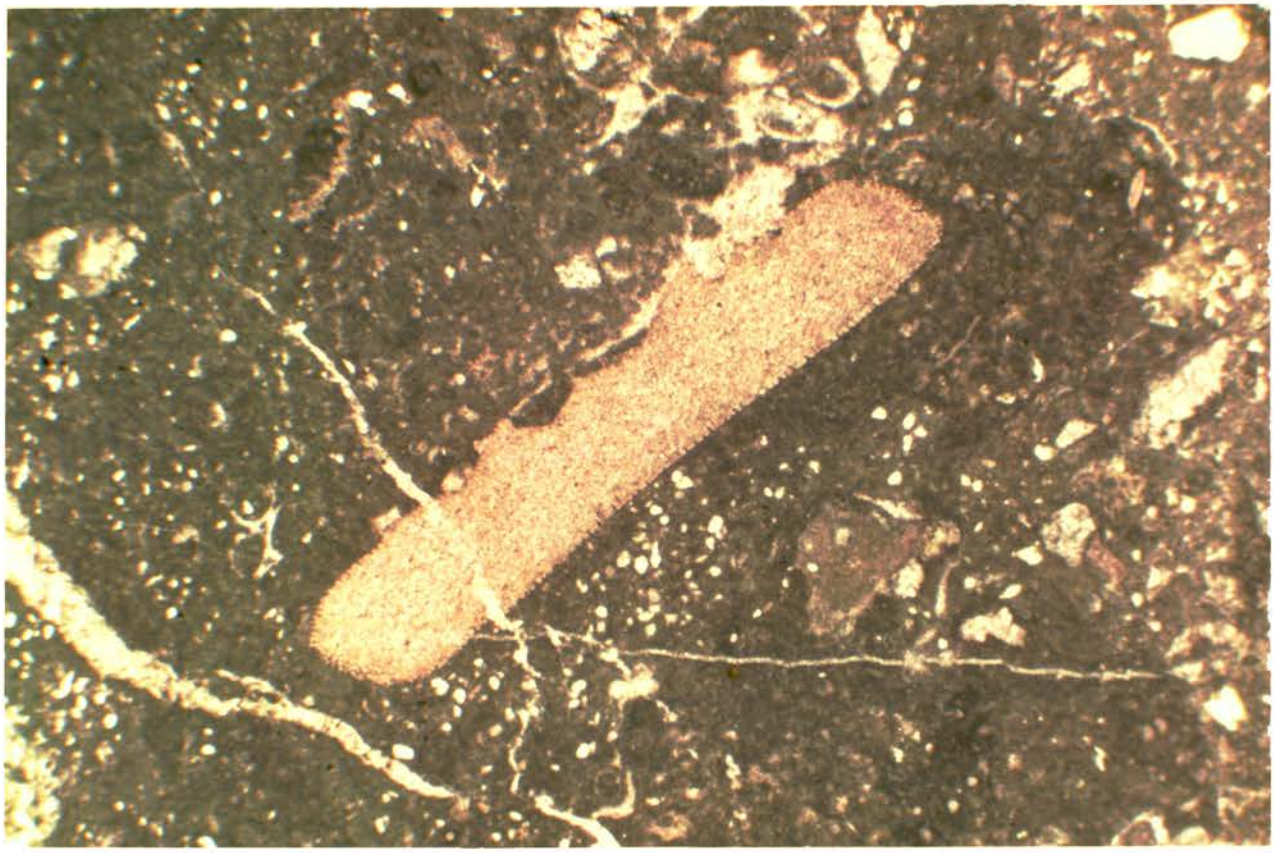

Plate 3-13

Resedimented grains in an oosparite (oolitic grainstone). The aggregates are made up of ooids and peloidal material set in a micritic matrix. Detrital quartz with authigenic overgrowths is abundant (sample 30/6). X 30 PPL

Plate 3-14

Late cementation in an oolitic grainstone (sample 30/7). The blue-stained ferroan calcite in the fracture (arrow) is late cement as it cuts across pre-existing grains (ooids and quartz) and cements. Detrital quartz with overgrowths is abundant. Note also the large aggregate grain composed of ooids in micrite matrix. X 50 PPL

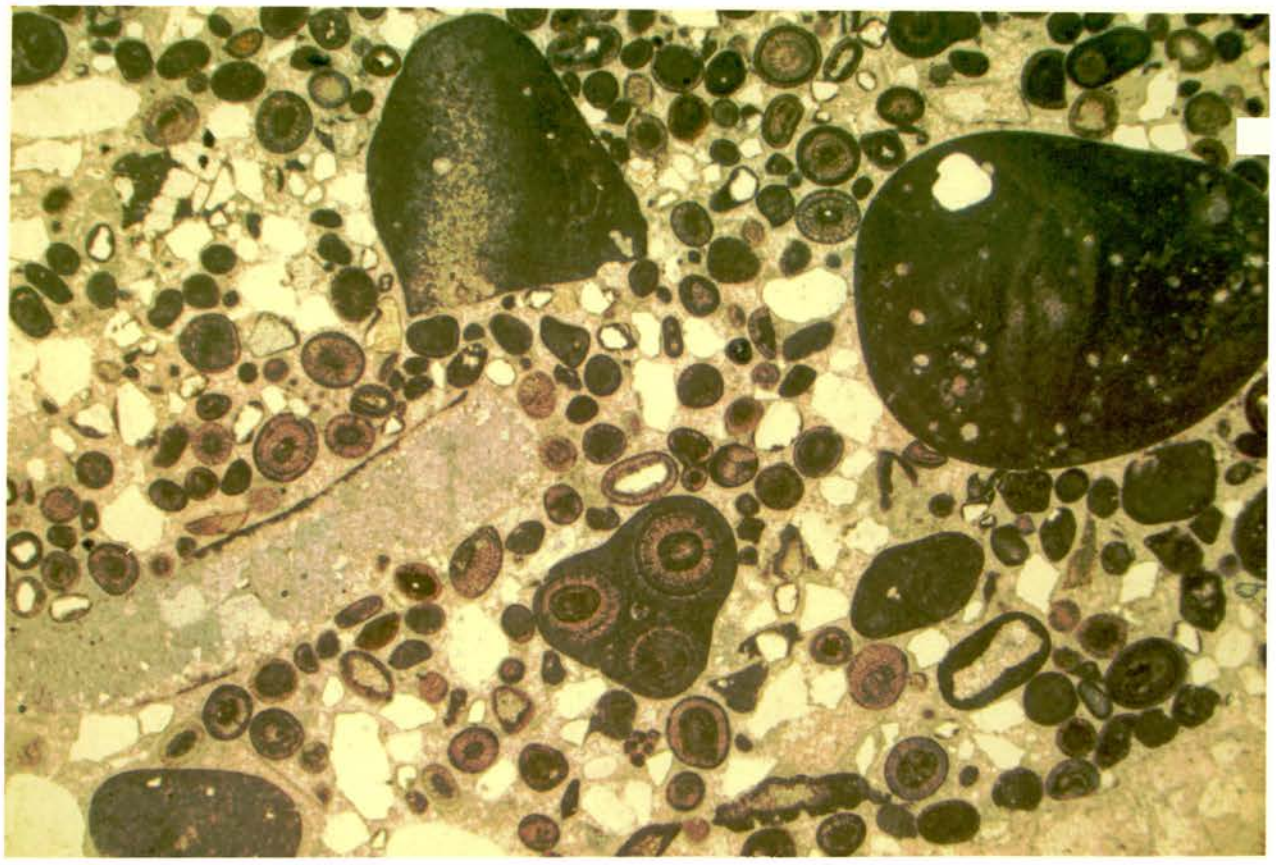

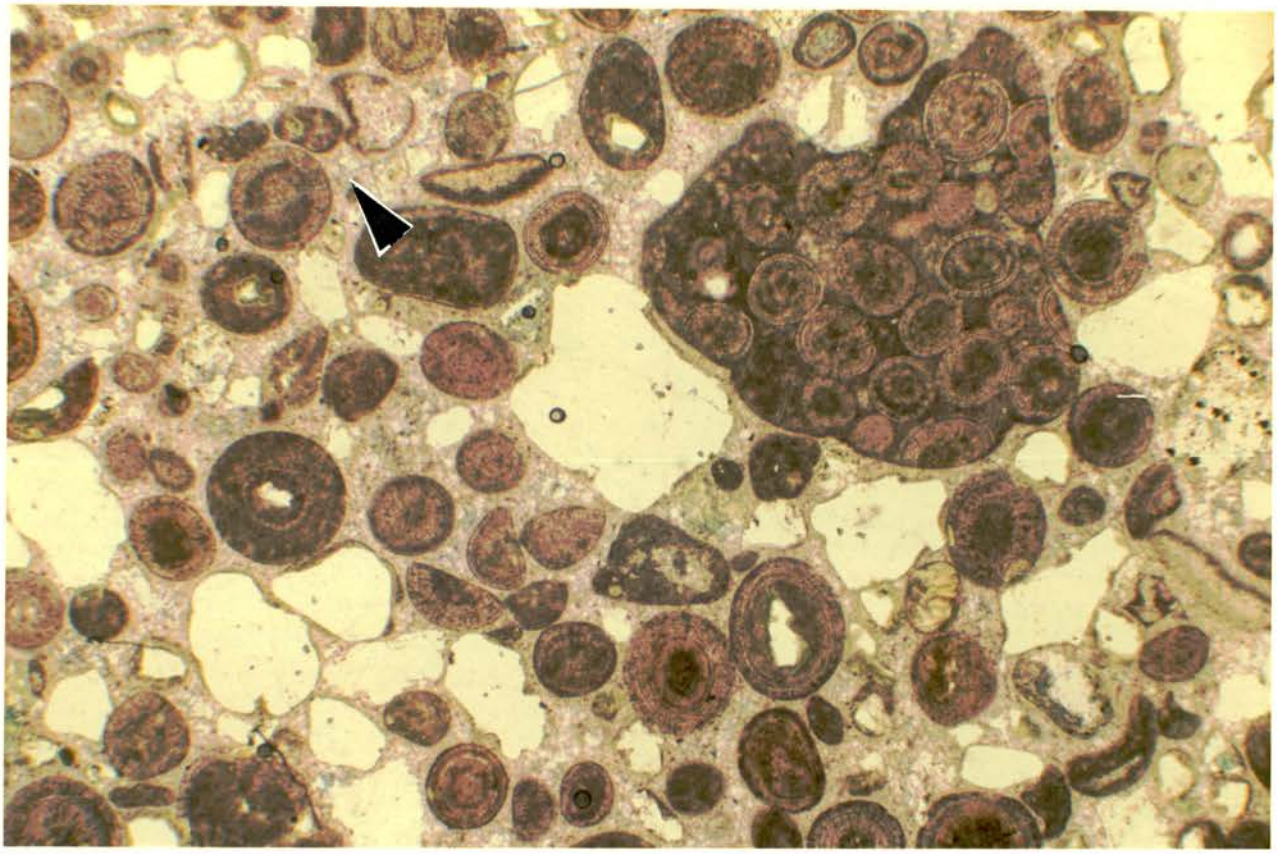

Plate 3-15

Neomorphic spar in coral (Sample 27/6) identified by the patchy distribution of grain size, remnant micritic patches and irregular, mostly non-planar crystal boundaries. X 50 PPL

Plate 3-16

Multiple cementation in a biomicrite (sample 27/4). The first-generation cement is the isopachous calcite precipitated on a micritic substrate followed by a later -generation coarsely-crystalline non-ferroan calcite (arrows). A third generation of faintly purplish-stained ferroan calcite occurs as vein cement. The rock is a coralline biomicrite in which the corals occur as the big rounded patches of neomorphic spar. X30 PPL

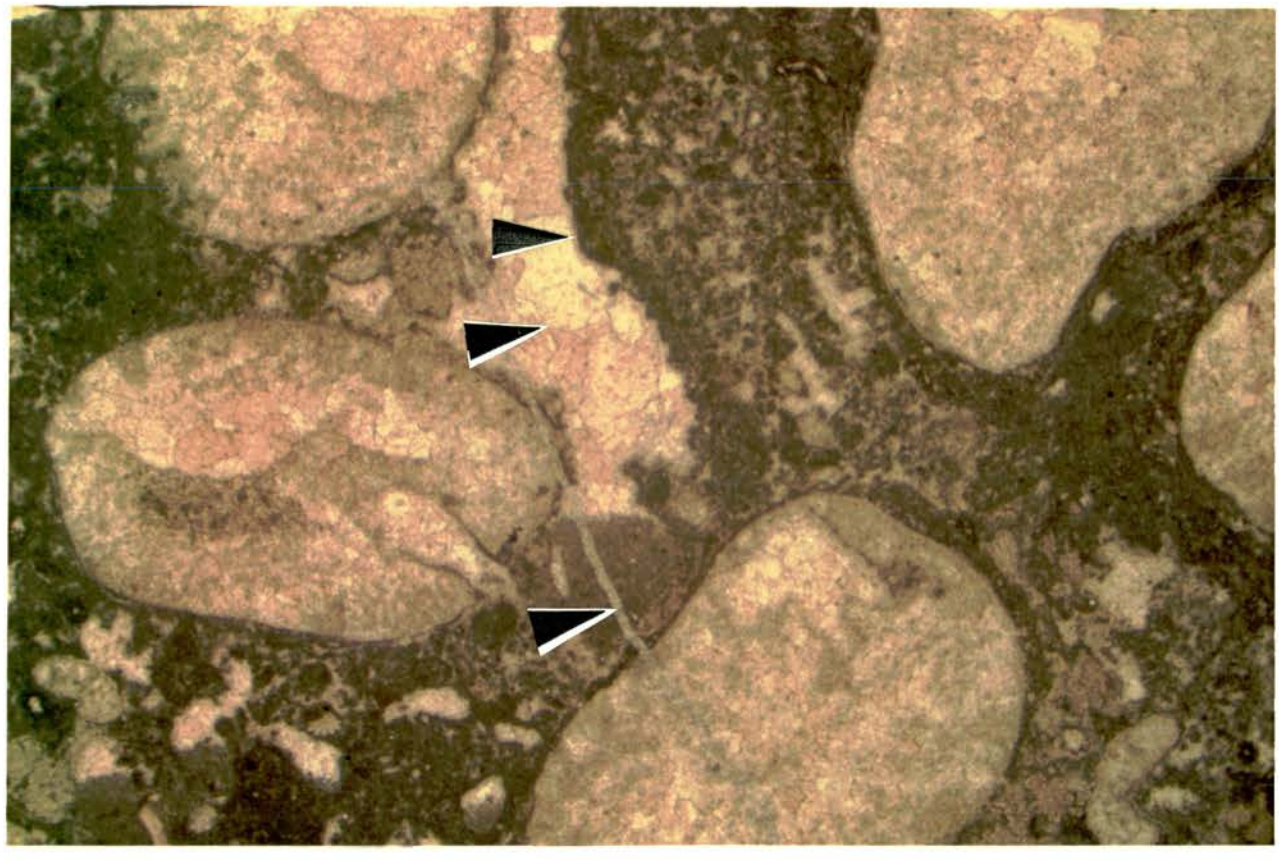

Plate 3-17

Saddle dolomite in a biomicrite from the Kambe Formation (sample 26/3). Note the characteristic undulose extinction. X 50 X-P

Plate 3-18

Same as above under PPL. Note the slight turquoise colour of the saddle dolomite in the stained section. X50 PPL

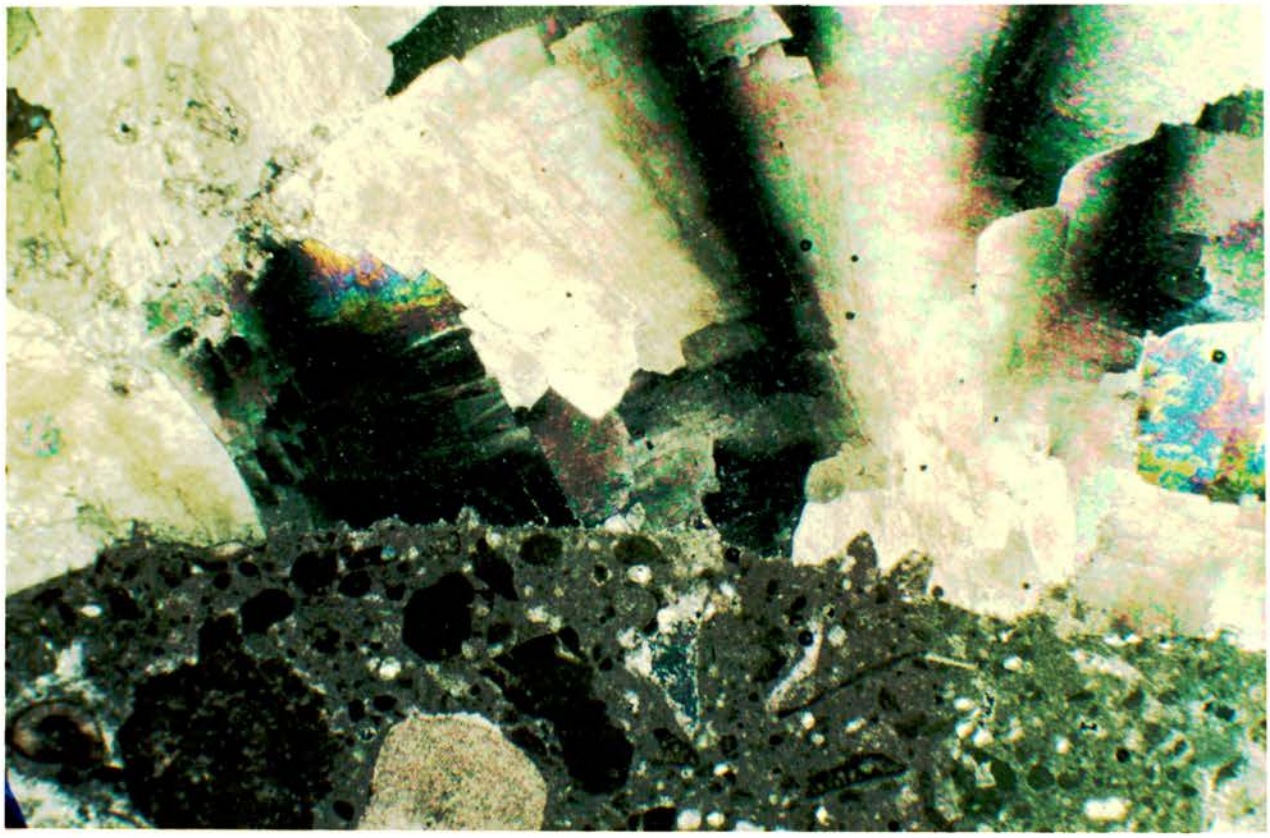

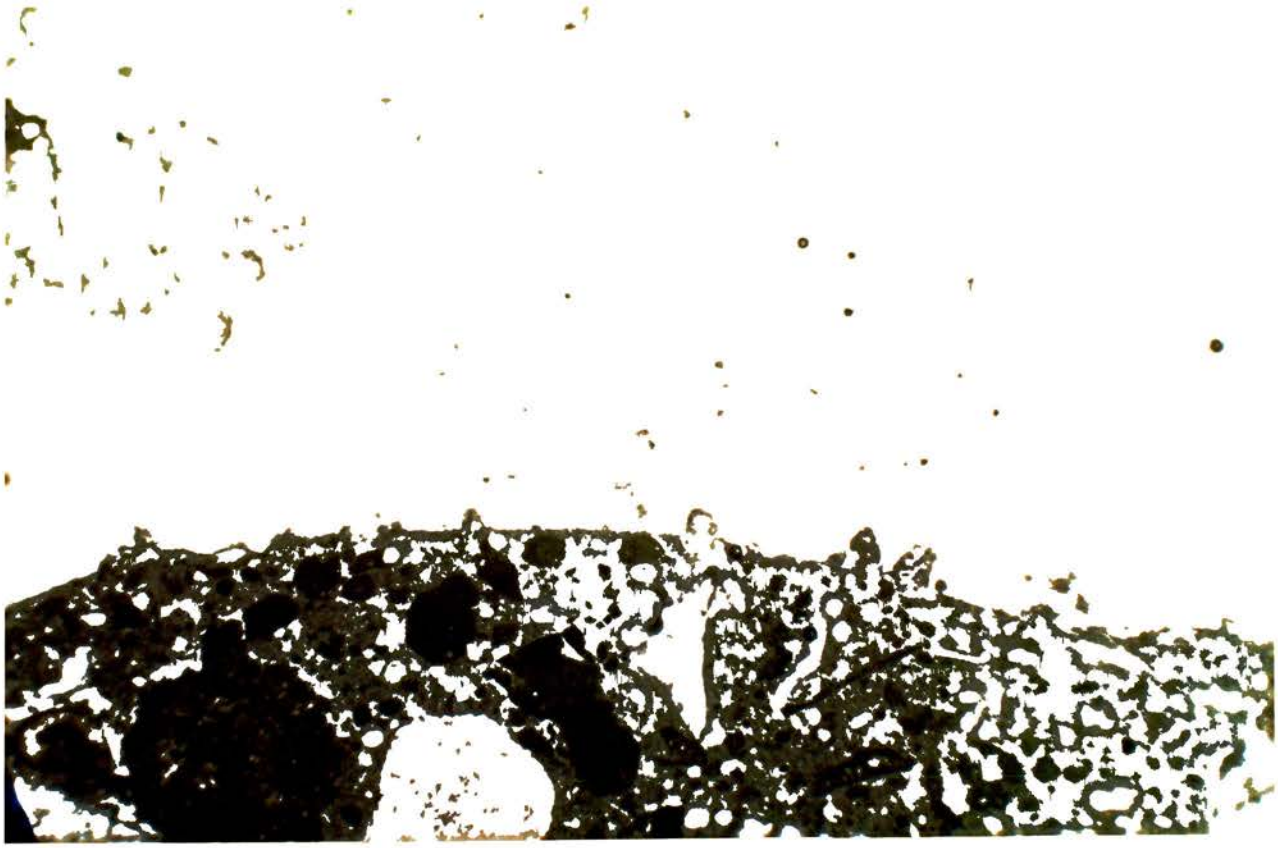

Plate 3-19

Radiaxial fibrous calcite in a biosparite (sample 3/2). from the Kambe Formation. Note the characteristic undulose extinction. X 50X-P

Plate 3-20

Same as above under PPL. The cement shows curved twin lamellae whose concave surfaces face away from the substrate (arrows). The cement is inclusion-rich and passes into Fe-rich (purple-stained) calcite. X 50

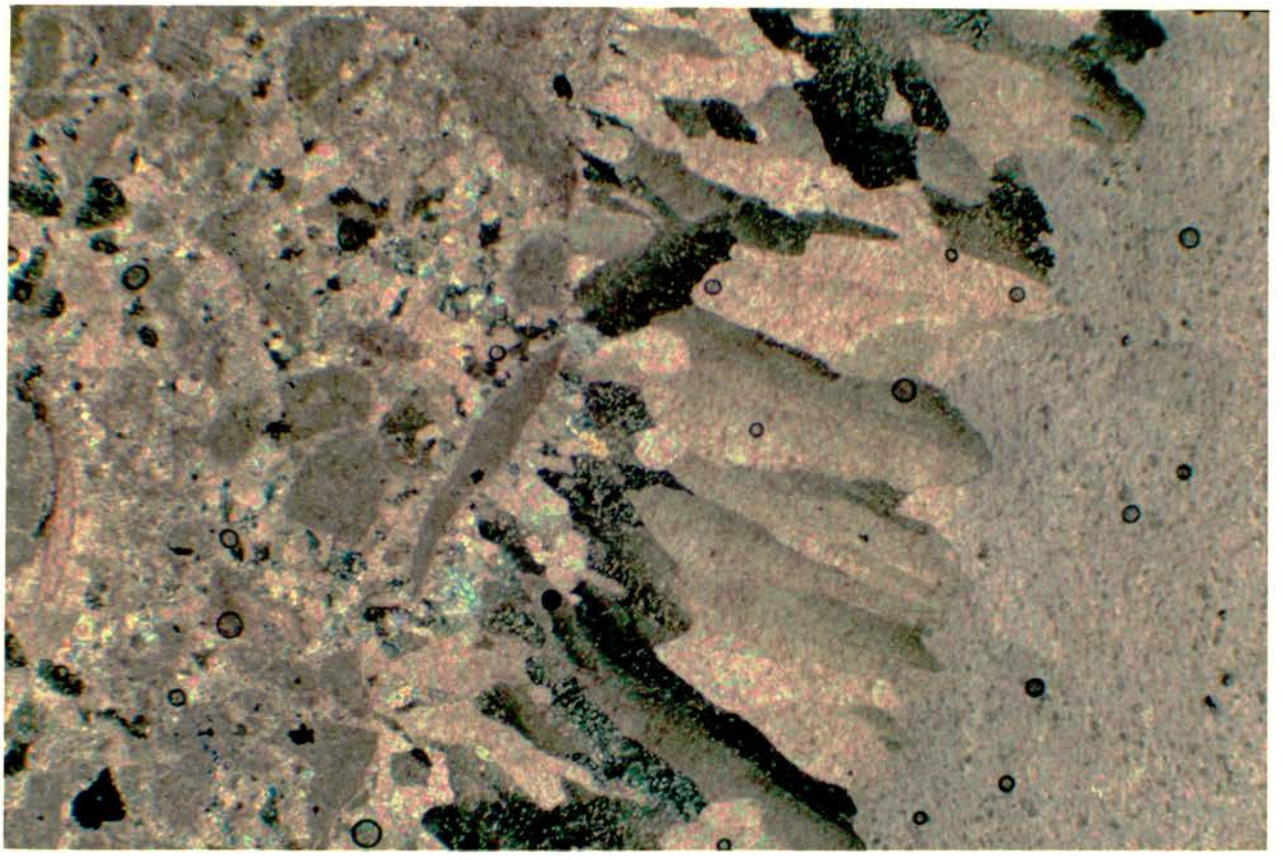

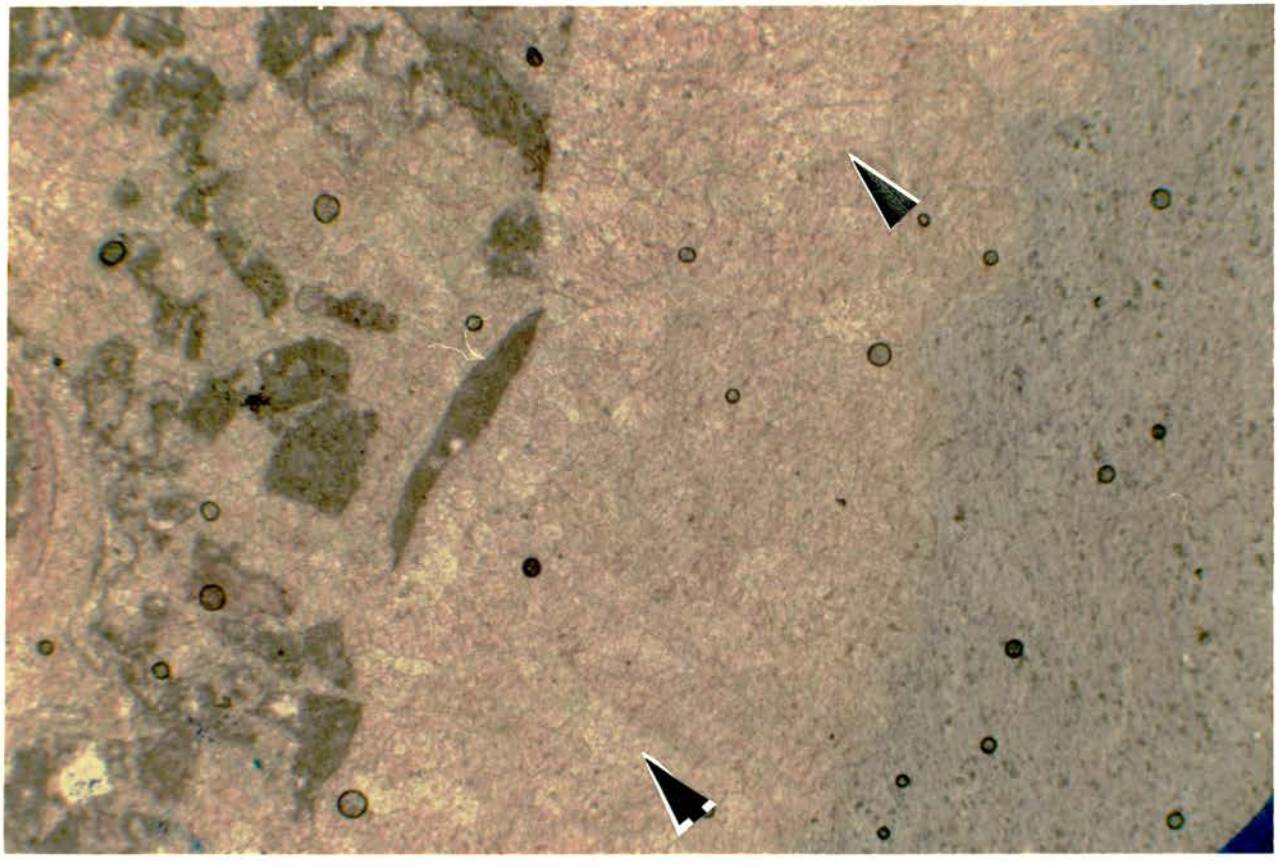

Plate 3-21

A micrite envelope marking the outline of an originally aragonitic gastropod which has since recrystallized into neomorphic spar. Unstained section. X 50 PPL

Plate 3-22

A poorly-washed oosparite from the Kambe limestones (sample 3/9) with both micritic and sparry calcite cement. X 50 PPL

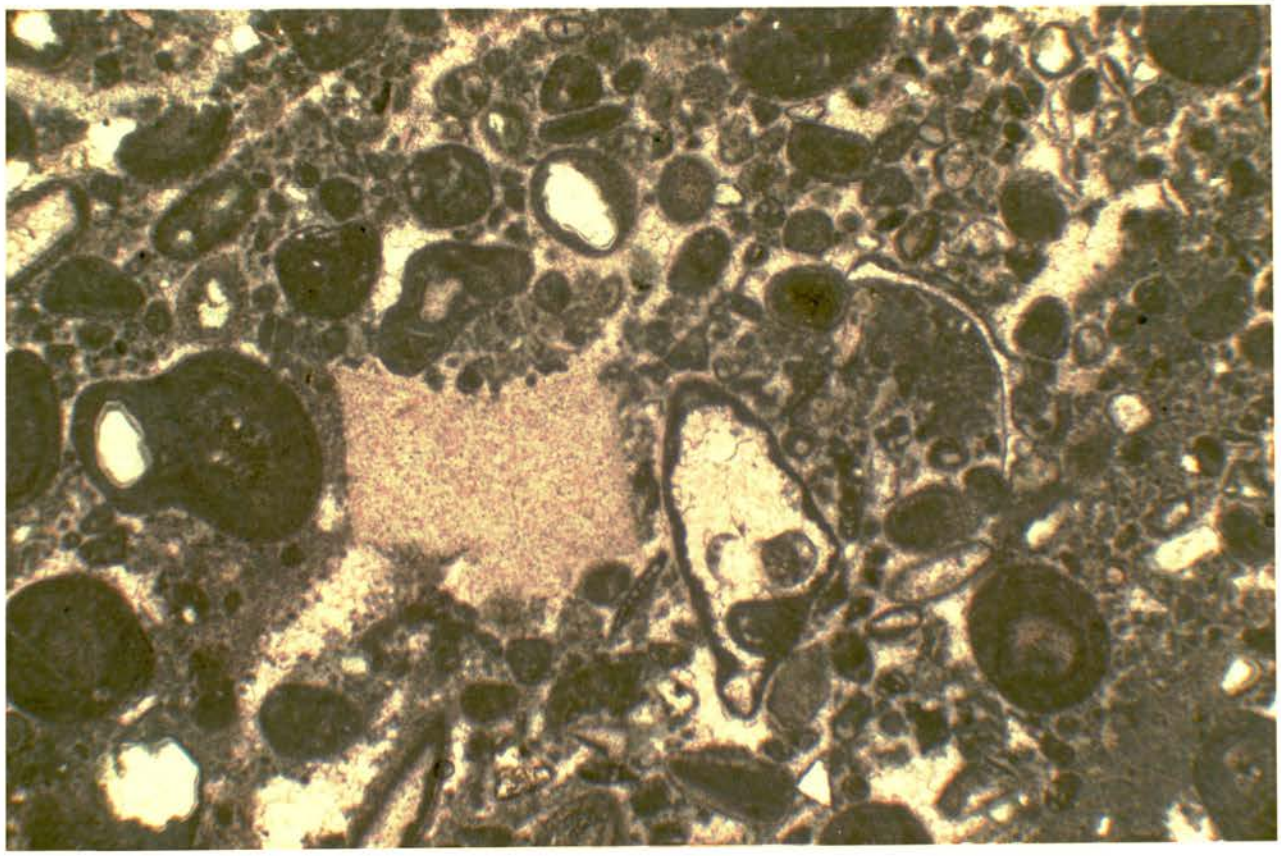

Plate 3-23

Syntaxial cementation around an echinoderm plate (arrow). The foliated bioclast is a brachiopod. X 50 X-P

Plate 3-24

Same as above under PPL

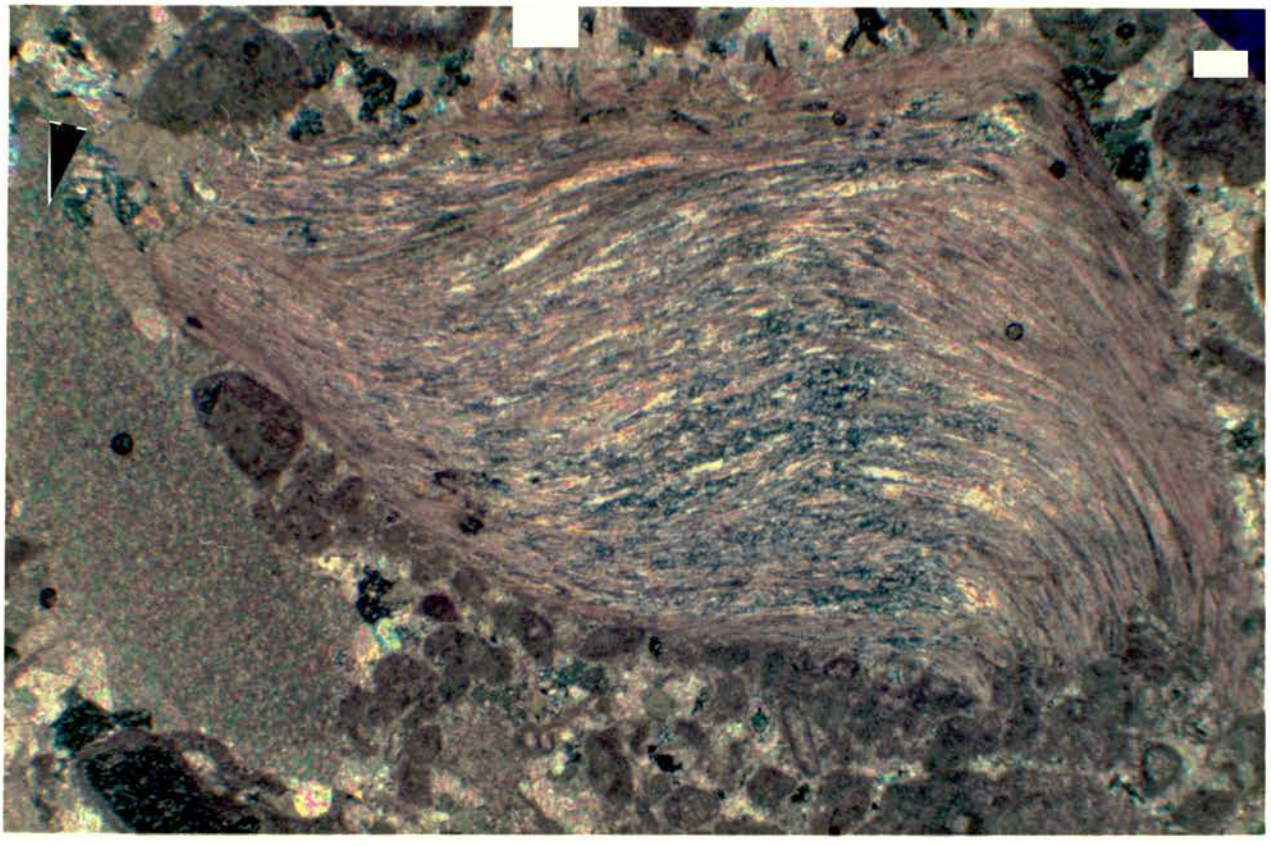

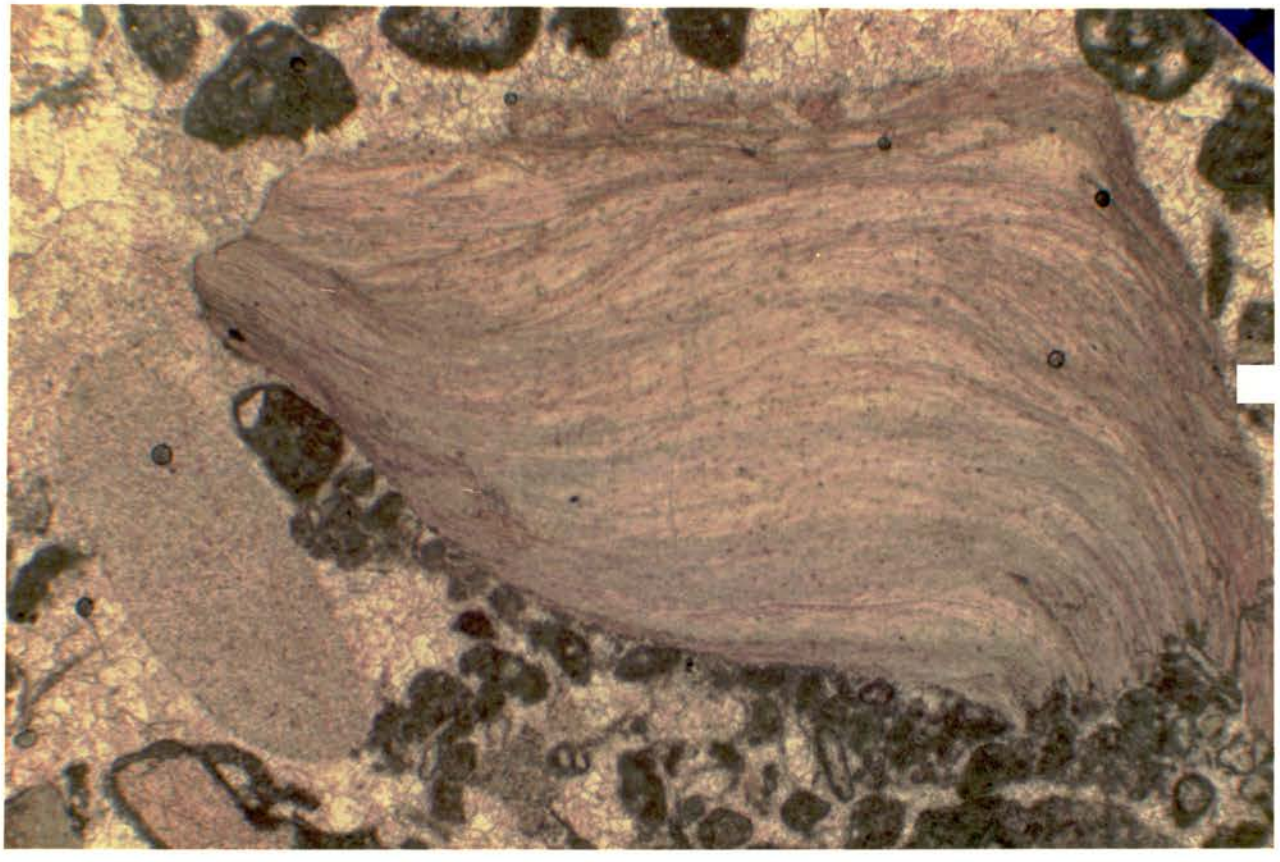

Plate 3-25

Foraminiferal-dolomitic pelsparite with black (probably bituminous) material (sample 4/8). X 50 PPL

Plate 3-26

Silty echinoderm pelmicrite (packstone) sample 4/12.
X 50 PPL

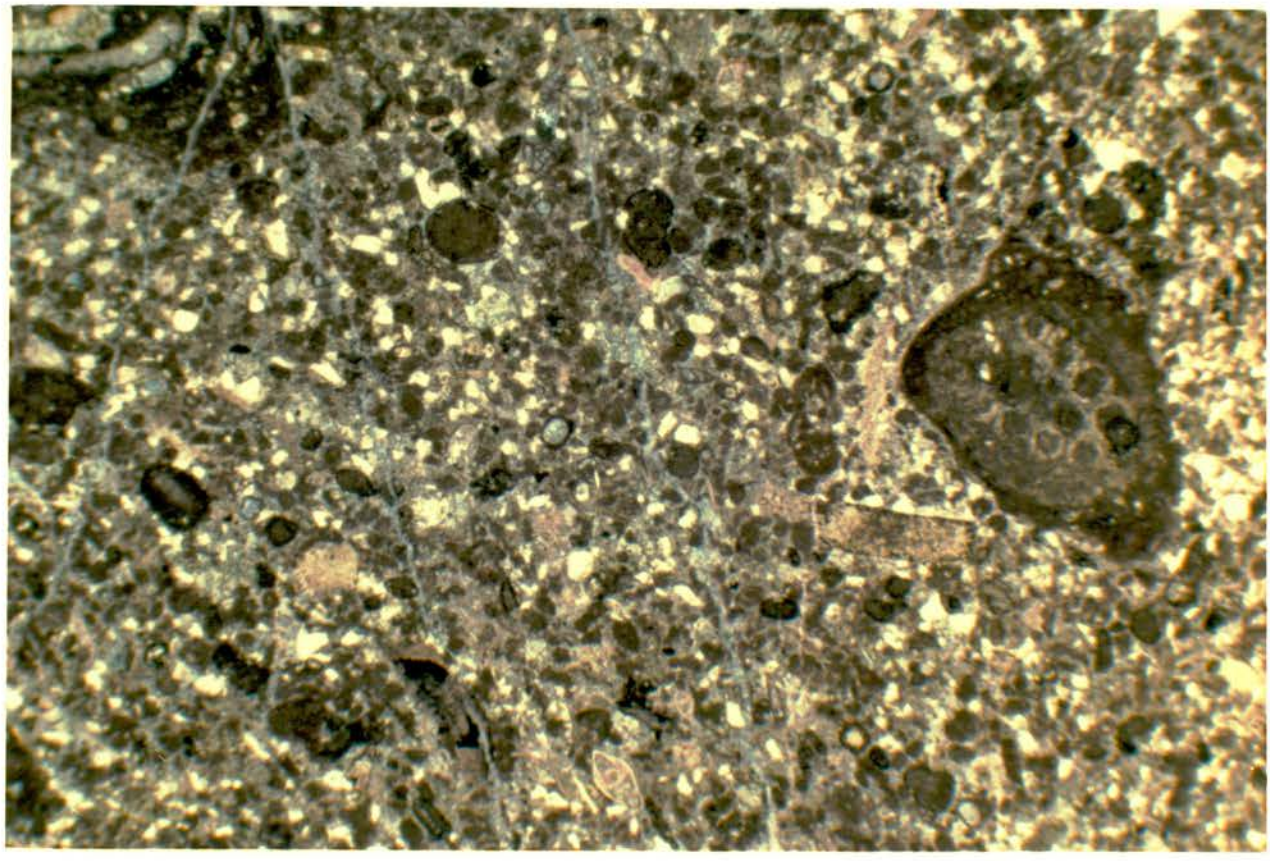

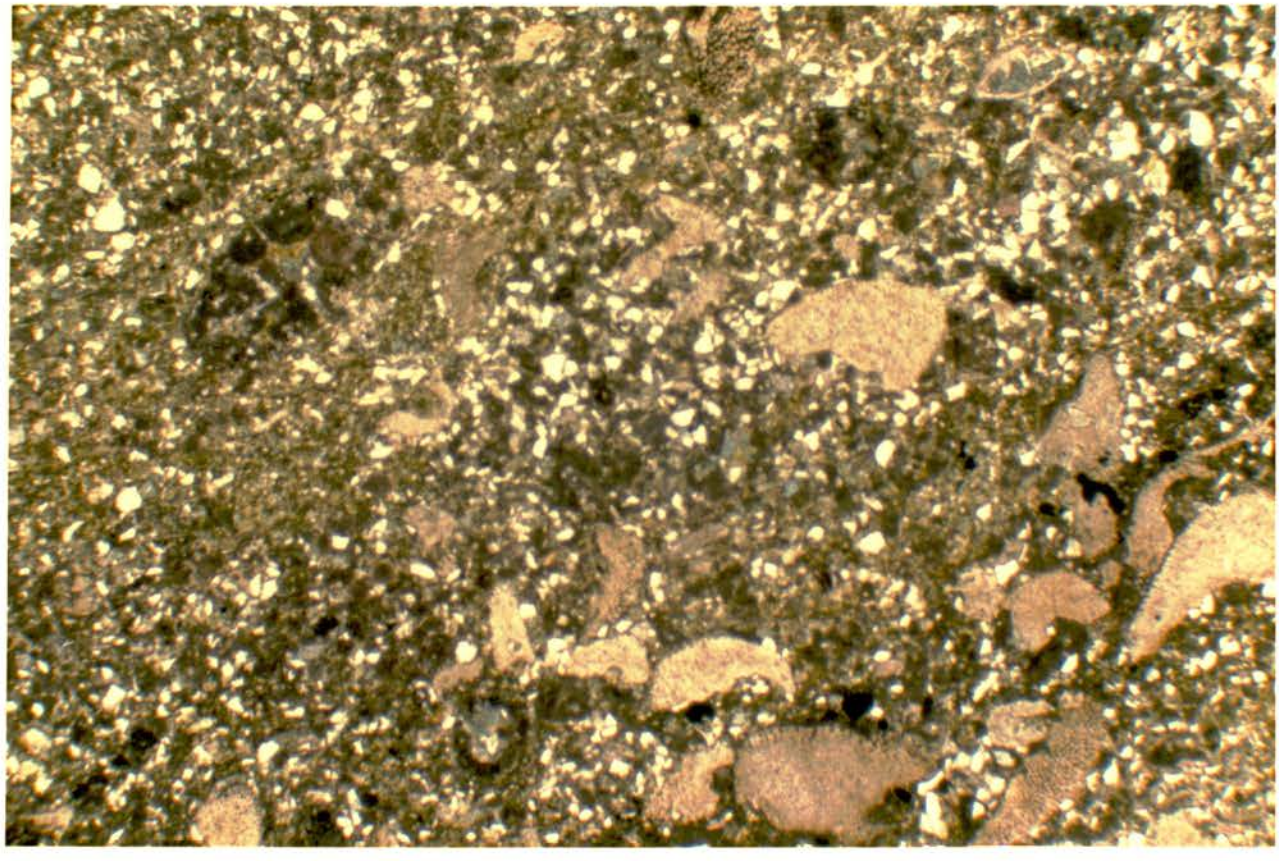

Plate 3-27

An articulated brachiopod (arrow) in a biopelmicrite (sample 4/14). X 50 PPL

Plate 3-28

A sparse biopelmicrite (wackestone) from the Kambe limestone. The bioclastic grains are mainly foraminifera and ostracodes (arrow). Late fracture (arrow) is probably tectonic.
X 30 PPL

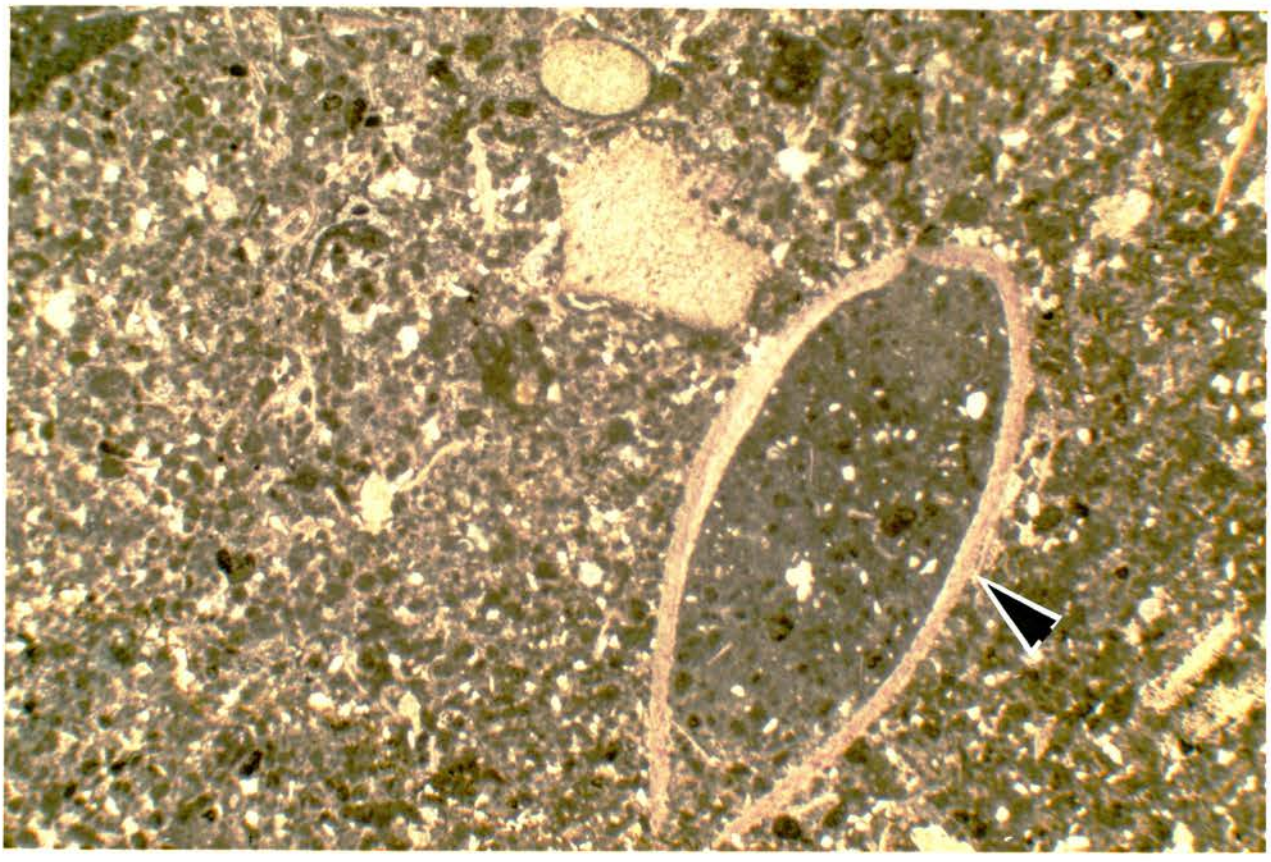

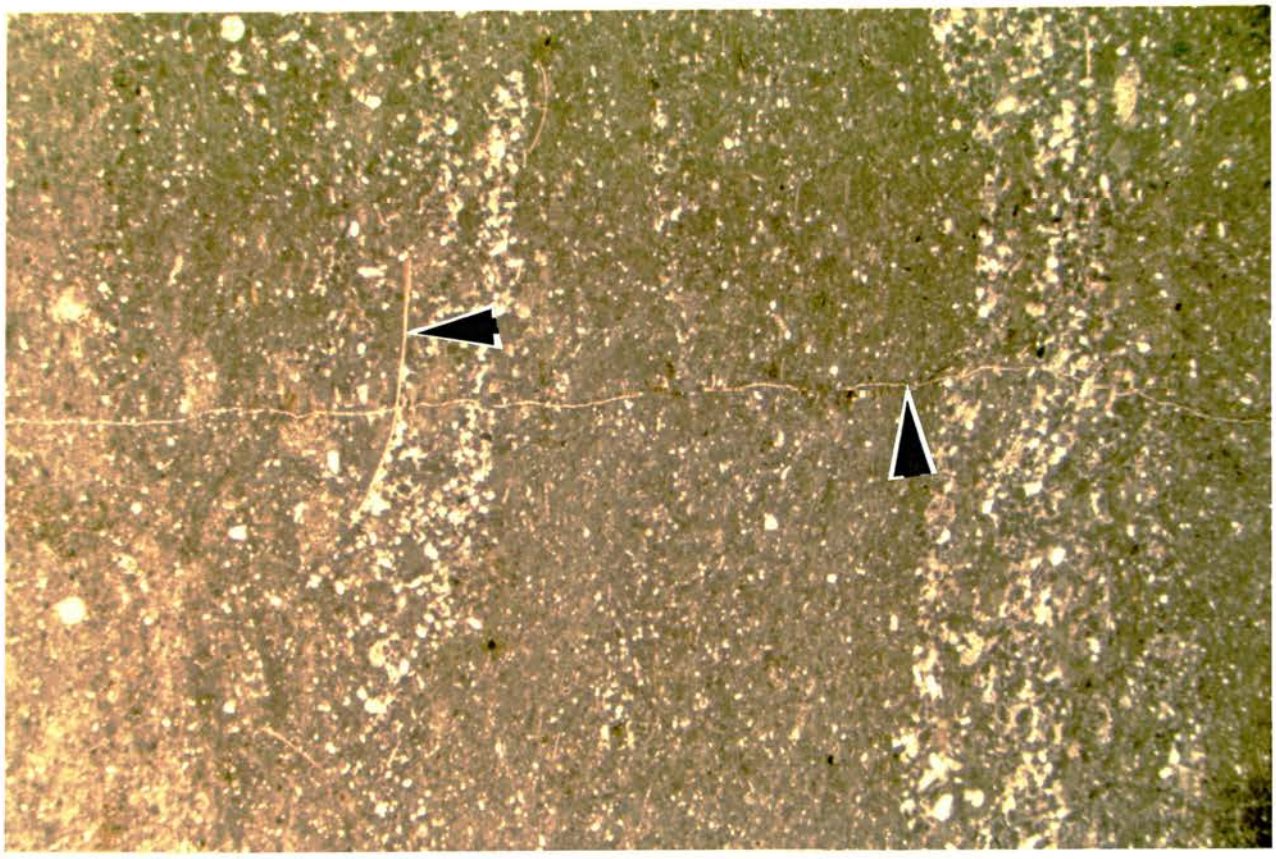

Plate 3-29

SEM photograph of the porous Freretown limestone (sample 30/2) showing the pore-lining calcite cement crystals. The pores are only lined and not filled. Some of the pores exceed 100m in diameter. X 400

Plate 3-30

SEM photograph of a quartzarenite (sample 3/11) of the Mazeras sandstones. The quartz grains (left) show a pitted appearance and have authigenic silica cement giving well developed crystal faces. Note the well-crystallized authigenic kaolinite (arrow) occurring as pseudohexagonal plates (booklets). X 1000

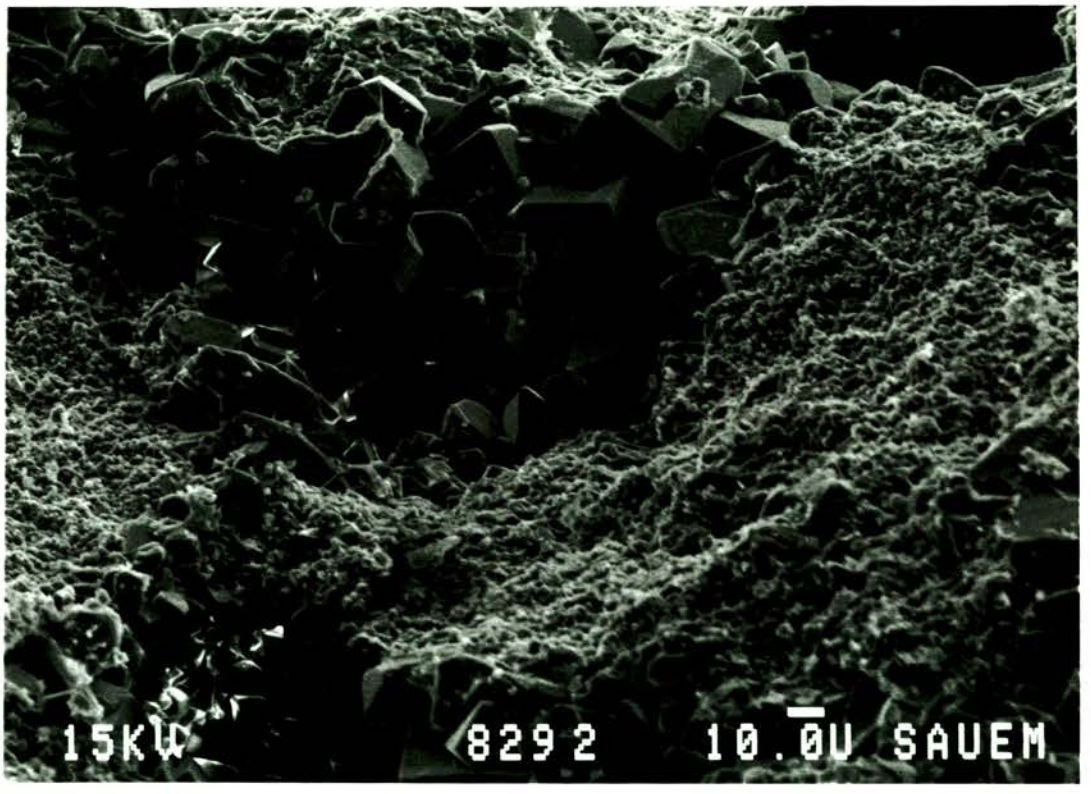
15KV
8292
10.0U SAUEM

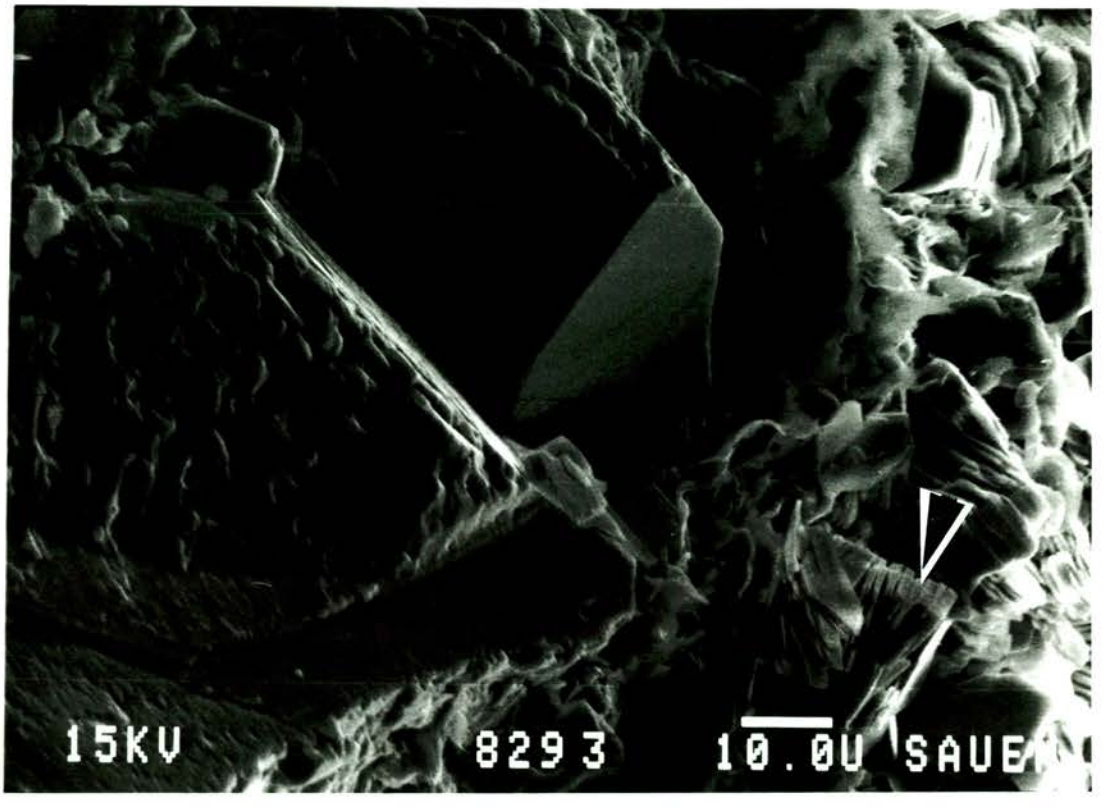
15KV
8293
10.0U SAUE

Plate 3-31

SEM photograph of an oosparite (sample 30/7). The grain on the right is quartz with authigenic overgrowths. X 200

Plate 3-32

Same as above showing multi-generation cement made of rim cement followed by coarser pore-filling calcite. X 200

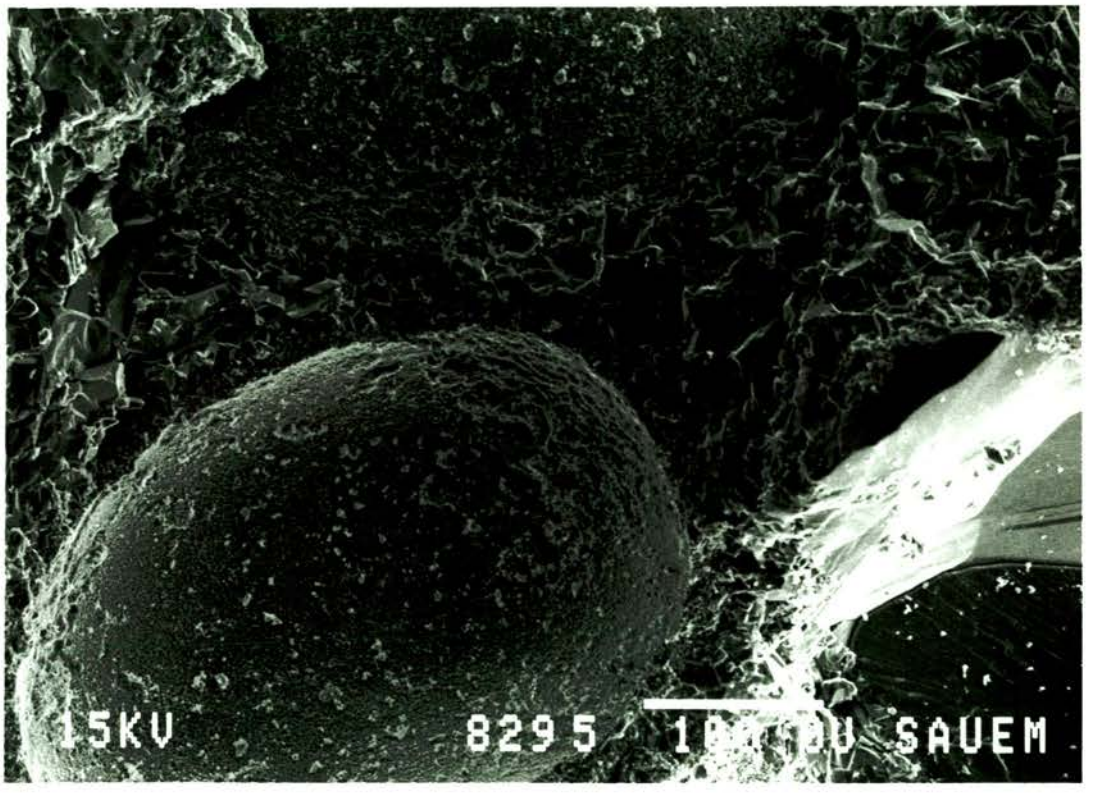
15KV
8295
SAUEM

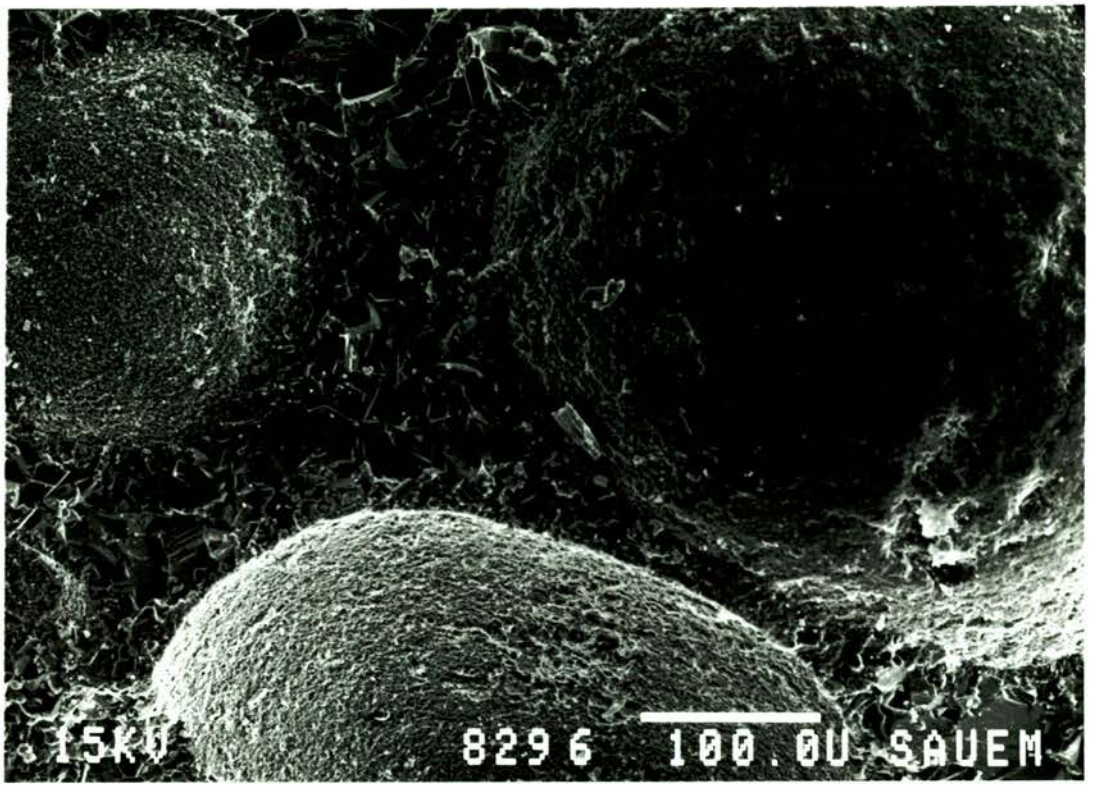
15KV
8296
100.0U SAUEM

4.0 DEPOSITIONAL ENVIRONMENTS

4.1 MAZERAS SANDSTONES

The limitations caused by the small number of samples available make it difficult to determine the depositional environment of the Mazeras sandstones with any degree of accuracy. Eight thin sections and one SEM sample were examined. Grain sizes vary from sample to sample ranging from fine to very coarse (gritty) sand. Mineralogical maturity determined from the feldspar content varies from immature (with abundant and relatively unaltered feldspars) to submature with trace amounts of altered feldspars. Petrographic differences are probably the result of sampling at different stratigraphic horizons of the Mazeras sandstones but this was not confirmed by field observations since no vertical sections were studied and sampling was mainly from small localized exposures.

It is, however, almost unanimously agreed by previous workers that the Mazeras Sandstones are fluvial-deltaic in origin. Caswell (1956) concluded that the lowermost parts of the Mazeras Formation are subaqueous deposits, the uppermost continental and between the two are deltaic deposits with which the silicified tree remains are associated. Coffin & Rabinowitz (1988) considered the Mazeras Sandstones to be deltaic while Walters & Linton (1973) indicated that, while the lower units are probably deltaic, the upper beds are likely to be aeolian sandstones representing coastal dunes

formed during arid conditions.

4.2 KAMBE LIMESTONES

The Kambe limestones were deposited during Middle Jurassic times when marine conditions became established in the Lamu Embayment (Coffin & Rabinowitz,1988). The model suggested in the present study for the deposition of the Kambe limestones considers them as a platform carbonate sequence that developed along a passive continental margin. This margin formed off the east coast of Africa as a result of the break-up of Gondwanaland and the rifting and drifting of Madagascar from Africa during Jurassic times between 160 and 130 ma (Bosellini,1986). From the palaeoposition of the African continent during the Jurassic (Lawyer,et al.1990), and also from the evidence of both the coral and the oolitic limestone varieties within the Kambe, (Caswell, 1956), it is clear that the limestone sequence was deposited in a shallow, warm tropical sea.

The model I have adopted for the deposition of the Kambe limestones involves deposition in a restricted marine shelf environment in which the restriction is produced not by any significant physiographic barriers but by the existence of a broad expanse of shallow water in an epeiric platform. Evidence for the broad shallow water platform is seen in the palaeogeographic map of eastern Africa (Figure 4-1) during the Jurassic which shows approximately 400km of continental shelf

between Kenya and Madagascar. Epeiric platforms were common in the Jurassic and although no good modern examples exist, the interior of the Great Bahama Bank and the Florida Bay are close analogues (Enos,1983; Sellwood,1986; Tucker & Wright,1990). The restriction in the shelf was presumably caused by the build-up of shelf-edge oolitic grainstone complexes in the manner shown in figure 4-2.

This model for the Kambe limestones is supported by both field observations and petrographic evidence. Field evidence is based mainly on two exposures with measurable vertical sections at the Kambe Limestone quarry and at the Rare River cliffs. The basal conglomerate at the Kambe Limestone quarry probably represents the lowermost unit in a shallowing-upward carbonate sequence (James,1979) and records the initial transgression over the underlying Mazeras sandstones. The actual unconformable contact between the Mazeras and the Kambe Formations is exposed at the Mwachi River section (Karanja,1984). The basal unit is a high energy deposit and the whole sequence is here interpreted as an "oolite-grainstone" cycle (Wilson,1975) or a "grainy sequence" (James,1979). The matrix of the conglomerate (sample 30/6) is an oosparite (oolitic grainstone).

The basal conglomerate is overlain by oolitic grainstones which are clear, cross-bedded lime sands with relatively impoverished faunas and were probably deposited as oolite-shoal facies in a sand belt parallel to the shelf

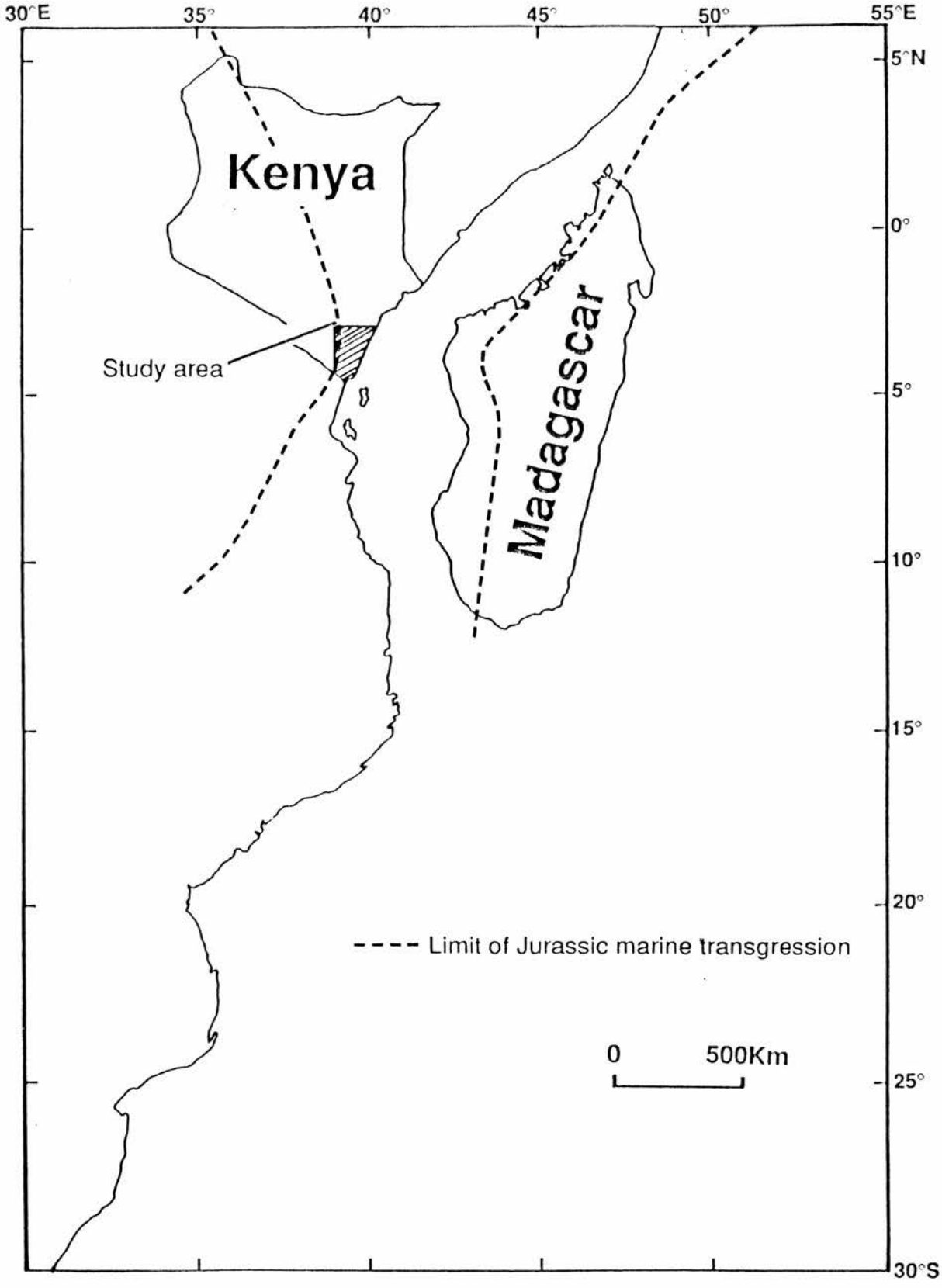

Figure 4-1
Palaeogeographic map of Eastern Africa during the Jurassic period (modified from Coffin and Rabinowitz,1988; Saggerson and Miller,1957)

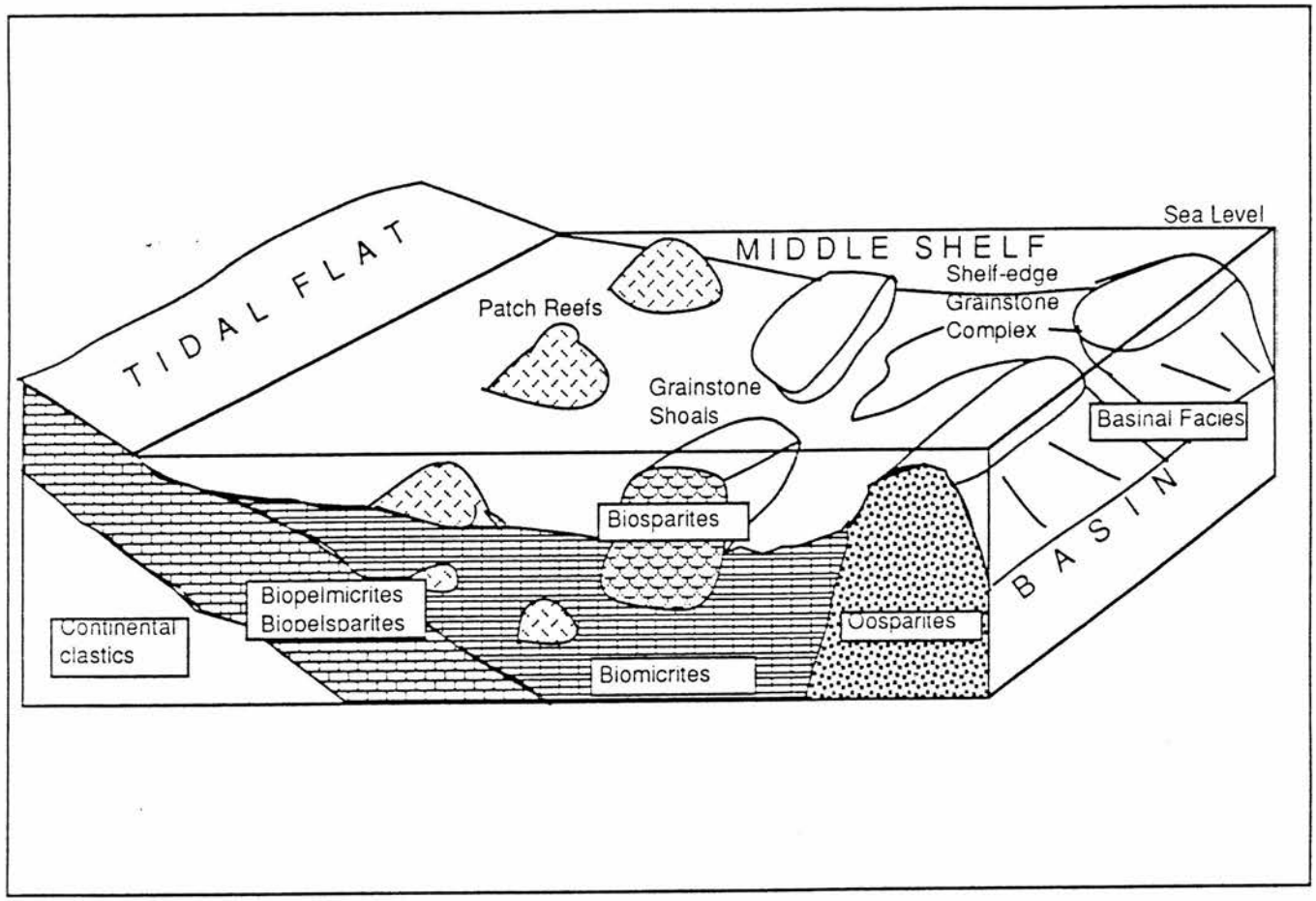

Figure 4-2
Depositional model for the Kambe limestones. Vertical scale greatly exergerated.

margin. The cross- bedding and the presence of a few shallow water fossils (including, brachiopods, echinoderms and bivalves) indicates high energy conditions of deposition on shallow shoals (Wilson & Jordan,1983). The excellent sorting of absolutely mud-free sediment is an
indication of accumulation on bars and shoals with high energy wave currents where the sediment was continuously moved to and fro. The oolite grainstones correspond to standard microfacies 15 of Wilson (1975) and the almost complete lack of fossils is an indication of the unstable nature of the continuously shifting substrate.

Above the oolitic limestone unit is a 14m thick, poorly-washed pelsparite (oolitic packstone) while the topmost unit is a biopelmicrite (bioclastic wackestone). The top unit (sample 31/10) is laminated and contains several 10cm-thick shale partings representing periodic interruptions of carbonate sedimentation by incursions of clay.

The oolitic packstone facies represents deposition shore-wards from an active sand shoal while the topmost biopelmicrite unit indicates deposition in quieter water farther away from the platform margin. This deposition model is similar to the one proposed for the Middle Jurassic of northwestern Europe where carbonate facies were deposited in shallow waters without reef-rimmed margins in epeiric platforms (Sellwood,1983).

The biomicrite and biosparite facies (bioclastic

grainstones and packstones) in the Kambe Formation correspond to standard microfacies 11 (Wilson,1975). The faunal assemblage indicates normal marine salinities and the bioclasts are commonly micritized. The sparite facies are probably the products of grainstone shoal environments in agitated water where lime mud is winnowed out. The biosparite and biomicrite facies may be associated with patch reefs and mud mounds scattered across the shelf and they sometimes contain ooids and lithoclasts of reworked carbonate material.

The biomicrite and biosparite facies are not represented in any of the typical vertical sequences of the Kambe Formation observed in the field. They were instead noted to occur in more localized outcrops probably due to the localized nature of organic build-ups (patch reefs and mud mounds) scattered throughout the shelf. The patch reef model would explain the localized high concentrations of corals in some samples and field outcrops. Shelf-edge reefs would be expected to be more regular in shape, elongate and parallel or perpendicular to shelf margin (Wilson & Jordan,1983). The corals are locally so abundant that the terms reefal and coral limestone have been used in the past to describe these facies of the Kambe limestones (Gregory, 1921; McKinnon-Wood,1930;1938). Exposed surfaces have been weathered into karstic surfaces to produce what Caswell (1956) referred to as "karstland topography". These features are normally formed in inner shelf environments and on emergent shoals and reef

flats or they may form on exposed shelf deposits. A sample (3/3) containing angular clasts set in sparry calcite cement is interpreted as a collapse breccia probably formed by dissolution of limestone on an exposed mud mound (Wilson & Jordan, 1983). The biopelmicrites and biopelsparites (peloidal grainstones to packstones) show faunal restriction with mainly miliolid foraminifera and echinoderm fragments as the dominant bioclasts. They are interpreted as falling within standard microfacies 16 grading to 19 (Wilson,1975). These facies are normally deposited in restricted marine shoals on tidal flats and levees or very restricted bays and ponds.

Field observations at the Rare River cliffs suggest deposition as a relatively low energy shoaling upward sequence (James,1979). Evidence for this is however not fully conclusive as neither the top section (inaccessible) nor the lower-most section (not exposed) were observed. The exposed section is a repetitive sequence of sandy dolomitic pelsparites and silty calcareous mudstones on the lower parts of the section and silty biopelmicrites and thinly laminated calcareous mudstones in the upper parts. The base of the shoaling-upwards cycle would probably be a transgressive unit (not observed) followed by a muddy carbonate with impoverished fauna capped by intertidal/ supratidal deposits (Enos,1983).

Dolomite and quartz silt are common and the dolomite is interpreted as primary (early diagenetic) due to its small crystal size and was probably formed in supratidal

environments (Shinn,1983). The occurrence of laminated calcrete horizons and black organic matter preserved in the sediments further supports the idea of deposition in supratidal environments. The absence of evaporitic minerals such as halite, gypsum /anhydrite suggests that either the climate was humid and that such minerals would form during the dry season and then get dissolved and washed away during the wet season or, as in the Bahamas case, evaporites are not always precipitated or preserved (Tucker & Wright,1990).

4.3 FRERETOWN LIMESTONES

Field observation was limited to one exposure in a disused quarry in the Freretown area. Only three samples were available for analysis and they all show severe faunal restriction where only two species (algae and foraminifera) are represented, but in very great numbers. The samples are classified as algal- foraminiferal grainstones.

They are equivalent to standard microfacies 18, the foraminiferal-dasycladacean grainstones common in tidal bars and channels of lagoons in restricted marine shoals. It is a typical and widespread Cretaceous and Tertiary facies of the most restricted marine environment of the bank interior (Wilson,1975).

5.0 DIAGENESIS

The diagenesis of the Kambe limestones is interpreted mainly on the basis of cement petrography, coupled with trace element geochemistry, stable isotope analysis and cathodoluminescence (CL) studies. Thin section and cathodoluminescence microscopy were used to observe the textural relationships between the different cement phases and grains. Cathodoluminescence petrography was used to study the various cement zones and interpreted in conjunction with geochemical analysis.

A total of 88 microprobe spot analyses were carried out on 9 selected samples of the Kambe limestones. The selected samples were mainly from the biosparite and oosparite facies as they provided cements which were coarse enough to be easily sampled. The elements analyzed were Ca, Fe, Mg and Mn for all the samples and Sr and Ba for some of the samples. The results are presented as raw data (Table 5-1) and numerical averages (Table 5-2) in ppm for the various elements. The same polished sections used for microprobe analysis were cleaned to remove the carbon coating and used for cathodoluminescence petrography. This order was not always followed and, in some cases, the polished sections were first used for cathodoluminescence and then carbon-coated for microprobe analysis. Establishing the cathodoluminescence pattern first was found to be very useful in determining the locations for microprobe analysis.

Sample	Analysis position	Elemental composition (ppm)				
		Fe	Mg	Mn	Sr	Ba
3/2	1 Vein cement	0000	1918	2540	NA	NA
	2	0000	1309	1634		
	3	0451	1930	0155		
	4	1228	0712	1255		
	5	0521	0591	0837		
	6	0163	1785	1208		
	7	0225	1308	0720		
	8	0000	2057	0000		
	9					
	10 Light-coloured vein cement	0000	1074	0457	NA	NA
	11 Dark-coloured vein cement	0808	0688	0945	NA	NA
	12 Micrite	0871	1013	1022	NA	NA
30/6	13 Dark-coloured rim cements	0000	5543	0457	NA	NA
	14	0000	4312	0527		
	15	0319	3540	2641		
	16	0000	4354	0380		
	17	0000	2515	1510		
	18	0000	2316	0000		
	19 Lighter-coloured pore-filling cement	4049	1671	4027	NA	NA
	20	2340	1815	9627		
26/3	21 Saddle dolomite cement	0707	4964	0302	NA	NA
	22 -darker zone	0389	5295	0418		
	23 -lighter zone	2254	3739	0340		
	24	1640	3781	0263		
	25 Dark-coloured euhedral crystal within cement	0241	0000	0441		
3/9	26 Dark pore-filling cement	0000	2378	0194	NA	NA
	27	0000	0168	0953		
	28	0645	0000	0039		
	29 Light-coloured pore-filling cement	0225	0850	1634	0000	0000
	30	0490	1411	1293	0000	0000
	31	0389	2931	1061	0668	0000
	32	0194	1206	0170	0161	0251
3/5	33 Micrite patches	0132	1381	0720	NA	NA
	34	0684	2186	0380		
	35 Dark-coloured zones in vein cement	0031	0422	0000	NA	NA
	36	0288	0296	5840		
	37 Light-coloured zones in vein cement	0257	0482	7087	NA	NA
	38	0287	0374	1371		
27/2	39 Rim cement	0233	0814	0821	0000	0000
	40	0000	0856	0441	0000	0564
	41	0567	4957	0108	0000	0000
	42	0334	3528	0000	0000	0358
	43	2021	3534	2409	0000	0815
	44	0000	2678	0271	0000	0663
	45	0278	3414	0108	0186	0564
	46	0000	1731	0612	0000	0206

(continued)

	47 Ooids	0684	2189	0380	NA	NA
	48	0334	2859	0496	0000	0000
	49	0326	3269	0054	0000	1585
	50	0140	2792	0000	0000	0054
	51	0140	1508	0225	0194	0000
	52	0000	3003	0945	0211	1290
	53	0047	2642	0604	0000	0000
	54	0000	3588	0387	0000	1206
	55	0326	3094	0325	0000	0815
	56 Light-coloured pore-filling cement	1656	2871	2238	NA	NA
	57	1943	3890	0380	NA	NA
	58	1858	4216	2006	0000	0981
	59	3035	4161	2742	0000	0000
	60	0000	1091	1053	0000	0054
	61	1788	2919	2688	0000	0054
	62 Dark-coloured pore-filling cement	0000	3124	0380	NA	NA
	63	0295	2714	0418	NA	NA
	64	0808	3088	2711	0000	0000
30/8	65 Dark-coloured pore-filling cement	0000	0488	0875		
	66	0000	1061	1440	NA	NA
	67	0000	0374	1022		
	68 Light-coloured pore-filling cement	1259	1466	13360	NA	NA
	69	3358	1484	5993		
	70	0358	1104	17566		
3/4	71 Dark-coloured vein cement	0000	0802	0457	NA	NA
	72	0031	1025	0573		
	73 Intermediate vein cement	1850	0296	2773	NA	NA
	74	2005	1363	3075		
	75 Light-coloured vein cement	2005	1158	5267	NA	NA
	76	1842	2720	5718		
30/9	77 Ooids	0266	1840	0720	NA	NA
	78	0583	1978	1071		
	79 Rim cements	0326	0862	3942	NA	NA
	80	4050	0977	2618	NA	NA
	81	1757	0965	10293	0000	0305
	82	1345	1158	11276	0389	0555
	83 Light-coloured pore-filling cement	2037	0446	7234	NA	NA
	84	1329	0784	6560		
	85 Dark-coloured pore-filling cement	0420	3251	1898	NA	NA
	86	0560	0814	4008	0389	0000
	87	4711	1466	2587	1125	0806
	88	0529	1496	1448	1573	0000
	89	1687	1019	1727	0186	0000

Table 5-1
Microprobe spot analysis data for the Kambe limestones (NA indicates positions not analyzed for the various elements)

Points Analysed	Samples	Analyses	Trace element concentration(ppm)				
			Fe	Mg	Mn	Sr	Ba
Vein cement (undifferentiated)	3/2	8	0324	1451	1044	NA	NA
Vein cement (light-coloured)	3/2,3/4, 3/5	5	0879	1162	3456	NA	NA
Vein cement (dark-coloured)	3/2,3/4, 3/5	5	0232	0647	1563	NA	NA
Vein cement (intermediate)	3/4	2	1928	0830	2924	NA	NA
Micrite	3/2,3/5	3	0562	1527	0707	NA	NA
Rim cements (undifferentated)	27/2, 30/9	12	0909	2098	2742	0058	0404
Rim cements (dark-coloured)	30/6	6	0053	3763	0919	NA	NA
Saddle dolomite -darker zone	26/3	2	0548	5130	0360	NA	NA
Saddle dolomite -lighter zone	26/3	2	1947	3760	0302	NA	NA
Pore-filling cement, dark coloured	3/9,27/2, 30/8, 30/9	12	0620	1577	1376	NA	NA
Pore-filling cement, light-coloured	3/9,30/6, 30/8, 30/9, 27/2	17	1548	1960	4672	0104	0161
Ooids	27/2, 30/9	11	0259	2615	0472	0051	0494
Shell,light-coloured	30/9	1	1687	1019	1727	0186	0000
Shell,dark-coloured	30/9	1	0529	1496	1448	1573	0000

Table 5-2
Average geochemical composition of the Kambe limestones. The numbers are arithmetic averages of the concentrations of the various elements in parts per million (ppm). NA indicates elements which were not analyzed for in some of the samples.

A total of 21 analyses were carried out on 10 samples for their carbon and oxygen stable isotope compositions. The results are presented as $\delta^{13}C$ and $\delta^{18}O$ in (permil) with reference to the PDB (Pee Dee Belemnite) standard. The $\delta^{18}O$ value with reference to the SMOW (Standard Mean Ocean Water) standard is also given (Table 5-3). Most of the isotopic analyses were carried out on the coarsely-crystalline vein cement as this was the most accessible. A number of whole rock analyses were also carried out.

5.1 RIM CEMENTS

These are common in most of the Kambe Limestone facies. They occur mostly as isopachous rims formed on the margins of grains. In the oolitic grainstone (oosparite) facies the rim cements form isopachous fringes around the ooids, sometimes with polygonal compromise boundaries between adjacent fringes. In the stained thin sections, rim cements occur as pink, non-ferroan calcite crystals.

Under cathodoluminescence, the rim cements occur as thin fringes of dark, non-luminescent crystals (equivalent to zone A cements in figure 5-1) around the interparticle pore margins. These are especially well-developed in the oolitic grainstone facies.

Trace element geochemical analysis of three samples with clearly distinguishable rim cements shows that out of 18 spot analyses for Fe, 8 have zero ppm concentration while the

maximum value is 4050 ppm. On the probe, the cement occurs as dark-grey and light-grey calcite crystals. On average, the dark-coloured rim cements contain 53 ppm Fe and are therefore essentially non-ferroan calcite. The dark-coloured rim cements show relatively high Mg contents of between 2316 and 5543 ppm and Mn content of up to 2641 ppm (Table 5-1). In the undifferentiated rim cements, the Mg content is up to 4957 ppm and the Mn concentration reaches 11,276 ppm. Sr and Ba concentrations are 389 and 815 ppm respectively. Eight out of ten spot analyses produced zero readings for Sr (Tables 5-1 and 5-2).

5.2 PORE-FILLING CEMENTS

These occur as inward-coarsening equant calcite in drusy mosaics and also as poikilotopic cements. Pore-filling cement post-dates the early-generation rim cement and occurs as both ferroan and non-ferroan calcite, the former occurring mostly towards the center of the pore-spaces. The pore-filling cements are generally more coarsely crystalline than the rim cements and they also occur as syntaxial overgrowths on echinoderm fragments.

Under cathodoluminescence, at least four main zones were identified in the pore-filling cement (Figure 5-1). These zones post-date the dark, non-luminescent rim cements (zone A cements) observed in the oolitic grainstones. Zone B is composed of a bright orange luminescent cement. This is

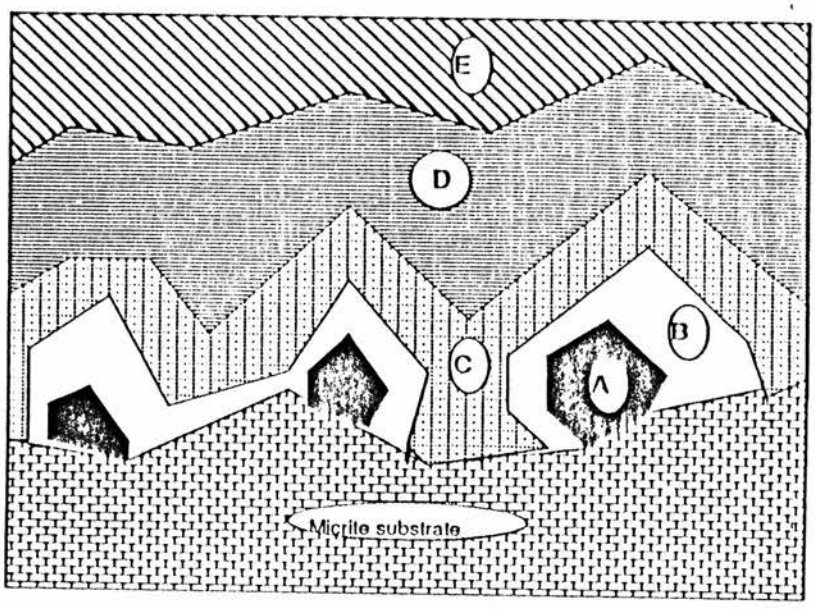

Figure 5-1
A typical cathodoluminescence pattern of the pore-filling cements from the Kambe limestones. Zone A is dark and non-luminescent, B is bright orange and C is dull brown with some bright bands. Zone D is dull brown with a few lighter-coloured patches while E is composed of alternating bright and dark-brown luminescent subzones.

followed by zone C, a dull brown luminescent zone with bright brown bands while the succeeding zone D is mainly dull brown with some lighter orange luminescent patches. The innermost zone E, (towards the center of the pore) is composed of thin subzones of alternating moderately bright and dull orange luminescence. The zoning presumably reflects differences in chemical composition of the pore waters during crystal growth. Most of the syntaxial overgrowths surrounding echinoderm fragments are composed of dark, non- luminescent cement.

Trace element geochemistry of the pore-filling cements shows that the zones which appear light-coloured under the microprobe contain up to 4049 ppm Fe. The dark-coloured pore-filling cements are generally low in Fe (with the exception of one value of 4711 ppm) content with a maximum

value of 808 ppm (Tables 5-1and 5-2). Lighter-coloured pore-filling cements show an average Fe content of 1548 ppm while the darker-coloured zones have, on average, 620 ppm Fe. The colour banding under cathodoluminescence and microprobe follow the same pattern except that the zonations under cathodoluminescence are much more finer. The CL is able to detect small differences in chemical composition of the crystal. The Mg content of the lighter-coloured zones of the pore-filling cement is up to 4612 ppm (with an average of 1960 ppm) while the darker zones contain, on average, 1577 ppm Mg with a maximum of 3251 ppm. Mn content varies from a maximum of 4003 ppm in the dark-coloured pore-filling cement to 17,566 ppm in the lighter-coloured zones. On average, the lighter zones contain 4672 ppm Mn compared with 1376 ppm in the darker ones. The lighter zones contain an average of 104 ppm Sr and 161 ppm Ba (Tables 5-1 and 5-2).

The dark-coloured crystals on the microprobe are poor in Fe and Mn while the lighter-coloured zones are particularly Mn-rich and contain intermediate amounts of Fe. The dark zones under the microprobe are non-luminescent under CL while the lighter zones are brightly luminescent. Under the CL, the luminescence is mostly a function of the Fe and Mn contents. Mn acts as the activator while the Fe is the inhibitor. The concentration of activators necessary for luminescence varies but generally, several tens of ppm of Mn are required and once the Fe concentration is beyond 2 wt % $FeCO_3$, the crystals do

not luminesce. In calcite and dolomite crystals, the luminescence and colour intensity relates to the ratio of Fe and Mn rather than to the actual concentrations of the elements. Other activators include Pb and rare earth elements while quenchers include Ni and Co (Tucker and Wright,1990).

Analysis of one sample for stable isotope composition produced values of -0.062 and -7.6 respectively for $\delta^{13}C_{pdb}$ and $\delta^{18}O_{pdb}$ (Table 5-3).

5.3 VEIN CEMENTS

Vein cement occurs as late-stage calcite, both ferroan and non-ferroan,which post-dates both the rim cements and the pore-filling cement. The veins cut through early cements and grains. Radiaxial fibrous calcite is a common type of vein cement in the Kambe limestones, especially in the biosparite facies. It occurs as inclusion-rich, non-ferroan, elongate calcite crystals with a radial fabric which pass into extremely coarse crystals of ferroan calcite. Some of the small veins are filled almost exclusively with crystals of ferroan calcite without the non-ferroan variety. Thin section staining revealed large-scale zoning of the coarse vein cements into pink-stained non-ferroan zones and bluish-purple ferroan ones.

Under cathodoluminescence the vein cements appear as dark non-luminescent bands, sometimes with a very thin brightly luminescent inner (presumably youngest) zone.

On the microprobe the vein cements appear as light, intermediate and dark-coloured zones. Geochemical analysis of the vein cements showed the dark-coloured zones to be low in Fe content (0 to 808 ppm, average 232) and the lighter zones to be ferroan with up to 3358 ppm Fe (average 879). The intermediate zone of vein cement contains between 1850 and 2005 ppm Fe with an average concentration of 324 ppm.

The Mg content of vein cement ranges from a maximum of 1025 ppm in the dark zone to 1363 ppm in the intermediate zone and 2720 ppm in the light-coloured zone. The average Mg concentrations are 647, 1451 and 1162 ppm for the dark, intermediate and light-coloured zones respectively.

Sample	Material sampled	δ13Cpdb	δ18Opdb	δ18Osmow
3/4a	Light coloured vein cement	0.368	-12.599	17.921
3/4b	Dark coloured vein cement	0.694	-3.847	26.944
3/4c	Whole rock	1.360	-3.831	26.961
26/3a	Saddle dolomite cement	3.179	-8.816	21.882
26/3b	Whole rock - dolomitic sample	2.655	-5.834	24.895
3/9a	Outer pore-filling cement	2.587	-3.080	27.734
3/9b	Inner pore-filling cement	2.871	-2.878	27.943
3/9c	Whole rock	2.867	-3.646	27.152
3/2a	Dark coloured vein cement	-0.324	-3.895	26.894
3/2b	Light coloured vein cement	0.302	-4.032	26.754
3/2c	Dark coloured vein cement	-0.811	-4.377	26.398
3/2d	Whole rock	1.244	-5.051	25.703
3/5a	Light coloured vein cement	1.095	-5.282	25.465
3/5b	Dark coloured vein cement	2.617	-2.518	28.314
3/5c	Whole rock	1.550	-4.802	25.960
3/5d	Clear late-fracture cement	1.693	-8.533	22.114
30/6	Pore-filling cement	-0.062	-7.600	23.075
30/7	Whole rock	0.959	-5.030	25.725
30/8	Whole rock	0.260	-6.302	24.413
30/9	Whole rock	-0.329	-4.939	25.819
30/10	Whole rock	0.071	-3.381	26.896

Table 5-3
Oxygen and carbon stable isotope data for the Kambe limestones. The figures are given in parts per thousand (permil).

Average Mn concentrations show a general increase from 1044 ppm in the undifferentiated zones (range 0 to 2540), 1563 ppm in the dark-coloured zones (range 457-5840), 2924 ppm in the intermediate zones (range 2773 to 3075) to 3456 ppm (range 457 to 7087) in the lighter-coloured zones (Tables 5-1 and 5-2).

Eight stable isotope analyses were carried out on 3 samples containing vein cement. The lighter-coloured vein cements contain between 0.302 and 1.693 $\delta^{13}C_{pdb}$ and from -4.032 to -12.599 $\delta^{18}O_{pdb}$ (Table 5-3). The isotopic composition of the darker-coloured vein cement varies between -0.324 and 2.617 $\delta^{13}C_{pdb}$ and from -2.518 to -4.377 $\delta^{18}O_{pdb}$.

5.4 DOLOMITE CEMENTS

Dolomite cements in the Kambe limestones occur as saddle (baroque) dolomite and also as discrete dolomite rhombs. The occurrence of saddle dolomite is not widespread and was identified in only one sample (26/3). Dolomite rhombs, probably both replacive and primary in origin, are common in the biopelmicrites and biopelsparites of the Kambe Formation. Crystalline dolomite occurs in one dolostone sample (27/10) which appeared to have undergone complete pervasive dolomitization to produce interlocked dolomite rhombohedra in a xenotopic mosaic. Dolomitization is commonly associated with dark brown (Fe ?) mineralization. Some of the dolomite has apparently reverted back to calcite by a dedolomitization

process to produce ferrous- mineral coated dedolomite rhombs. This was revealed in stained thin sections by the presence of unstained rhombs associated with blue-stained dolomite.

Microprobe analysis of the saddle dolomite cement revealed two zones, a dark and a light-coloured one. The darker zone is less ferroan, with a maximum Fe concentration of 707 ppm (Tables 5-1 and 5-2). This zone contains up to 5295 ppm Mg and 418 ppm Mn. The light-coloured zone is more ferroan with up to 2254 ppm Fe, 3781 ppm Mg and 340 ppm Mn. The main difference between the two zones is in their Fe content. The Mg concentration is too low for dolomite and a possible explanation for this is that the microprobe analysis might have been performed on a spot that has undergone dedolomitization. The Mg content is high enough to support a dolomite or a dolomitic precursor.

Carbon and oxygen stable isotope analysis produced values of 3.179 $\delta^{13}C_{pdb}$ and -8.816 $\delta^{18}O_{pdb}$ (Table 5-3) for the saddle dolomite cement.

5.5 DISCUSSION AND INTERPRETATION

The order of cementation for the Kambe limestones is rim cements followed by pore-filling cements and finally vein cements and dolomite. The cementation and diagenesis of carbonates can take place in many settings. These include the marine environment during deposition of the sediment, in near-surface environments where fresh-water penetrates the

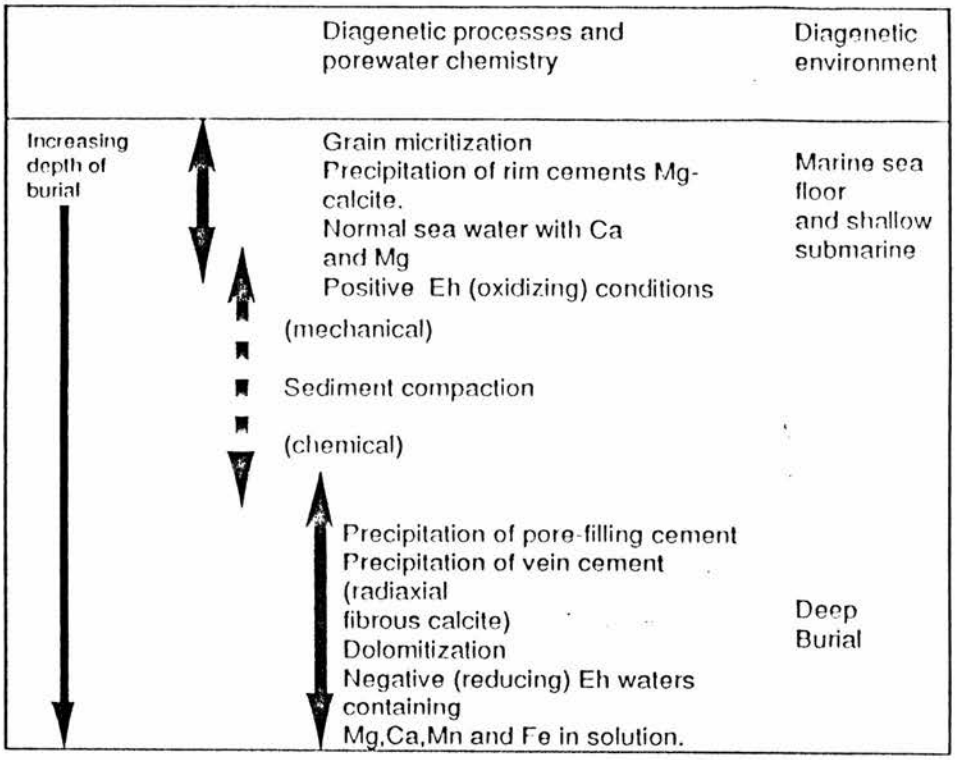

Table 5-4
A summary of the diagenetic processes, products and environments for the Kambe limestones

deposits, in subaerial settings produced by sea-level fall, in mixing zones between waters of different chemistries or in the brines of the deeper subsurface (Harris *et al*,1985). The nature of the end-product of diagenesis is determined by the composition of the original sediment, the nature of the interstitial fluids and their movements and the physical-chemical processes and the time scale involved (Scoffin,1987). Shallow marine carbonates enter the burial environment through one of two routes. They may be buried directly from the marine environment or they may be affected by meteoric processes first (Tucker and Wright,1990).

A two-stage diagenetic model is suggested here for the Kambe limestones. Table 5-4 shows a summary of the processes, products and environments of the diagenesis of the Kambe

limestones according to the adopted diagenetic model. This model involves an early diagenetic phase on or near the environment of deposition (sea-floor to shallow marine diagenesis) followed by late diagenesis in the deep burial environment. Figure 5-2 shows a plot of d13 C and d18 O values for the Kambe limestones. The values are within the range of marine limestones and the general depletion in $\delta^{18}O$ is characteristic of deep burial late cements. Most of the material analyzed for isotopic composition was sampled from the deep burial cements. The depletion in $\delta^{18}O$ is believed to result from absence of meteoric diagenesis and subaerial exposure in the Kambe limestones is inferred from the lack of significant depletion in $\delta^{13}C$ as shown in figures 5-3 and 5-4. Limestones which have suffered meteoric diagenesis and meteoric exposure would be expected to show shifts of $\delta^{13}C$ towards more negative values (Allan and Matthews,1982; Walkden and Williams,1991).

5.5.1 Shallow Marine Diagenesis

The early stage of diagenesis in the shallow marine environment occurs at the sediment-water interface or just below it. Diagenesis on the sea-floor mainly involves the precipitation of cements and the alteration of grains by microbial micritization and boring by organisms. In this environment the sediment is subjected to alternating erosion and deposition and prolonged exposure to sea-water

supersaturated with respect to $CaCO_3$ (especially in shallow tropical seas). Micritization of grains is most prevalent in the quiet water locations while cementation is widespread in areas of high current activity (Bathurst,1971; Tucker and Wright,1990).

5.5.1.1 *Micritization*

In the Kambe limestones micritization of grains is prevalent, especially in the biomicrite and the biopelmicrite facies. This probably took place within a stagnant marine phreatic environment in which there was little sediment or pore-water movement (Tucker and Wright,1990). In such environments, cementation is limited and this is consistent with the low amounts of cement in the biomicrites and biopelmicrites of the Kambe limestones. Formation of micrite

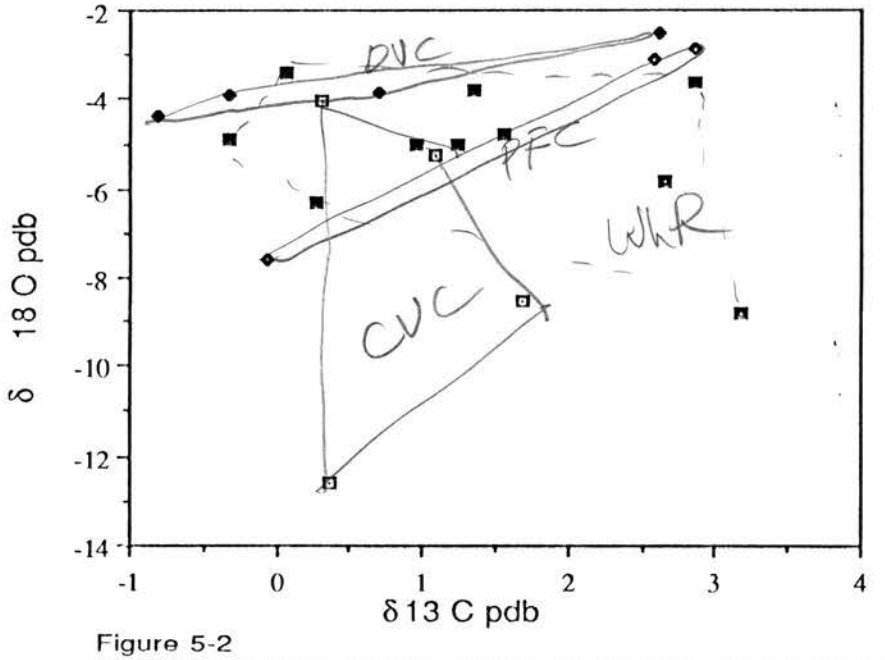

Figure 5-2
Carbon and oxygen stable isotope plot for the Kambe Limestones.
□ clear vein cements ◆ dark vein cements ■ saddle dolomite
◇ pore-filling cements ■ whole rock samples

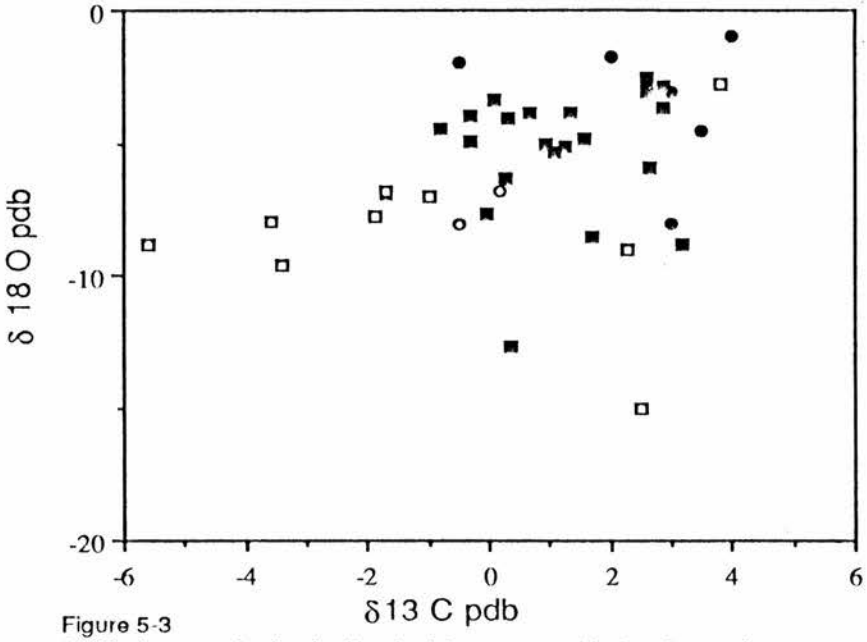

Figure 5-3
Stable isotope plot for the Kambe Limestones with data form other sources for comparison.
■ Kambe Limestone ▫ Walkden & Williams,1991 o Wilkinson et al, 1985
● Moldovanyi & Lohmann,1982

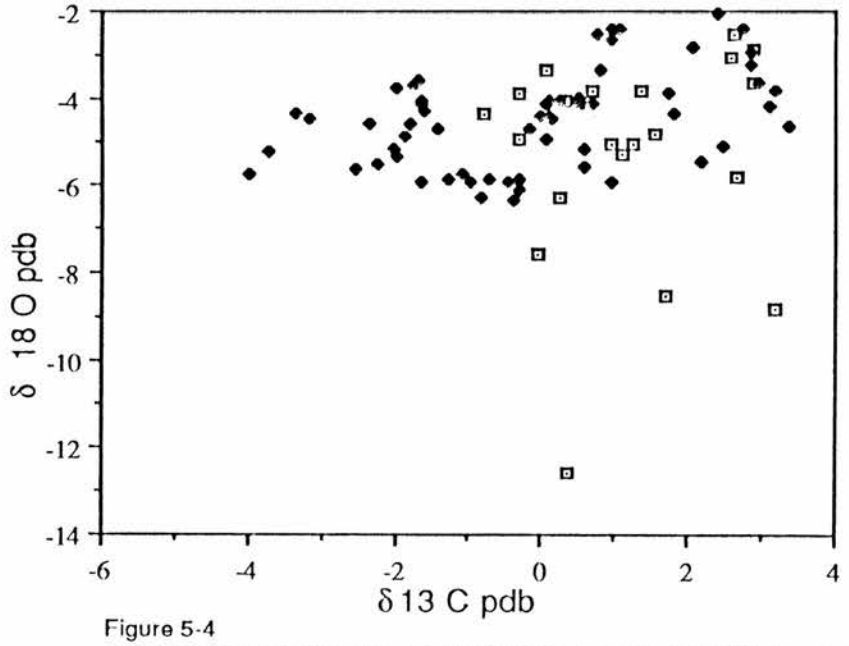

Figure 5-4
Stable isotope plots for the Kambe Limestone compared with those of a limestone that has undergone subaerial exposure and meteoric diagenesis.
▫ Kambe Limestones ◆ Allan & Matthews,1982

envelopes around bioclastic grains and the hardening of faecal pellets to produce the high proportion of peloids is believed to have taken place in this environment. Micrite envelopes from precipitation at high temperature (Walls et al,1979). The result from the centripetal micritization of grains (Bathurst,1971). Prezbindowski (1985) reported that micrite envelopes as the products of marine diagenesis are ubiquitous in the carbonates of the Stuart City Trend, with a mineralogy of Mg-calcite subsequently stabilized to calcite (1230 ppm Mg^{2+}).

5.5.1.2 *Cementation*

Cementation in the shallow marine environment occurs mainly in the active marine phreatic zone where pore-waters are continually replenished, especially in reefs and sand shoals. The cements are initially deposited within the bioclasts in intraskeletal pores, shells and tests. The cementation of intergranular pore-space results in the formation of hardgrounds (Tucker and Wright,1990). This cementation model is applicable to the Kambe Limestone oosparite and biosparite facies. The product of this cementation process is the first-generation of isopachous rim cements on the margins of grains and within the intraskeletal pore-space.

The first-generation cement is rim cement. This is non-luminescent and includes material which is

undifferentiated or dark-coloured on the microprobe. The Fe content is low (average 53 ppm in the dark zones and 909 ppm in the undifferentiated zone). The higher average values of Fe in the undifferentiated rim cements could be the result of precursor high-Mg calcite preferentially taking up iron in the pore-waters (Tucker and Wright,1990). The high Mg content (averaging 2098 ppm in the undifferentiated zones and 3763 ppm in the dark zones) is consistent with calcite of marine origin. This cement generation was precipitated as high-Mg calcite which has since stabilized to low-Mg calcite. The high-Mg calcite precursor is supported by the high Mg concentration and the low Sr (average 58 ppm) content of the rim cement. Low Sr is indicative of a lack of aragonite or aragonite-dominated precursors. Originally aragonitic cements would have high Sr content (1900 ppm) and lower Mg (200 ppm) while calcite-dominated precursors would be expected to have high Mg (3700 ppm) and Sr as low as 400 ppm (Scoffin,1987). Calcite-precursor cements were presumably deposited as both equant and acicular high-Mg calcites which subsequently stabilized to low-Mg calcite during migration of thin fluid fronts, a process which resulted in retention of the original crystal morphology (Wilkinson *et al*,1985). Originally calcitic, isopachous cements are reported to be a common occurrence in Jurassic hardgrounds (Sandberg,1985 ; Meyers and Lohmann,1985).

The isotopic composition of the early marine cements

was not determined. This was due to their small crystal sizes which made them very difficult to sample. Whole rock isotopic compositions for 4 samples of the Kambe Limestone oosparites averaged $\delta^{13}C = +0.29$ and $\delta^{18}O = -4.9$. This compares reasonably well with typical $\delta^{13}C$ and $\delta^{18}O$ values for limestones of marine origin and their early cements, of $\delta^{13}C = +1$, $\delta^{18}O = -2$ and $\delta^{13}C = -1$ and $\delta^{18}O = -4$, respectively (Scoffin,1987). The average isotopic values for the Kambe Limestone oosparites are within the range reported for common marine limestone (Hudson,1977).

5.5.2 Late Burial Diagenesis

The most important feature of deep burial diagenesis in the Kambe limestones was the precipitation of cements. Compaction, though evident from the presence of broken micrite envelopes and the occasional splayed oolitic laminae is interpreted as having been an insignificant feature of deep burial diagenesis. Absence of sutured grain contacts in the oolitic facies testifies to the lack of appreciable compaction effects. Stylolites which would normally result from mechanical compaction are also absent. The small amount of compaction noted is thought to have occurred during and after shallow marine diagenesis but before late burial cementation. It is suggested that precipitation of shallow diagenetic cements played a significant role in the restriction of the effects of mechanical compaction caused by sediment loading.

5.5.2.1 *Late burial cements*

Burial cements post-date early cements and compaction features. They are commonly coarse-grained and poikilotopic because they grow at relatively low levels of supersaturation (Scholle and Halley,1985). Increased temperature with burial (dependent on the geothermal gradient) speeds up reactions such as dolomite precipitation. In the Kambe limestones, a geothermal gradient of 30°C /km (as reported from the Kencan-1 well) indicates maximum temperatures of between 60° and 130°C for the Jurassic limestones (taking 1152m and 3595m as the Formation top and bottom respectively).

In the Kambe limestones late burial cementation is represented by coarse pore-filling equant spar, coarse fracture-filling radiaxial fibrous calcite and saddle dolomite. Poikilotopic and syntaxial spar are also common late burial cements. Poikilotopic spar may have resulted from the very slow nucleation rate of calcite and very slow growth in pore fluids only just supersaturated with respect to $CaCO_3$. Syntaxial calcite is a common feature of grainstones containing echinoderm fragments and the crystals may be large enough to show poikilotopic texture (Tucker and Wright,1990).

The pore-filling cements are slightly ferroan (with up to 0.61 mole % $FeCO_3$) especially towards the centers of the pores. Some of the pore-filling cements have a very high Mn concentration, above 17,000 ppm (Table 5-1). These inner-pore

cements are marked by a bright subzoned luminescent band. The subzones indicate relatively short periods of pore-water stagnation and the precipitation of Mn-bearing calcite. The zone marks the onset of permanently reducing conditions where Mn^{2+} is present in pore-water and Fe^{2+} is removed out through sulphate reduction (Tucker and Wright,1990). Sector zoning in calcites and dolomites often indicates very small differences in the Mn^{2+} concentrations between different zones (Reeder and Grams,1987).

On a ternary plot showing the concentrations of the trace elements in the Kambe limestones, almost all the cements plot along the Mg-Mn line (Figure 5-5 and 5-6). The values are plotted as percentages of the trace element out of a total of the three elements (Mn + Mg + Fe =100%). As would be expected, there is a general increase in Mn and Fe from very low in the ooids and micrite to moderate in the rim cements and the highest values are in the vein cements (Figure 5-5). The pore-filling cements show a wide range of trace element concentration from low to high Mn and low to moderate Fe (Figure 5-6). Mg is the dominant trace element in the Kambe limestones and this is consistent with the argument that the grains and cements were originally composed of magnesian calcite. Both Fe and Mn are assumed to be in their divalent state which is unlikely in open marine waters and many meteoric waters where the Fe is oxidized to Fe^{3+} and Mn to Mn^{3+} or Mn^{4+} (Tucker and Wright,1990). The much larger radii of the

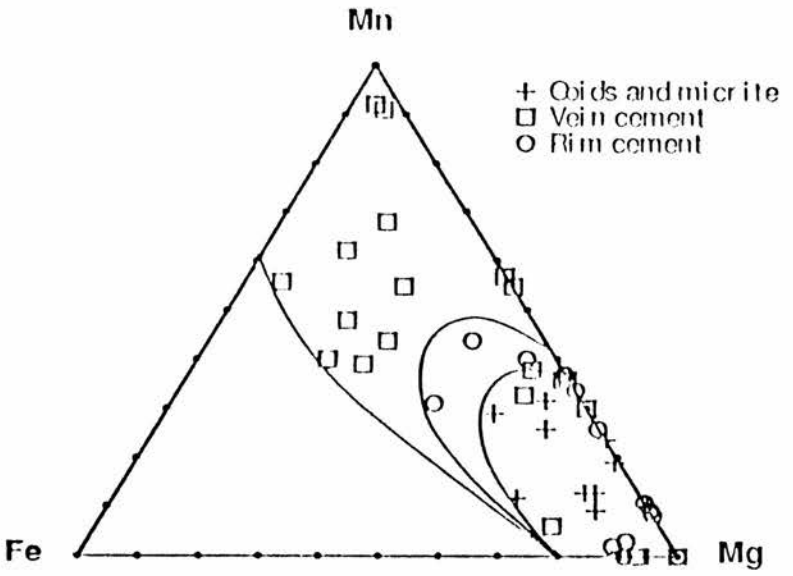

Figure 5-5
A triangular plot for the trace element composition of the ooids, micrite, vein cements and rim cements of the Kambe limestones.

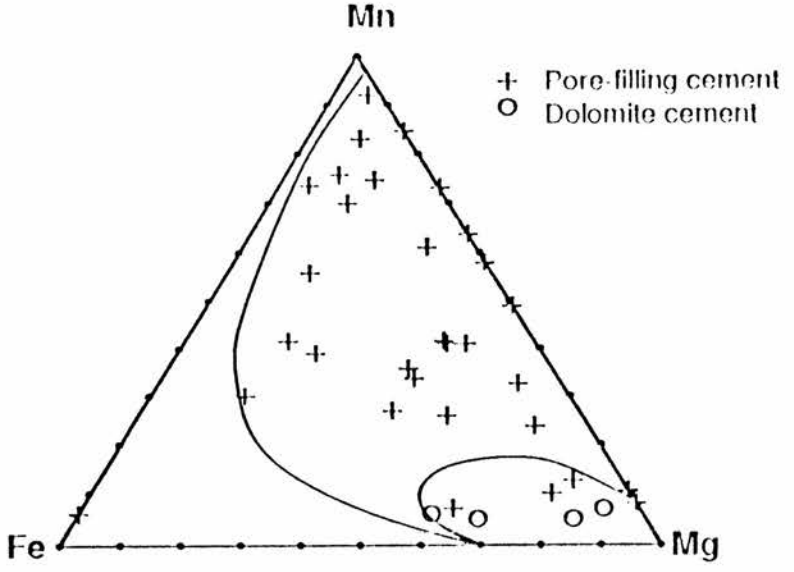

Figure 5-6
A triangular plot for the trace element composition of the vein and dolomite cements from the Kambe limestones.

oxidized ions make them unsuitable for substitution into the calcite lattice. Mg is not affected by changes in redox potential. Calcites rich in Fe and Mn are likely to be formed in the deeper burial environment which offers favourable redox conditions.

The average isotopic composition of the pore-filling spar is $\delta^{13}C = +2.7$ and $\delta^{18}O = -3$. These values are within the ranges reported for common marine limestones (Hudson,1977).

Radiaxial fibrous calcites have been recognized as common cavity-fill cements in marine phreatic environments (Kendall,1985). The radiaxial crystals are inclusion-rich and were probably magnesian calcites originally. In the Kambe limestones, the radiaxial crystals contain up to 1.12 mole % $MgCO_3$ indicative of formerly high-Mg calcite. The Fe and Mg concentrations vary between the different zones of the radiaxial crystals. Alternating clear and inclusion-rich bands indicate the crystal growth zones.

The vein cements in the Kambe limestones have an overall average isotopic composition of $\delta^{13}C= +1$ and $\delta^{18}O = -5$ (Table 5-3 and figure 5-2). The average values vary from +0.9 to +0.5 for $\delta^{13}C$ and -7.6 to -3.7 for $\delta^{18}O$ in the clear vein cement and the dark vein cement respectively. The isotopic values are within the range of Jurassic late cements and marine limestones (Hudson,1977). Prezbindowski (1985) reported values for the isotopic composition of Cretaceous radiaxial fibrous calcites from the Stuart City Trend

averaging $\delta^{13}C$= +2 and $\delta^{18}O$ = -2.5 which he concluded was compatible with precipitation from water of $\delta^{18}O$ = 0 to +1 and indicated little or no neomorphic alteration. The depletion in $\delta^{18}O$, as in the Kambe Limestone cements (Figure 5-2), may have resulted from isotopic re-equilibration at elevated burial temperatures where the original $\delta^{13}C$ values are retained while $\delta^{18}O$ becomes lighter (Walls et al,1979).

Using the oxygen isotope fractionation for palaeotemperature reconstruction (Craig,1965) and assuming a Jurassic sea-water $\delta^{18}O$ value of -1 (Hudson,1977), the Kambe Limestone radiaxial fibrous calcite cements appear to have been precipitated at temperatures of between 35 and 50°C. This indicates minimum burial depths of between 330 and 830m (assuming the present geothermal gradient of 30°C/km and a surface temperature of 25°C). Homogenization temperatures of fluid inclusions in the vein cements are in the range of 59° to 95°C. Some of the fluid inclusions in the Kambe Limestone burial cements contain hydrocarbons. This was confirmed by dull-orange fluorescence when the thin sections were viewed under ultraviolet light.

Baroque (saddle) dolomite in the Kambe limestones contains up to 0.4 mole % $FeCO_3$ and between 1.54 and 2.58 mole % $MgCO_3$. It is relatively poor in Mn (418 ppm Mn). The high Fe content supports a burial origin for the saddle dolomite since burial cements containing high concentrations of Fe are common products of environments where formation waters were saline

and reducing (Glover and Read,1983). Late diagenetic and post-tectonic precipitation of saddle dolomite is indicated by its occurrence in veins, stylolites and tectonic breccias and its association with hydrocarbon occurrences and base metal sulphide mineralization (Radke and Mathis,1980).

The isotopic composition of the saddle dolomite is approximately $\delta^{13}C = +3$ and $\delta^{18}O = -9$ (Table 5-3 and Figure 5-2). This oxygen isotope composition is indicative of precipitation at temperatures of between 80° and 85°C (using the fractionation conversion after Land,1983). This is within the reported temperature range of saddle dolomite formation of between 60° and 150°C (Radke and Mathis,1980). The depletion in $\delta^{18}O$ of burial dolomites indicates precipitation at high temperatures and/or from depleted waters (Tucker and Wright,1990).

Plate 5-1

A cathodoluminescence photograph of a Kambe Limestone oosparite (sample 30/6). Note the first-generation, non-luminescent, rim cement (arrows) which is succeeded by coarser, luminescent , pore-filling cement. Early compaction is evident from the lack of early cement at the grain contacts (lower right). X 100

Plate 5-2

Cathodoluminescence photograph of another Kambe Limestone oosparite (sample 27/2). The pore-filling cements show about 5 major cathodoluminescence bands (marked in black). The arrow indicates the direction of crystal growth. Note evidence of early compaction and the zoning in the ooids. X 50

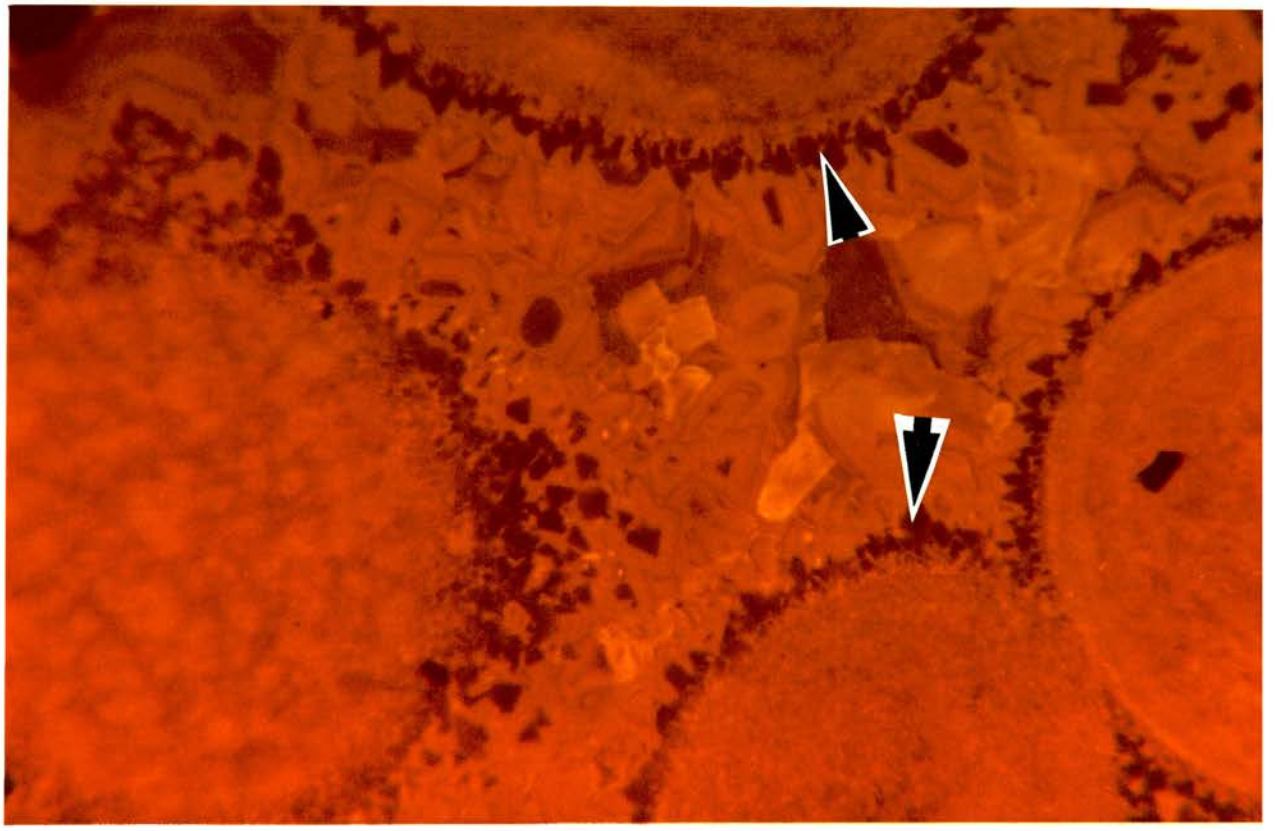

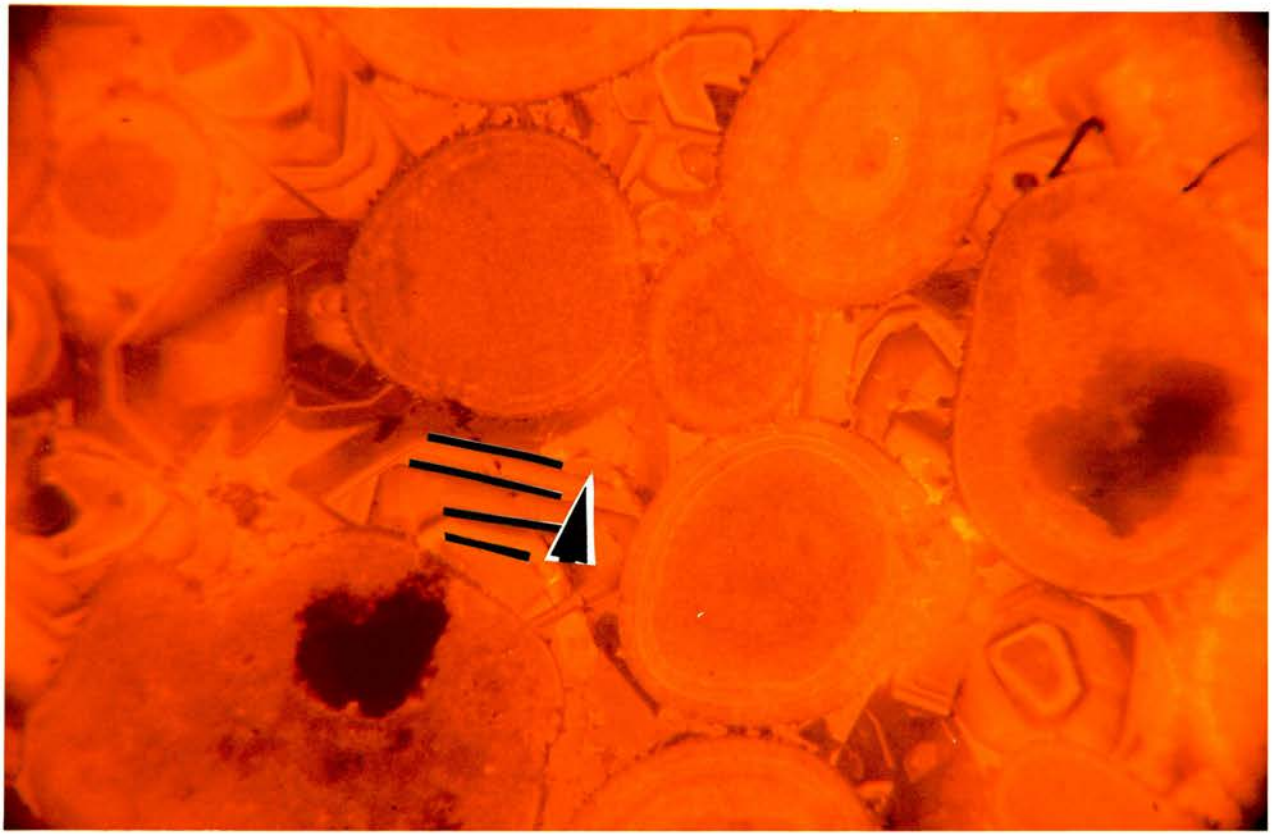

Plate 5-3

The typical cathodoluminescence pattern of the Kambe Limestone pore-filling cement (sample 3/9). 5 zones are identified (arrowed) with the pore center towards the right (see figure 5-1 for interpretation of the zones). X 50

Plate 5-4

A different view of the Kambe Limestone pore-filling cement. X 50

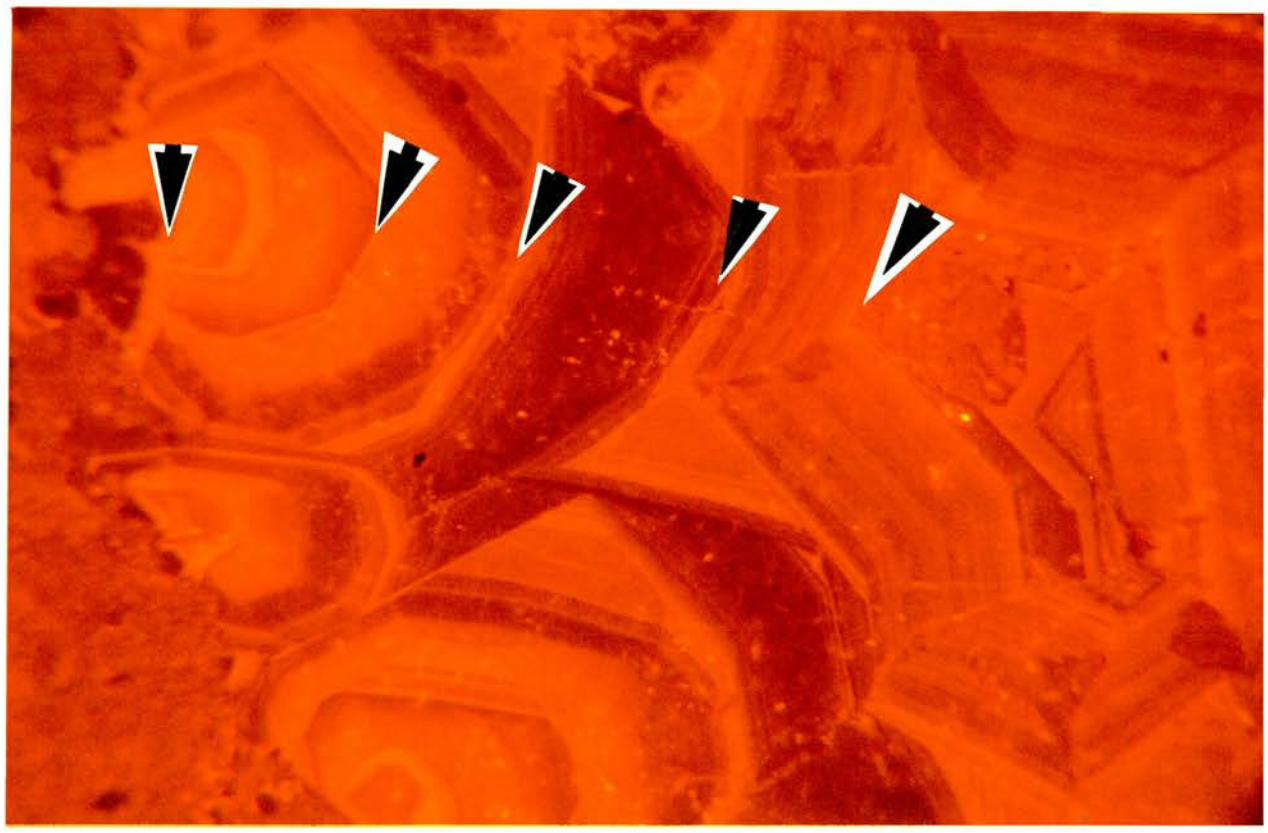

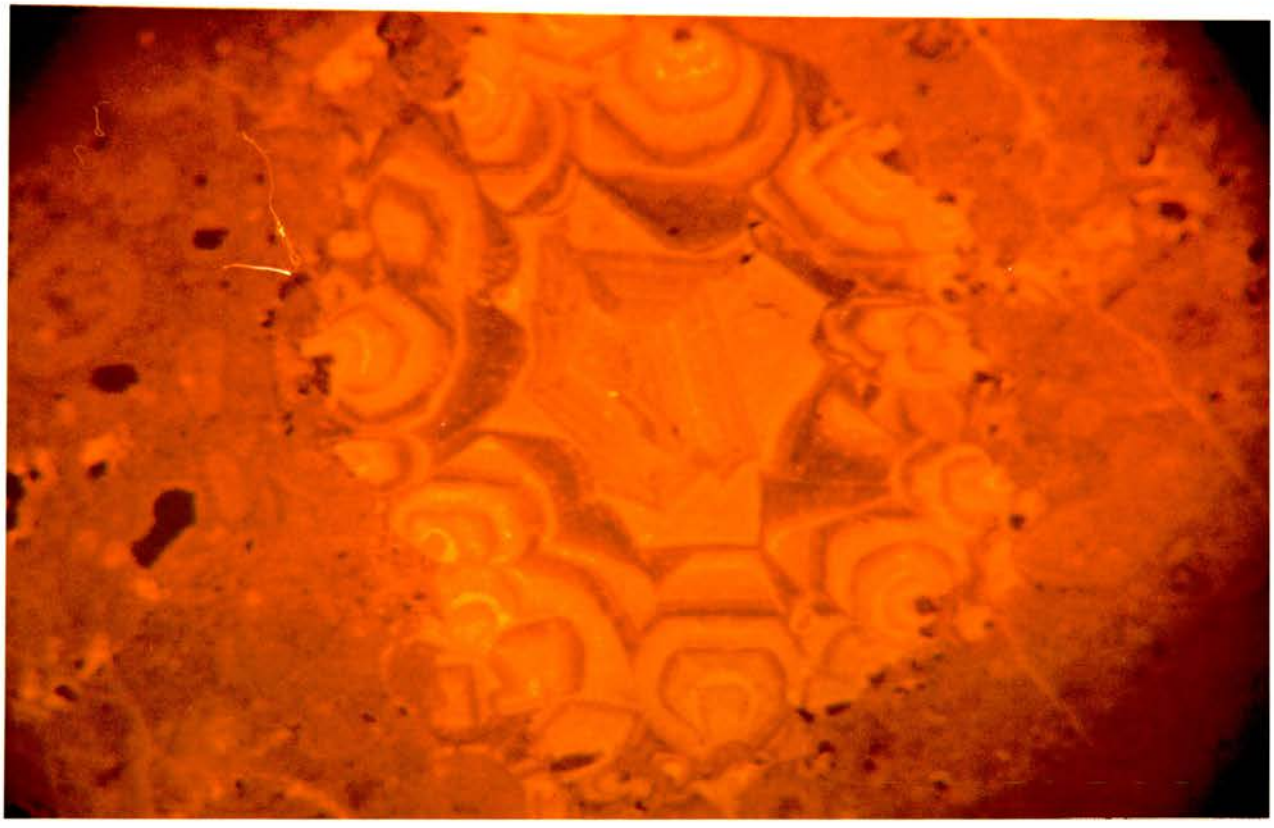

Plate 5-5

The cathodoluminescence pattern displayed by cement precipitated on a brachiopod shell fragment in an oosparite (sample 27/2). The cement shows a columnar habit but the overall cathodoluminescence pattern is similar to previous pictures i.e. a non-luminescent zone followed by banded zones of varying luminescence. X 125

Plate 5-6

The cathodoluminescence pattern of cement filling a recrystallized gastropod in an oosparite (sample 27/2). Note the mainly non-luminescent inner cement while the outer parts of the gastropod contain luminescent cement. X 125

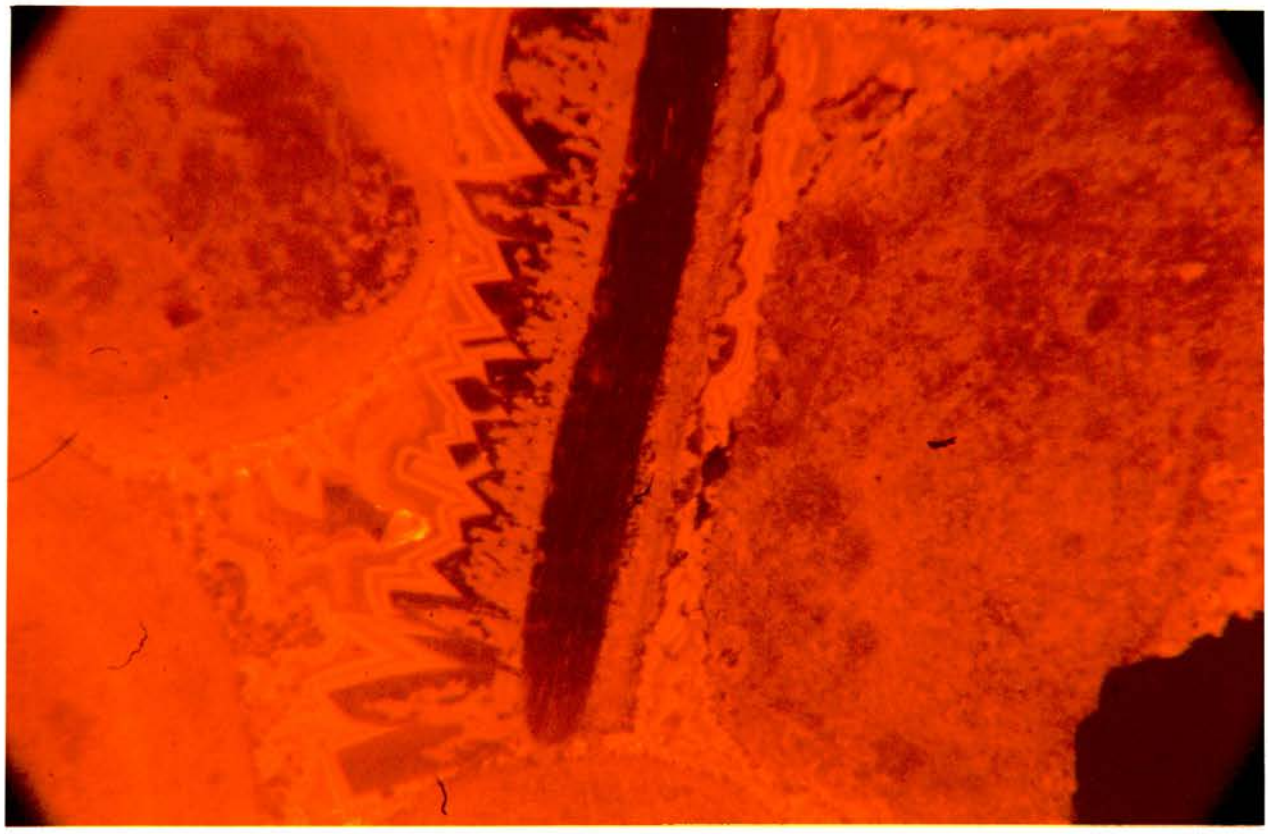

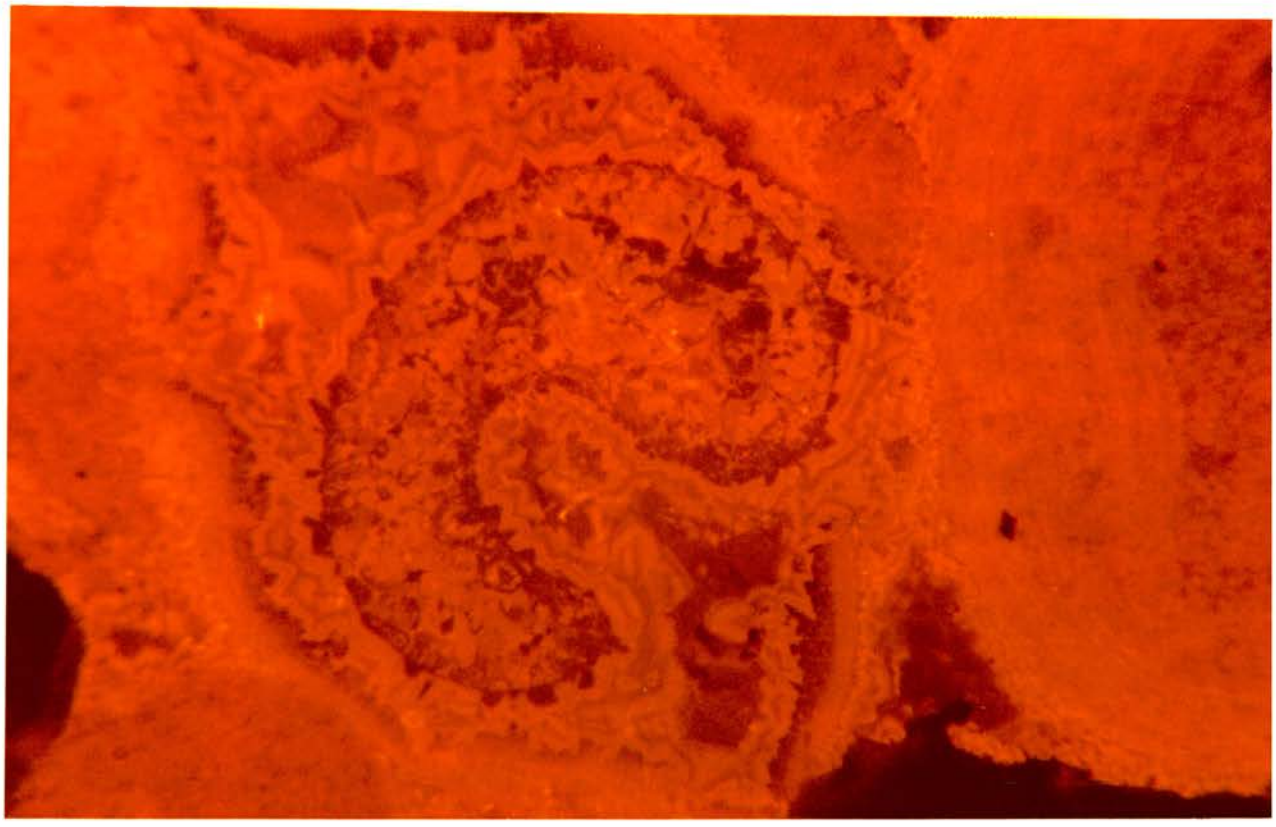

Plate 5-7

A backscatter photograph of a Kambe Limestone oosparite (sample 30/6). Microprobe analyses were carried out on the ooids and the light and dark-coloured zones of the pore-filling cement. The dark cement was found to be Fe- and Mn-deficient while the lighter-coloured zones were found to Mn-rich and contained intermediate amounts of Fe (Table 5-1 and 5-2).

Plate 5-8

In this backscatter photograph of an oosparite (sample 30/8), the early rim (dark) cement can be distinguished from the later pore-filling (lighter-coloured) cement. The rim cement would appear non-luminescent on the CL.

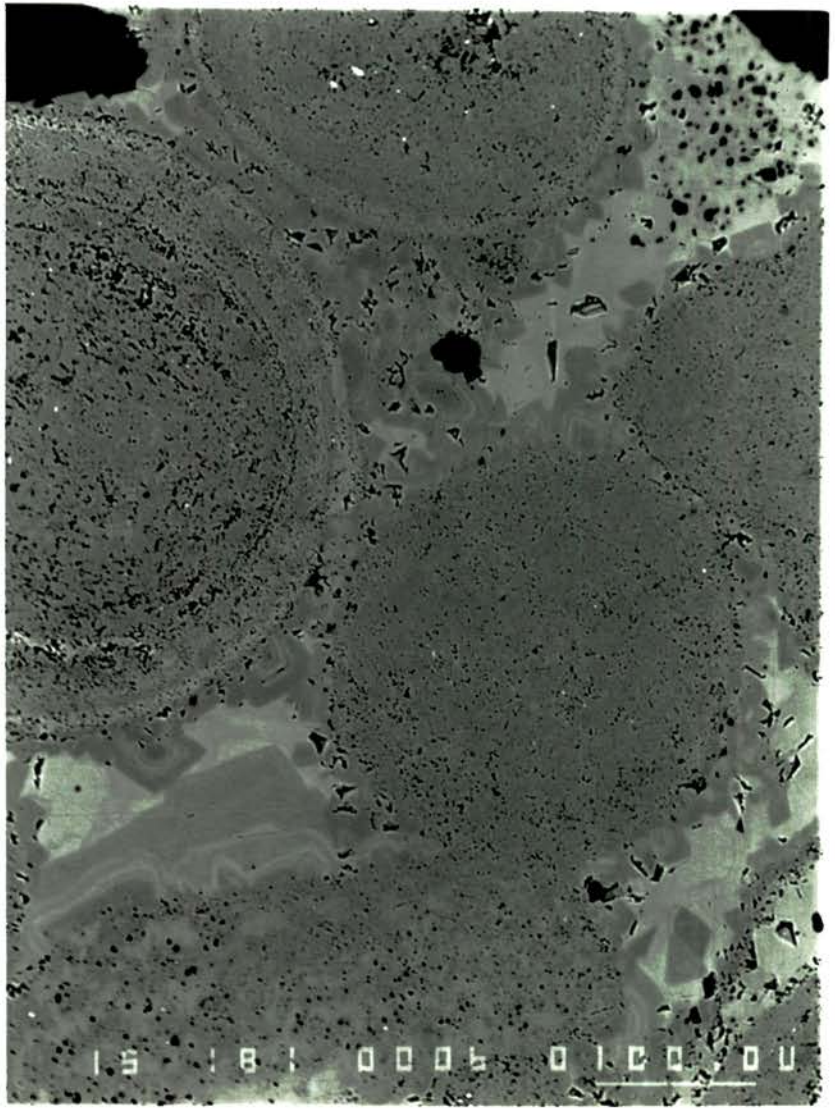

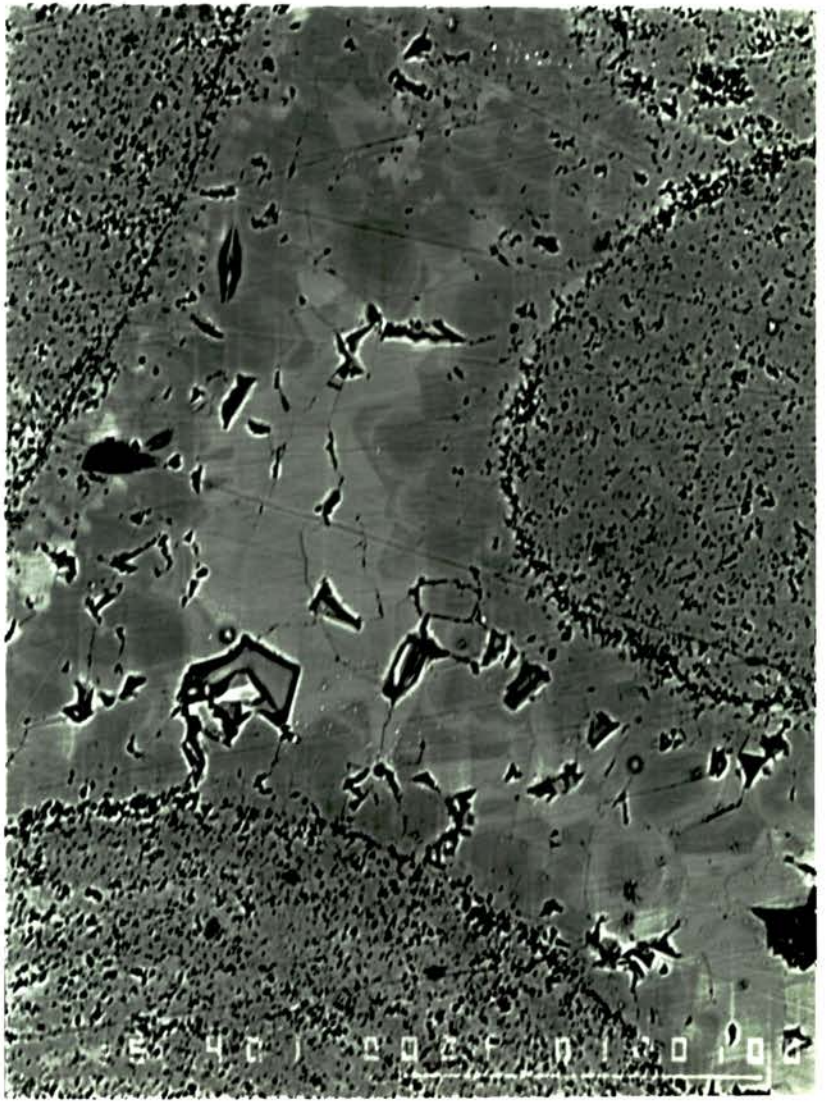

6.0 SUMMARY AND CONCLUSIONS

A review of the stratigraphy of the Lamu Embayment was carried out from published data sources, along with a consideration of the basin development. The evolution of the Lamu Embayment followed a path typical of the development of Atlantic-type passive margins i.e. starting with continental rifting followed by initiation of sea-floor spreading and finally the formation of the mature passive margin.

A petrographic study of the Jurassic/Cretaceous sediments has concentrated mainly on the Kambe limestones and 6 petrofacies have been recognized based mainly on their composition. A few samples of the Mazeras sandstones have also been investigated.

Based on facies analysis, a model for the deposition of the Kambe limestones is suggested. The facies association indicates deposition in a restricted marine shelf environment.

On the evidence of cement petrography, isotopic composition and trace element geochemistry, diagenesis of the Kambe limestones took place in two stages. Early diagenesis occurred on the seafloor and shallow burial environments where early rim cements were precipitated and bioclastic grains were micritized. Late diagenesis took place in the deep burial environment where pore-filling cements and vein cements were precipitated. Some dolomitization occurred during deep burial.

Based on thin section porosity evaluation, the Mazeras

sandstones have poor reservoir rock potential with porosity ranging from 3.1% to 7.8%. This is partly due to the extensive cementation by quartz overgrowths and clay. Most of the porosity is secondary, resulting from the leaching and dissolution of feldspars probably enhanced by surface weathering. The secondary pores appear to be well interconnected and the rock may have some (? significant) permeability. This needs to be quantified and the subsurface porosity might be expected to even lower than the reported values. It should be borne in mind that the small number of samples examined may not be fully representative of the Mazeras Formation.

A total of 20 samples from various facies of the Kambe limestones were point-counted for porosity evaluation. Out of these, 11 had below 1% porosity while the highest value was only 4.7%. This means that the Kambe limestones have poor reservoir rock potential. Extensive cementation by calcite in the submarine and deep burial environments is to blame for the porosity occlusion. Late fractures that might have enhanced porosity have been filled with calcite cement and there is no evidence of secondary dissolution. Dolomitization is not extensive but where present, it significantly improves the porosity of the Kambe limestones.

Some fluid inclusions in the coarse vein cements contain hydrocarbons signifying that at some time during or prior to the emplacement of these cements, hydrocarbons had been

generated within the basin.

The dark grey biopelmicrites from the Rare River section of the Kambe Formation may contain sufficient organic matter to be of interest as source rock but this was not quantified.

The samples from the Freretown Limestones have good to excellent porosity ranging from 15.7% to 24.2%. If the same kind of porosity exists in the subsurface, then the Freretown Limestone are excellent reservoir targets.

REFERENCES

Adams,A.E., MacKenzie,W.S. and Guilford,C. 1984. *Atlas of Sedimentary Rocks under the Microscope.* Longman, London.104p

Allen,P.A. and Allen,J.R. 1990. *Basin Analysis: Principles and Applications.* Blackwell, Oxford.451p

Bathurst,R.G.C.1971.Carbonate Sediments and their Diagenesis. *Developments in Sedimentology,* **12**. Elsevier, Amsterdam.

Bosellini,A.1986. East Africa Continental Margins. *Geology* **14**,76-78

Canon,R.T.,Simiyu-Siambi,W.M.N. and Karanja,F.M.1981. The Proto-Indian Ocean and a probable Palaeozoic/Mesozoic triradial rift system in East Africa. *Earth and Planetary Science Letters* **52**, 419-426

Caswell,P.V.1953. Geology of the Mombasa-Kwale Area. *Geological Survey of Kenya Report* No.**24**

Caswell,P.V.1956. Geology of the Kilifi-Mazeras area. *Geological Survey of Kenya Report* No.**34**

Coffin,M.F. and Rabinowitz,P.D.1988. Evolution of the Conjugate East African-Madagascan Margins and the Western Somali Basin. *Geological Society of America Special Paper* **226**, 77p.

Craig,H.1965. The measurement of oxygen isotope palaeotemperatures. In: *Stable isotopes in oceanographic studies and palaeotemperatures* (Ed. by E.Tongiorpi). Consiglio Nazionale delle Richerche, Laboratorio di

Geologia Nucleare, Pisa, 1-24

Dickson,J.A.D.1966. Carbonate identification and genesis as revealed by staining. *Journal of Sedimentary Petrology* **36**,491-505

Dodson,R.G.1966. Geology of the Lali Hills-Dakadima Area. *Geological Survey of Kenya Report* No.**76**

Dunham,R.J.1962. Classification of Carbonate Rocks according to Depositional Texture.In: *Classification of Carbonate Rocks* (Ed. by W.E.Ham). American Association of Petroleum Geologists Memoir **1**, 108-121

Enos,P.1983. Shelf.In: *Carbonate Depositional Environments* (Ed. by P.A.Scholle,D.G.Bebout and C.H.Moore). American Association of Petroleum Geologists Memoir **33**, 507-538

Folk,R.L.1962.Spectral subdivision of limestone types. In:*Classification of Carbonate Rocks* (Ed. by W.E.Ham). American Association of Petroleum Geologists Memoir **1**, 62-84

Folk,R.L.1974. *Petrology of Sedimentary Rocks*. Hemphills, Austin, Texas.154p.

Gregory,J.W.1921.*The Rift Valleys and Geology of East Africa*. Seeley, London

Grover,G.Jr and Read,J.F.1983. Palaeoaquifer and deep burial related cements defined by regional cathodoluminescence patterns, Middle Ordovician carbonates, Virginia. *The American Association of Petroleum Geologists Bulletin* **67**, 1275-1303

Heckel,P.H.1972. Recognition of shallow marine environments. In : *Recognition of ancient sedimentary environments* (Ed. by J.K.Rigby and W.K.Hamblin). Special Publication of the Society of Economic Palaeontologists and Mineralogists **16**, 226-286

Hudson,J.D.1977. Stable isotopes and limestone lithification. *Journal of the Geological Society, London* **133**, 637-660

James,N.P.1979. Facies models 10. Shallowing-upwards sequences in carbonates. In: *Facies Models* (Ed. by R.G.Walker) Geoscience Canada Reprint Series 1, 109-119.

Karanja,F.M.1980. Geology of the Mapotea-Silaloni Area. Coastal Geology Project, North Coast. *Geological Survey of Kenya Report*

Karanja,F.M.1984. *Excursion Guide to the Geology of the Mombasa Lamu Basin west of Mombasa*. Ministry of Energy & Regional Development. Nairobi, Kenya

Kendall,A.C.1985. Radiaxial fibrous calcite:a reappraisal. In:*Carbonate cements* (Ed. by N.Schneidermann and P.M.Harris). Special Publication of the society of Economic Palaeontologists and Mineralogists **36**, 59-77

Kent,P.E.1972. Mesozoic history of the East coast of Africa. *Nature* **238**, 147-148

Kent,P.E. 1982. The Somali ocean Basin and the continental margin of East Africa. In :*The ocean Basins and Margins, The Indian Ocean* (Ed. by A.E.M.Nairn and F.G.Stehli) **6**, 185-204

Kent,P.E. and Perry,J.T.O'B.1973. The development of the Indian Ocean margin in Tanzania. In: *Sedimentary Basins of the African coasts, part 2. South* (Ed. by G.Blant). Association of African Geological Surveys Paris 113-131

Land,L.S.1983. The application of stable isotopes to the study of the origin of dolomite and to problems of diagenesis of clastic sediments. In: *Stable isotopes in sedimentary geology* (Ed. by M.A.Arthur and T.F. Anderson). Society of Economic Palaeontologists and Mineralogists short course No.**10**, 4.1-4.22

Lawyer,L.A., Coffin,M.F. and Gahagan,L.1990. The Mesozoic breakup of Gondwanaland. *Paper presented at the Indian Ocean 1st regional seminar on petroleum exploration.* Seychelles, 1990.

Majewske,O.P.1969. *Recognition of Fossil fragments in Rocks and Thin Sections.* E.J.Berill, Leider, Netherlands

McKinnon-Wood,M.1930. Reports on the Geological collections from the coastlands of Kenya colony. *Monographs of the Geological Department of the Hunterian Museum Glasgow University* **IV**, 232p

McKinnon-Wood,M.1938. On a second Collection of Fossils and Rocks From Kenya. *Monographs of the Geological Department of the Hunterian Museum Glasgow University* **V**, 116p

Meyers,W.M. and Lohmann,K.C.1985. Isotope geochemistry of regionally extensive calcite cement zones and marine

components. In: *Carbonate cements* (Ed. by N.Schneidermann and P.M. Harris).Special Publication of the Society of Economic Palaeontologists and mineralogists **36**, 223-239

Miller,J.M.1952. Geology of the Mariakani-MacKinnon Road Area. *Geological Survey of Kenya Report* No.**20**

Moldovanyi,E.P. and Lohmann,K.C.1984. Isotopic and petrographic record of phreatic diagenesis: Lower Cretaceous Sligo and Cupido Formations. *Journal of Sedimentary Petrology* **54**, 972-985

Nyagah, K.1992. *Stratigraphy,depositional history and environments of deposition of Cretaceous through Tertiary strata in the Lamu Basin, Southeast Kenya and implications on hydrocarbon exploration.* National Oil Corporation of Kenya Unpublished report.

Prezbindowski,D.R.1985. Burial cementation-is it important? A case study, Stuart City Trend,South central Texas. In : *Carbonate cements* (Ed. by N.Schneidermann and P.M.Harris). Special Publication of the Society of Economic Palaeontologists and mineralogists **36**, 241-264

Rabinowitz,P.D.,Coffin,M.F.and Falvey,D.1982. Salt diapirs bordering the continental margin of northern Kenya and southern Somalia. *Science* **215**, 663-665

Rabinowitz,P.D.,Coffin,M.F. and Falvey,D.1983. The separation of Africa and Madagascar. *Science* **220**, 67-69

Radke,B.M. and Mathis,R.L.1980. On the Formation and Occurrence of Saddle Dolomite. *Journal of Sedimentary*

Petrology **50**, 1149-1168

Rais-Assa,R.1988. Stratigraphy and geodynamics of the Mombasa Basin (Kenya) in relation to the genesis of the proto-Indian Ocean. *Geological Magazine* **125**, 141-147

Reeder,R.J. and Grams,J.C.1987. Sector zoning in calcite cement crystals: implications for trace element distribution in carbonates. *Geochimica et Cosmochimica Acta* **51**, 187-194

Reeves,C.V.,Karanja,F.M. and MacLeod,I.N. 1986. Geophysical evidence for a Jurassic triple-junction in Kenya. *Earth and Planetary Science Letters* **81**,299-311

Saggerson,E.P. and Miller,J.M.1957. Geology of the Takabba-Wergudud area, Mandera District. *Geological Survey of Kenya Report* No.**40**, 42p

Sandberg,P.1985. Aragonite cements and their occurrence in ancient limestones. In: *Carbonate cements* (Ed. by N.Schneidermann and P.M.Harris). Special Publication of the Society of Economic Palaeontologists and mineralogists **36**, 33-57

Sanders,L.D.1959. Geology of the Mid-Galana Area. *Geological Survey of Kenya Report* No. **46**

Scholle,P.A.1978. A colour illustrated guide to carbonate rock constituents, cements and porosities. *American Association of Petroleum Geologists Memoir* **27**,241p

Scholle,P.A. and Halley,R.B.1985. Burial diagenesis: out of sight,out of mind !. In: *Carbonate cements* (Ed. by

N.Schneidermann and P.M.Harris) Special Publication of the Society of Economic Palaeontologists and mineralogists **36**, 309-334

Scoffin,T.P.1987. *An introduction to carbonate sediments and rocks*. Blackie & Son, Glasgow. 247p

Sellwood,B.W.1986. Shallow Marine Carbonate Environments. In: *Sedimentary Environments and Facies* (Ed. by H.G.Reading). 2nd ed. Blackwell. 283-343.

Shinn,E.A.1983. Tidal Flat Environments. In: *Carbonate Depositional Environments* (Ed. by P.A.Scholle,D.G.Bebout and C.H.Moore). American Association of Petroleum Geologists Memoir **33**, 173-210.

Thompson,A.O.1956. Geology of the Malindi Area. *Geological Survey of Kenya Report* No.**36**

Tucker,M.E. and Wright,V.P.1990. *Carbonate Sedimentology*. Blackwell. 482p.

Walkden,G.M. and Williams,D.O.1991. The diagenesis of the Dinantian Derbyshire-East Midland carbonate Shelf,Central England. *Sedimentology* **38**,643-670

Walls,R.A.,Mountjoy,E.W. and Fritz,P.1979. Isotopic composition and diagenetic history of carbonate cements in Devonian Golden Spike Reef,Alberta,Canada. *Bulletin of the Geological society of America* **90**, 963-982

Walters,R. and Linton,R.E.1973. The Sedimentary Basin of coastal Kenya. In: *Sedimentary Basins of African coasts* (Ed. by G.Blant). Association of African Geological

Surveys. Paris. 133-158.

Western Atlas International, Inc.1990. *The hydrocarbon potential of Kenya*. Integrated Technical Report. National Oil Corporation of Kenya, v.**1**. 185p

Wilkinson.B.H.,Smith,A.L. and Lohmann,K.C.1985. Sparry calcite marine cement in Upper Jurassic Limestones of Southeastern Wyoming. In: *Carbonate cements* (Ed. by N.Schneidermann and P.Harris). Special Publication of the Society of Economic Palaeontologists and mineralogists **36**, 169-184

Williams,L.A.J.1962. Geology of the Hadu-Fundi Isa Area north of Malindi. *Geological Survey of Kenya Report* No.**52**

Wilson,J.L.1975. *Carbonate Facies in Geologic History*. Springer- Verlag, Berlin.471p.

Wilson,J.L. and Jordan,C.1983. Middle Shelf Environments. In: *Carbonate Depositional Environments* (Ed. by P.A.Scholle, D.G.Bebout and C.H.Moore). American Association of Petroleum Geologists Memoir **33**, 298-343.